Dissertation

Submitted to the

Combined Faculties for the Natural Sciences and Mathematics

the Ruperto-Carola University of Heidelberg, Germany

for the degree of

Doctor of Natural Sciences

A Genetic Approach towards Identification of Factors Affecting Quinine Responses in *P. falciparum*

Presented by

Astutiati Nurhasanah

born in Jakarta, Indonesia

Gedruckt mit Unterstützung des Deutschen Akademischen Austauschdiesntes (DAAD)

Dissertation
Submitted to the
Combined Faculties for the Natural Sciences and Mathematics
of the Ruperto-Carola University of Heidelberg, Germany
for the degree of
Doctor of Natural Sciences

Presented by
Astutiati Nurhasanah
born in Jakarta, Indonesia

Oral examination: .....

Genetic Approach towards Identification of Factors Affecting Quinine Responses in *P. falciparum*

Referees: Prof. Dr. Michael Lanzer

Prof. Dr. Christine Clayton

Ich erkläre hiermit, dass ich die vorgelegte Dissertation selbst verfasst und mich dabei keiner anderen als der von mir ausdrücklich bezeichneten Quellen und Hilfen bedient habe.

Ich erkläre hiermit, dass ich an keiner anderen Stelle ein Prüfungsverfahren beantragt bzw. die Dissertation in dieser oder anderer Form bereits anderweitig als Prüfungsarbeit verwendet oder einer anderen Fakultät als Dissertation vorgelegt habe.

Die vorliegende Arbeit wurde am Hygieneinstitut, Abteilung Parasitologie der Universität Heidelberg in der Zeit vom Oktober 2005 bis April 2009 unter der Leitung von Prof. Dr. Michael Lanzer durchgeführt.

Publications resulting from this work:

Sybille Mayer[§], Astutiati Nurhasanah[§], Cecilia P. Sanchez, Wilfred D. Stein, and Michael Lanzer ([§] Both authors contribute equally) “Genetic linkage analysis of quinine responses reveals a novel locus synergistically associated with *pfcrt* in *Plasmodium falciparum*”. Submitted to PNAS.

Acknowledgment

First of all I would like to thank Prof. Dr. Michael Lanzer for the opportunity he had given me in working in his lab, his trust and his constant support during the years of my PhD.

I also would like to thank Prof. Wilfred Stein for the collaboration, support and his priceless input to the work.

I am very grateful to the Deutscher Akademischer Austauschdienst (DAAD) for the scholarship they gave me, without which, it would have been hardly possible for me to finish this work.

My heartfelt appreciation goes to Sybille Mayer, for the collaboration and (of course!) also the friendship, we had during the years I spent in Lanzer's lab.

And to the other members of Lanzer's lab, the past and the current, big big thanks to you (Anurag, Yvonne, Alex, Sebastiano, Tim, Theodora, Phillipp, Doro, Nicole and our 'super TAs' Marina and Eli, and all the others whom I failed to mention here) for the good time I had all these years. All of you had really made my stay in Germany truly memorable.

Last but not least I would like to thank my family and friends, for their love and support through these years. Especially to my Indonesian friends (who are as dear to me as my own family), thank you for making my staying away from home felt easier☺ (*Terimakasih untuk semuanya ya..*). Last but not least, to my husband and dearest friend, Tomi, for everything.

Abbreviations

^3H	Tritium, tritiated
ABC	ATP Binding Cassette
BLAST	Basic Local Alignment Search Tool
BSA	Bovine Serum Albumin
$CaCl_2$	Calcium Chloride
Chrom.	Chromosome
Ci	Curie
cM	centiMorgan
CQ	Chloroquine
CQR	Chloroquine Resistant
CQS	Chloroquine Sensitive
CSA	Chondroitin sulphate A
D	Dd2
DHFR	Dihydrofolate reductase
DHPS	Dihydropteroate synthase
DNA	Deoxyribonucleic Acid
dNTP	Deoxyribonucleoside triphosphate
DPAP1	dipeptidyl aminopeptidase 1
EBA	Erythrocyte binding antigen
EDTA	Ethylene Diaminotetraacetate
et al	*et alii* (Latin) – and others
EtBr	Ethidium Bromide
f	Femto
F	regression variance
fL	femtoLiter
FV	Food vacuole
FVM	Food vacuolar membrane
fwd	Forward
gDNA	Genomic DNA
Glu	Glutamine
Gly	Glycine
GmbH	Gesellschaft mit beschränkter Haftung
H	Hydrogen or HB3
H_2O	Water
H_2O_2	Hydrogen peroxide
HAP	histoaspartic protease
HCl	Hydrochloric Acid
HEPES	N-(2-Hydroxylethyl)piperacin-N´-(2-ethylsulphonacid)
His	Histidine
HRP2	Histidine rich protein 2
IC_{90}	90% Inhibition Concentration
ICAM1	Intracellular adhesion molecule 1
iRBC	Infected red blood cell
K	Lycine
k	Kilo
K & D	Kyte and Doolittle
K76T	Threonine substitution to Lycine at amino acid 76
Kb	Kilobases
KCl	Potassium chloride
KCl	Potassium Chloride

L	Liter
LOD	Logarithm of odds
m	Milli or meter
M	Molar
MACS	Magnet Activated Cell Sorter
Met	Methionine
$MgCl_2$	Magnesium Chloride
$MgSO_4$	Magnesiumsulphate
min	Minute
ml	Milliliter
mm^2	Millimeter square
mm^3	Millimeter cubic
MR4	Malaria Research and Reference Reagent Resource Center
MS	Micro satellites
MSD	multiple membrane spanning domain
MSP	Merozoite surface protein
n	Nano
N_2	Nitrogen
NaCl	Sodium chloride
NaOH	Sodium hydroxide
NBD	nucleotide binding domain
NCBI	National Center for Biotechnology Information
O_2	Oxygen
P.	Plasmodium
PBS	Phosphate Buffered Saline
PCR	Polymerase Chain Reaction
Pf	Plasmodium falciparum
PfCRT	*Plasmodium falciparum* chloroquine resistant transporter (protein name)
pfcrt	*Plasmodium falciparum* chloroquine resistant transporter (gene name name)
PfEMP1	*Plasmodium falciparum* erythrocyte membrane protein 1 (protein name)
pfemp1	*Plasmodium falciparum* erythrocyte membrane protein 1 (gene name name)
pfmdr1	*Plasmodium falciparum* multidrugresistant gene
PfNHE	*Plasmodium falciparum* Sodium Hydrogen Exchanger (protein name)
pfnhe	*Plasmodium falciparum* Sodium Hydrogen Exchanger (gene name)
P-gp	P-glycoprotein
pH	Potential hydrogenii
pLDH	*Plasmodium* lactose dehydrogenase
Plm	plasmepsin
PV	Parasitophorous Vacuole
PVM	Parasitophorous Vacuolar Membrane
QN	Quinine
QN IC_{90}	90% inhibition concentration of quinine
QN-VP IC_{90}	90% inhibition concentration of quinine in the presence of verapamil
QTL	Quantitative Trait Loci
R or r	Pearson regression
RBC	Red Blood Cell
RDT	Rapid diagnostic test
rev	Reverse

RFLP	Restriction fragment length polymorphisms
rpm	rotations per minute
RPMI	Rosewell Park Memorial Institute
RT	Room Temperature
SDS	Sodium Dodecyl Sulphate
sec	Second
Ser	Serine
STS	Sequence Tagged Site
T	Threonine
TAE	Tris/acetic acid/EDTA
Taq	Thermus aquaticus
TE	Tris/ EDTA
TKM	Tris-KCl-Magnesium
TMD	Transmembrane domain
TMHMM	Transmembrane domain Hidden Markov Model
Tris	tris (hydroxymethyl)-aminomethane
TVN	Tubulovesicular Network
U	Units
US	United States
UV	Ultra Violet
V	Volt
v/v	volume to volume
vol	Volume
VP	Verapamil
w/v	weight to volume
WHO	World Health Organization
x	Times
θ	recombination frequency
µ	Micro

Table of Contents

Table of Figures

List of Tables

Summary

Although PfCRT has been implicated as the main factor affecting chloroqune accumulation and resistance in *Plasmodium falciparum*, quinine accumulation and resistance have long been suspected to be affected by more than one genetic factor. Prior studies demonstrated that reduced quinine accumulation did not necessarily cause increased quinine resistance (Sanchez *et al.*, 2008b), indicating that resistance and accumulation did not share all factors affecting them.

In this study, the initial accumulation levels of radio-labelled quinine in the progeny set of the HB3 x Dd2 genetic cross were investigated and quantitative trait loci (QTL) analysis was performed based on these data. By measuring the initial quinine accumulation, a read-out defined by processes contributing to early quinine accumulation, such as facilitating, transporting or partitioning processes, would be obtained, thereby isolating these processes from the later events that cause cell death, such as inhibition of haem mineralisation or of some enzymatic function. The IC_{90} data of the same progeny set (Ferdig *et al.*, 2004) were reanalysed and comparing the QTL analysis data obtained from quinine initial accumulation and IC_{90} levels allowed isolation of factors affecting only cell deaths from those that also affected drug transport.

A novel locus in chromosome 7, B5M12, seems to have a major effect to both quinine accumulation and IC_{90}. The locus acts synergistically with *pfcrt*. Two loci in chromosome 13, VAPA and C13M73, showed major effect on quinine IC_{90}, but had no effect to the accumulation. Despite the prediction that the putative NA^+/H^+ exchanger (PfNHE) is involved in quinine resistance, the result revealed that the putative gene was not located within these two peaks. The Dd2 alleles of VAPA and C13M73 were associated with higher quinine IC_{90}. The secondary scan showed the involvement of *pfmdr1* in both quinine accumulation and IC_{90}. Interestingly, the Dd2-type *pfmdr1* contributes to an increase in the initial quinine accumulation, and, correspondingly, to an increase in the sensitivity to quinine (the IC_{90} being decreased).

Zusammenfassung

In *Plasmodium falciparum* gilt PfCRT seit langem als Hauptfaktor bei der Chloroquinakkumulation und –resistenz. Die Chininakkumulation und –resistenz scheint jedoch weit komplexer zu sein, und es wird vermutet, dass mehrere Faktoren hierbei eine Rolle spielen. Früherer Untersuchungen haben gezeigt, dass eine verminderte Chininakkumulation nicht zwingend mit einer höheren Resistenz einhergeht (Sanchez *et al.*, 2008b), daher kann die Akkumulation von anderen Faktoren beeinflusst sein wie der Resistenz.

In dieser Arbeit wurde die initiale Akkumulation von radioaktivem Chinin in den F1 Nachkommen oder den parentalen Stämmen HB3 und Dd2 untersucht und anschließend eine QTL-Analyse („quantitative trait loci analysis“) der Daten durchgeführt. Da die frühe Chininakkumulation bestimmt wurde, erhält man einen Einblick in Prozesse wie dem erleichternden Transport und Kompartimentierung. Dadurch konnte man diese Prozesse von späteren Ereignissen, die den Zelltod durch die Inhibition der Hämmineralisierung oder anderer enymatischer Prozesse, trennen. IC_{90} Daten (Ferdig *et al.*, 2004) der Stämme der selben Kreuzung wurden erneut analysiert und mit der QTL-Analyse der initialen Chininakkumulation verglichen. Hierbei konnten Faktoren, die den Zelltod beeinflussen von Faktoren die die frühe Akkumulation beeinträchtigen, separiert werden.

Ein neuer Lokus auf Chromosom 7, B5M12, schien die Chininakkumulation und den IC_{90} zu beeinflussen. Dieser Lokus interagierte synergistisch mit *pfcrt*. Zwei Loki auf Chromosom 13, VAPA und C13M73, hatten einen bedeutenden Effekt auf den Chinin IC_{90} aber keinen Effekt auf die Akkumulation. Frühere Untersuchungen zeigten einen möglichen Einfluss des Na^+/H^+ Austauschers (PfNHE) auf den IC_{90}, allerdings konnte die Lokalisation dieses Gens auf dem Chromosom nicht im Maximum nachgewiesen werden und besaß demnach nicht den höchsten „LOD-Score“. Das Dd2 Allel von VAPA und C13M73 wurde mit erhöhtem Chinin IC_{90} in Verbindung gebracht. In einem zweiten Scan, ohne Berücksichtigung von *pfcrt*, konnte ein Einfluss von *pfmdr1* auf die Akkumulation sowie auf den IC_{90} nachgewiesen werden. Interessanterweise führte *pfmdr1* von Dd2 zu einer erhöhten initialen Chininakkumulation und führte außerdem zu einer erhöhten Chininsensitivität, d.h. zu einem verringerten IC_{90} Wert.

1. Introduction

1.1. Malaria

Malaria is caused by a protozoan parasite from the genus *Plasmodium*¸ which belongs to the Phylum: Apicomplexa; Class: Sporozoa; Order: Coccidia; Suborder: Haemosporidiae; Family: Plasmodiidae. There are more than 100 species of *Plasmodium* that can infect various animal species such as reptiles, birds and various mammals. However, only five species infect humans, *Plasmodium falciparum, Plasmodium vivax, Plasmodium ovale, Plasmodium malariae,* and *Plasmodium knowlesi*, which is only recently known to infect human, as well as monkey, its conventional host (Cox-Singh *et al.*, 2008, White, 2008). *P. falciparum* causes the majority infection in Africa and is responsible for most severe diseases and mortality. The least common malaria parasite is *P. ovale*, which is restricted to West Africa, while *P. malariae* is found worldwide, but also with relatively low frequency. The most widespread malaria parasite is *P. vivax* but infections with this species are rarely fatal (Tuteja, 2007). *P. vivax* and *ovale* form resting stages in the liver (hypnozoites) that, once reactivated, can cause a clinical relapse many months after the initial infection (Greenwood *et al.*, 2005). The parasite is transmitted by female *Anopheles* mosquitos. Of approximately 400 species of *Anopheles* throughout the world, about 60 are natural malaria vectors, and 30 are of major importance (Tuteja, 2007).

1.1.1. Malaria; the Origin and History

DNA-sequencing studies show that *P. falciparum* originated 165 million years ago, probably in the Central Lakes area of Africa (Retief & Cilliers, 2006). Because of its intolerance of temperatures below 20ºC, it probably migrated to the Mediterranean area only after the last Ice Age, approximately 15,000-20,000 years ago. *P. vivax* and *P. malariae* probably originated in South-East Asia, and being tolerant of colder temperatures, possibly moved west at an earlier stage (Retief & Cilliers, 2006).

The characteristic periodic fevers of malaria are recorded from every civilized society from China in 2700 BC through the writings of Greek, Roman, Assyrian, Indian, Arabic, and European physicians up to the 19th century. The earliest detailed accounts are those of Hippocrates in the 5th century BC, and thereafter there are increasing numbers of references to the disease in Greece and Italy and throughout

the Roman Empire as its occurrence became commonplace in Europe and elsewhere (Cox, 2002).

The term malaria itself is derived from medieval Italian 'mala aria' meaning 'bad air' and was first used probably by Carnaro in a publication of 1440 (Retief & Cilliers, 2006). The term came from early association of the disease with marshy areas. Theories regarding malaria's miasmatic origins remained until late 19th century, when Charles Louis Alphonse Laveran in 1880 discovered the causative parasite in human blood (Retief & Cilliers, 2006) and Ronald Ross discovered that mosquitos transmitted the malaria (Tuteja, 2007). The complete sporogonic cycle of *P. falciparum*, *P. vivax* and *P. malariae* was demonstrated by Giovanni Batista Grassi and a team of Italian investigators including Amico Bignami and Giuseppe Bastianelli (Shortt, 1951).

1.1.2. Malaria; the Global Impact

Malaria is a global disease, affecting a large number of countries and causing a great deal of mortality and morbidity worldwide and throughout the history of mankind. It was estimated that in 2007, around 2.37 billion people, or about 35% of the world population, live in areas where there is some risk of *P. falciparum* transmission (Guerra *et al.*, 2008). In the year 2006, there were an estimated 247 million cases of malaria occurred worldwide (World Health Organisation, 2008). Eighty six percent of these cases occurred in African regions, whereas 80% of the rests occurred in India, Sudan, Myanmar, Bangladesh, Indonesia, Papua New Guinea, and Pakistan (World Health Organisation, 2008). In the same year, approximately 881,000 deaths occurred from malaria, of which 91% were in Africa, which is a malaria high risk area (World Health Organisation, 2008).

Figure 1.1. presents the global malaria distribution at the end of 2007. Although low-risk areas cover a large number of people living across a wide geographical area, they produce a relatively small number of malaria cases each year, less than 2 million, and account for less than 3% of cases reported by countries in 2006 (World Health Organisation, 2008).

Malaria infection during pregnancy is a very serious public health problem in tropical and sub-tropical regions all over the world. In areas with low malaria transmission, adult women often do not have significant level of immunity to malaria that they become ill when infected with *P. falciparum.* In this area the risk of severe malaria is 2-3 higher in pregnant women than in non-pregnant women. Maternal death may result directly from severe malaria or indirectly from malaria-related severe anaemia.

In addition, malaria may result in a range of adverse pregnancy outcomes, including low birth weight, spontaneous abortion, and neonatal death (World Health Organisation, 2003). In areas with high malaria transmission, adults normally have sufficient immunity against malaria that, even during pregnancy, *P. falciparum* infection does not usually result in fever or other clinical symptoms. The principal impact of malaria infection is malaria-related anaemia in the mother and the presence of parasites in the placenta, resulting impairment of foetal nutrition, which contributes to low birth weight and is a leading cause of poorer infant survival and development (World Health Organisation, 2003). In areas of Africa with high malaria transmission, *P. falciparum* infection during pregnancy is estimated to cause 10 000 maternal deaths each year, 8% to 14% of all low birth weight babies, and 3% to 8% of all infant deaths (World Health Organisation, 2001).

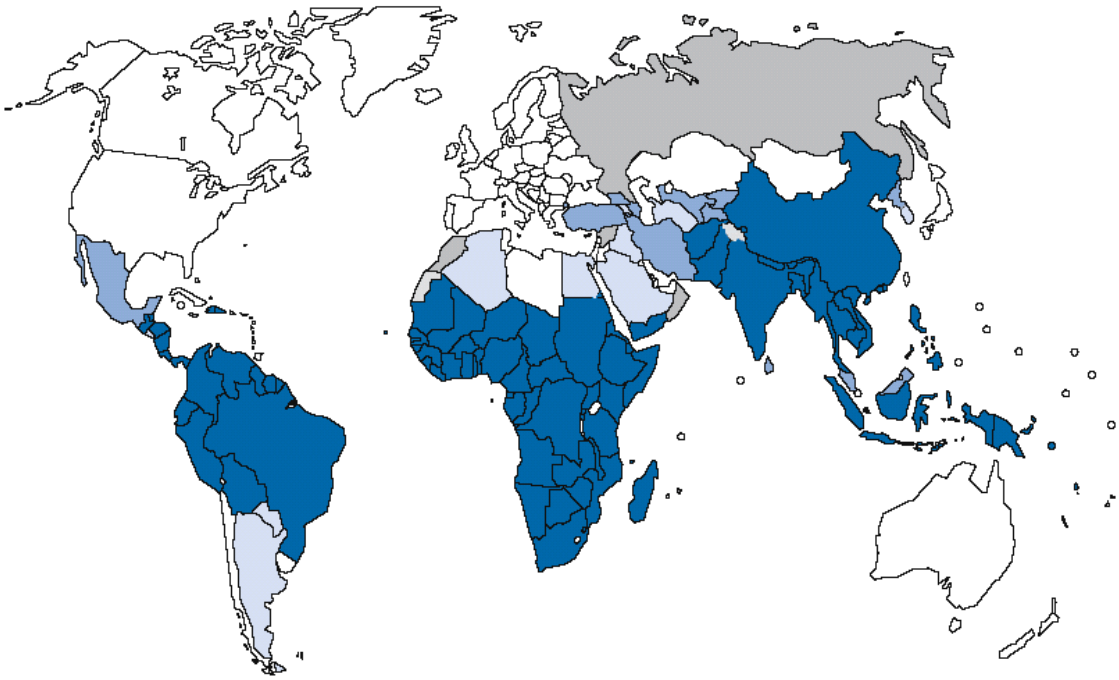

Figure 1.1. Global malaria distribution end 2007 (World Health Organisation, 2008)

The malaria distribution map shows malaria free countries and malaria endemic countries in phases of control, pre elimination, elimination and prevention of reintroduction.

malaria-free and/or no on-going local transmission for over a decade

Elimination

Control

Prevention of Introduction

Pre-elimination

Malaria is also a major cause of disease and mortality of children. Every 40 seconds a child dies of malaria, resulting a daily loss of more than 2000 young lives all over the world (Sachs & Malaney, 2002). In 2006, it was still the fourth leading cause of deaths of children under five years old, after neonatal conditions, pneumonia and

diarrhoea and in 2007, 85% of malaria mortality were of children under 5 years old (World Health Organisation, 2009). The effect to children extends beyond mortality and morbidity, since malaria also reduces attendance to school and can impair intellectual development (Greenwood *et al.*, 2005).

In addition to the mortality and morbidity, there is also a strong correlation of malaria to the economy. This correlation is, however, complex and works both ways. Poverty sustains the conditions where malaria thrives, and malaria impedes economic growth and keeps communities in poverty (Sachs & Malaney, 2002). Recent studies to estimate the economic burden of malaria in endemic countries showed that the direct cost of one episode of malaria to a household was US$6.87 in Ghana,US$4.80 in Uganda, and US$4.50 in Mali (Teklehaimanot & Mejia, 2008). Cross country regressions over 25 years period (1965–1990) estimated that the annual economic growth of countries with intensive malaria is 1.3% less in comparison to countries where malaria is not endemic, even after controlling for factors such as initial poverty, economic policy, tropical location, and life expectancy. On the contrary, 10% reduction in malaria was associated with 0.3% higher growth (Gallup & Sachs, 2001).

1.1.3. Clinical Manifestations

The clinical disease can be categorised into uncomplicated and severe malaria, and the clinical manifestations might vary in the presentation and severity. ranging from no symptoms at all, fever, chill, flu-like symptoms (Malaria In Armenia, 2002), metabolic acidosis, hypoglicaemia kidney failures and comatose in severe and complicated malaria (Patel *et al.*, 2003), severe anaemia (World Health Organisation, 2001) and congenital malaria (Maitra *et al.*, 1993) in cases of malaria during pregnancy. However, when diagnosed early enough and treated correctly, malaria can be handled relatively easily.

The classical malaria attack lasts 6-10 hours. It consists of a cold stage (sensation of cold, shivering), a hot stage (fever, headaches, vomiting; seizures in young children), and finally a sweating stage (sweats, return to normal temperature, tiredness). Classically the attacks occur every second day with the "tertian" parasites (*P. falciparum, P. vivax,* and *P. ovale*) and every third day with the "quartan" parasite (*P. malariae*). Some of these symptoms are related to the release of TNF-α during schizonts release (Kwiatkowski *et al.*, 1989). Parasite egress in *P. falciparum* is, however, often unsynchronised, leading to persistent spiking fever or daily fibril paroxysms (Rasti *et al.*, 2004).

Severe malaria normally results from sequestration of the parasites to various organs, such as the heart, lung, kidneys, subcutaneous tissues and placenta (Miller *et al.*, 2002). The sequestration occurs by interaction of parasites-derived proteins on the surface of infected red blood cells (RBCs) with certain molecules expressed on uninfected RBCs, endothelial cells as well as placental cells (Baruch, 1999). Several human proteins are implicated in the specific manifestations of malaria, for example chondroitin sulphate A (CSA), which plays role in parasites adhesion to placenta and intercellular adhesion molecule 1 (ICAM1) in cerebral malaria (Miller *et al.*, 2002).

Malaria is normally diagnosed using a combination of clinical observations, case history and diagnostic tests, principally microscopic blood examinations (Tuteja, 2007). Thin blood film is normally used for routine estimation of parasitaemia, since it is easier to see and count the parasites and the blood. A thick blood film concentrates the layers of red blood cells (RBC) on a small surface by a factor of 20 to 30 and provides enhanced sensitivity of the blood film technique. The sensitivity of the thick blood film procedure operated by an experienced technician is about 50 parasites/µl of blood (assuming a total RBC count of 5 x 10^6/µl of blood), which is equivalent to 0.001% of infected RBC (iRBC) (Moody, 2002). A rapid diagnostic test (RDT) is also available, although expensive and most likely not affordable for most people living in the malaria endemic areas. The test is based on recognition histidine rich protein 2 (HRP2), lactose dehydrogenase (LDH) and aldolase (Moody, 2002). HRP2 is a water-soluble protein produced by asexual stages and young gametocytes of *P. falciparum* (Rock *et al.*, 1987). It is expressed on the RBC membrane surface, and because of its abundance in *P. falciparum*, it is the first antigen used for RDT (Moody, 2002). pLDH, an enzyme found in the glycolytic pathway of the malaria parasite, is produced by sexual and asexual stages of the parasite (Makler *et al.*, 1998). Different isomers of pLDH for each of the four *Plasmodium spp*. infecting humans exist, and their detection constitutes a second approach to RDT development (Moody, 2002). Aldolase, which is also a glycolytic enzyme (Meier *et al.*, 1992), have been suggested as target antigens for RDT for species other than *P. falciparum* (Moody, 2002).

1.1.4. Life Cycle

The life cycle of malaria parasites is extremely complex, involving alternating hosts, the invertebrate *Anopheles* mosquitoes and vertebrate humans. Due to this complicated life cycle, the parasites requires specialised protein expression for survival in both the invertebrate and vertebrate hosts, for both intracellular and

extracellular survival, for the invasion of a variety of cell types and for the evasion of host immune responses (Tuteja, 2007).

Malaria in humans develops via two phases, an exoerythrocytic (hepatic) and an erythrocytic phase. The parasite life cycle is described in Figure 1.2.

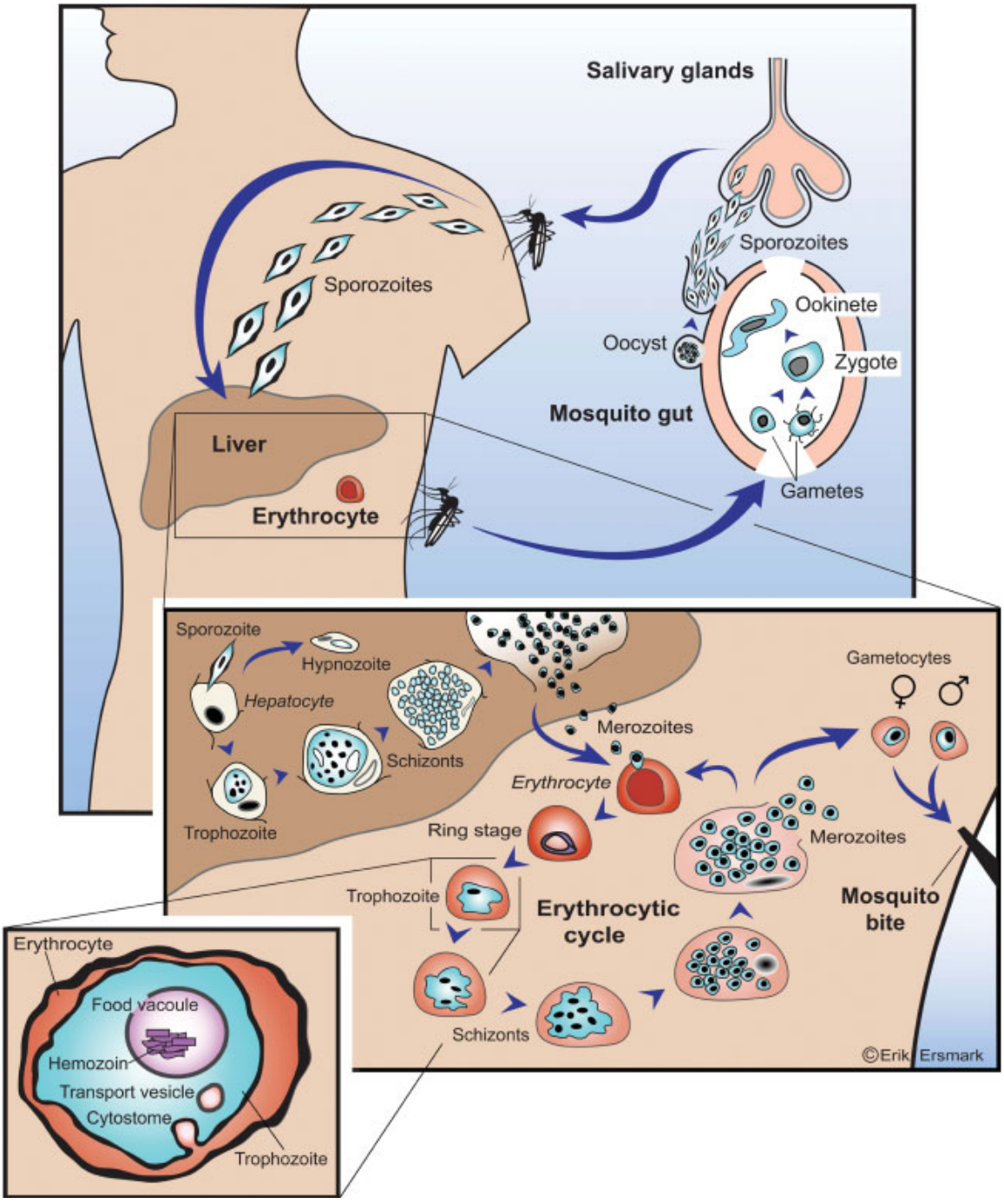

Figure 1.2. The life cycle of the malaria parasite in the human host and the mosquito vector. (Ersmark *et al.*, 2006)
The trophozoite stage in the erythrocytic cycle is enlarged.

The infectious stage sporozoites of *Plasmodium* residing in the salivary glands of the mosquitoes are injected to human during blood meal. Previously, it was thought that sporozoites move rapidly away from the site of injection as soon as they are injected to the human hosts. However, a recent study using rodent malaria parasites (*P. yoelii*) showed that, at least in this case, the majority of infective sporozoites remain at the injection site for hours, with only slow release into the circulation (Yamauchi *et al.*, 2007). Once in the bloodstream, *P. falciparum* and *P. malariae* sporozoites reach the liver and enter the hepatocytes. where each sporozoite immediately develops into a tissue schizont containing 10,000–30,000 merozoites that will be released into the bloodstream by rupturing the schizonts. In *P. vivax and ovale*, however, some sporozoites turn into hypnozoites, a form that can remain dormant in the liver cells, causing relapses months or even years after the initial infection. *P. falciparum* and *P. malariae* lack this persistent liver stage.

The mechanisms of hepatocytes invasion is not yet well understood, but studies have shown that a series of migration through several hepatocytes seem to be important for completion of the life cycle (Mota *et al.*, 2001). The receptors on sporozoites responsible for hepatocyte invasion are mainly the thrombospondin domains on the circumsporozoite protein and on thrombospondin-related adhesive protein. The whole time taken to complete the tissue phase varies depending on the species; 8-25 days for *P. falciparum*, 8-27 for *vivax*. 9-17 days for *ovale*, and 15-30 days for *malariae* (Tuteja, 2007).

Merozoites released into the bloodstream again evade the host immune system by invading erythrocytes. The erythrocyte invasion process is complicated and involving several phases, initial recognition and reversible attachment of the merozoite to the erythrocyte membrane; reorientation and junction formation between the apical end of the merozoite (irreversible attachment) and the release of substances from the rhoptry and microneme organelles, leading to formation of the parasitophorous vacuole; movement of the junction and invagination of the erythrocyte membrane around the merozoite accompanied by removal of the merozoite's surface coat; and resealing of the parasitophorous vacuole and erythrocyte membranes after completion of merozoite invasion (Miller *et al.*, 2002)

Asexual division starts inside the erythrocyte. Here, the parasites develop through different stages starting with the early trophozoíte stage known as the ring stage, where the parasites then enlarge accompanied by highly active metabolism including glycolysis of large amounts of imported glucose, ingestion of host cytoplasm and the proteolysis of haemoglobin into constituent amino acids. The end of the trophozoite stage is marked by multiple rounds of nuclear division without cytokinesis resulting in

the formation of schizonts. Each mature schizont contains around 20 merozoites and these are released after lysis of the RBC to invade further uninfected RBCs. This repetitive intraerythrocytic cycle of invasion–multiplication–release–invasion continues, taking about 48 h in *P. falciparum*, *P. ovale* and *P. vivax* infections and 72 h in *P. malariae* infection. This release coincides with the sharp increases in body temperature during the progression of the disease.

Several of the molecules involved in invasion are members of larger gene families Merozoite surface proteins (MSP)1 to MSP4 are integral membrane proteins identified on the surface of developing and free merozoites, which are involved in the initial recognition of the erythrocytes via interactions with sialic acid residues and are likely to be important for invasion because antibodies directed against these proteins can block this process (Cowman & Crabb, 2002). Erythrocyte binding antigen 175 (EBA-175) is a *P. falciparum* protein binds the major glycoprotein (glycophorin A) found on human erythrocytes during invasion (Miller *et al.*, 2002). The structure of EBA-175 has striking similarities to the Duffy antigen-binding proteins of *P. vivax* that are essential for successful invasion by this species. After invasion, the principal parasite ligand known as *P. falciparum* erythrocyte membrane protein 1 (PfEMP1), which is encoded by *var* multigene family, is expressed at the surface of the infected RBC (Chen *et al.*, 2000). The extensive diversity in the var gene family is mainly responsible for the evasion of specific immune responses and many of these genes are expressed in the parasite population, but at any given time during an infection, parasites within infected cells express only a single *var* gene due to its unique gene activation and switching mechanism (Chen *et al.*, 2000).

The sexual cycle begins when a gametocyte is ingested during the bite of a female Anopheles mosquito. Depending on their sex, the gametocytes are transformed into male or female gametes in the gut of the mosquito. Gametes of the opposite sex merge to form diploid zygotes, which develop into ookinetes, which, in turn move to the mid-gut surface where they are converted into oocysts. Within the oocyst, several hundreds sporozoites are formed and later liberated to enable transport of the infectious sporozoites to the mosquito salivary glands. The mosquito is now able to transmit the infection during the next human bite, continuing the parasite life cycle (Ersmark *et al.*, 2006).

1.1.5. Chemotherapy

Despite the consistent effort to develop a potent malaria vaccine, clinically proven vaccines are continuously absent that the prevention and treatment of disease still

has to rely on chemoprophylaxis and chemotherapy. However, since the discovery of the first synthetic antimalarial drug, chloroquine, during the 1930s, only a small number of substances have been proven to be suitable for licensing as drugs for human use, an to make the matter worse, there is a growing number of resistance to these compounds (Hyde, 2007). Thus, the repertoire of clinically valid and effective antimalarial drugs is really limited.

Traditionally, antimalarial drugs are classified into the stages of parasite being targetted by the drugs, blood schizonticides acting on the asexual intraerythrocytic stages of the parasites, tissue schizonticides killing hepatic schizonts, and thus preventing the invasion of erythrocytes, acting in a causally prophylactic manner, whereas hypnozoiticides killing persistent intrahepatic stages of *P. vivax* and *P. ovale*, thus preventing relapses from these dormant stages, and gametocytocides destroying intraerythrocytic sexual forms of the parasites and preventing transmission from human to mosquito (Schlitzer, 2007). As there are no dormant liver stages in *P. falciparum* malaria, blood schizonticidal drugs are sufficient to cure the infection. In cases of *P. vivax* and *P. ovale*, a combination of blood schizonticides and tissue schizonticides is required.

The first chemically synthesised and most commonly used drugs for malaria treatment and prophylaxis are from the quinoline group. All drugs in this group are derivatives of quinine, the active compound present in *Chinchona* bark and the oldest antimalaria known in the Western world. Despite the dissemination of resistant parasites all over the world in the last 40 years, chloroquine is up to now still the most important drug for prophylaxis and treatment of this disease, due to its safety, low cost and excellent activity (Wiesner *et al.*, 2003). Primaquine, another member of quinoline group, has a unique spectrum of activity, including reliable efficacy to against primary and latent liver stages as well as gametocytes. Thus, although primaquine cannot be used to treat symptomatic malaria, the drug is used to eradicate hypnozoites of *P. vivax* and *ovale*, which are responsible for relapsing infections (Shapiro & Goldberg, 2005, Foley & Tilley, 1998).

The second most commonly used drug after chloroquine is the antifolate combination sulfadoxin-pyrimethamin, or also known as fansidar (Wiesner *et al.*, 2003). Antifolates work by inhibiting the folate biosynthesis of parasites. Humans depend on the dietary intake of pre-formed dihydrofolate as an essential nutrient, which is then reduced to tetrahydrofolate, and used in the biosynthesis of thymine, purine nucleotides, and several amino acids (Met, Gly, Ser, Glu, and His). On the other hand, *Plasmodia* can synthesise dihydrofolate from simple precursors as well as use exogenous dihydrofolate via a salvage pathway (Schlitzer, 2007). Dihydropteroate

synthase (DHPS) and dihydrofolate reductase (DHFR) are the two key enzymes used as targets of the antifolate drugs. DHPS is completely absent in humans, whereas protozoal DHFR is sufficiently different from the one of human that allow the development of selective inhibitors. The disruption of folate synthesis by DHFR and DHPS inhibitors leads to decreased levels of fully reduced tetrahydrofolate, which in turn decreases glycine to serine conversion, methionine conversion, and lower thymidylate levels with a subsequent arrest of DNA replication (Gregson & Plowe, 2005). Antimalarial antifolate drugs, such as pyrimethamine, proguanil and the family of sulfa drugs, were introduced in the 1940s, but resistance arose rapidly, that it is necessary to use the drugs in combination therapy. Mutations in the genes *pfdhfr* and *pfdhps* are responsible for conferring resistance to this family of drugs (Gregson & Plowe, 2005)

Artemisinin is derived from the 'qing hao' weed (*Artemisia annua*), or also known as 'sweet wormwood' or 'annual wormwood', which has been used as traditional Chinese medicine to treat fever and symptoms of malaria since hundreds of years (Shapiro & Goldberg, 2005). The active ingredients of 'qing hao', called 'qinghaosu' and now known as artemisinin, was first extracted and crystallised in 1971 (Woodrow *et al.*, 2005). Since then, an array of semi-synthetic artemisinin derivatives with improved potency and bioavailability has been developed, including dihydroarthemisinin, arthemeter and athesunate.

Arthemisinins kill all species of *Plasmodium* that infect humans (Woodrow *et al.*, 2005) and active against both asexual and sexual blood stages, thus reducing transmission of the parasites (Schlitzer, 2007, Wiesner *et al.*, 2003). The asexual stages are the most susceptible, with artemisinins decreasing the parasite biomass up to 10,000-fold per asexual cycle (Woodrow *et al.*, 2005), making them the most active and rapid acting antimalarial drugs known today. In common with other antimalarials, artemisinins act predominantly against the large ring stage of infection when parasites are beginning to become most metabolically active, but, in contrast with other currently useful antimalarials, artemisinins also target tiny ring stages of infection present only a few hours after infection (Woodrow *et al.*, 2005, Schlitzer, 2007).

The activity of artemisinins depends on the cleavage of endoperoxidase bridge presents in the middle of the substance by Fe^{+2}, leading to formation of C-centred radicals. Previously it was thought that the C-centred radicals formation occurs in the food vacuole (FV), that the released radicals act more or less indiscriminately with different proteins, inhibiting multiple enzymes and preventing haem detoxification (Schlitzer, 2007). However, a more recent research suggested that the radicals

formation occurs in the cytoplasm catalysed by a cytoplasmic Fe^{+2} source, producing radicals acting specifically on a protein, called PfATP6, which is related to mammalian SERCA (Sarcoplasmic endoplasmic reticulum Ca^{+2} ATPase) (Eckstein-Ludwig *et al.*, 2003).

Several antibiotics known to be active against bacteria also show activity against malaria. The activity depends on the presence of mitochondria and apicoplast that have their own DNA and bacteria-like machinery for replication, transcription, and translation. The mitochondrial genome is relatively small (6 kb), encoding only three proteins, whereas all other proteins and rRNAs have to be imported from the cytosol. The apicoplast genome is considerably larger (35 kb), including housekeeping genes responsible for the maintenance, whereas most proteins involved in the metabolic pathways are encoded in and imported from the nucleus (Schlitzer, 2007). Antibiotics like rifampicin is thought to inhibits the RNA synthesis in the apicoplast by inhibiting the RNA polymerase, whereas antibiotics like tetracycline, macrolides and lincosemides are considered to inhibit the protein synthesis in apicoplast (Wiesner *et al.*, 2003, Schlitzer, 2007).

1.2. Quinine

Quinine (QN) is originally the plasmodicidal alkaloid present in the powdered bark of cinchona tree. As mentioned above, QN belongs to the quinoline group of drugs and due to its soluble character, QN is used mainly a intravenous formulation for treatment of complicated malaria, when oral medication is not possible (Wiesner *et al.*, 2003).

1.2.1. Quinoline drugs – The Discovery and History

The quinolines represent one of the most successful yet poorly understood classes of drugs. Notable examples of the quinoline compounds include the 4-aminoquinoline chloroquine, the 8-aminoquinoline primaquine, and the quinolinemethanols mefloquine and QN. Until the emergence of drug-resistant parasites, these drugs were the most effective means to treat malaria.

The bark of *Cinchona officinalis* had been the traditional medicine of the indigenous Peruvians to treat shivering. In 1633, an Agustinian named Calancha, of Lima, Peru, wrote that a powder of cinchona “given as a beverage, cures the fevers and tertians”. By 1640, cinchona was used to treat fevers in Europe. It was mainly distributed in the continent by the Jesuit monks and used in the form of powder, extract or infusion

(Shapiro & Goldberg, 2005). In 1810 a crude mixture of crystalline alkaloids was extracted from cinchona bark by Gomes, in Portugal (Foley & Tilley, 1998) and in 1820, QN, the active compound of the bark was first isolated by Pelletier and Caventou (Shapiro & Goldberg, 2005), making malaria one of the diseases treated with pure substance (Wiesner *et al.*, 2003).

In 1856 William Henry Perkin tried to synthesise QN, though unsuccessful. Instead, his effort led to the discovery of the first synthetic dye called 'mauve' (Schlitzer, 2007), which later led to development to even more synthetic dyes. Microbiologists used these dyes for staining microorganisms, to enhance the visibility under microscope. Paul Ehrlich noticed that methylene blue was particularly effective in staining malaria parasites and rationalised that it could also be toxic to the parasite (Schlitzer, 2007). In 1891, Ehrlich and Guttmann cured two malaria patients with methylene blue, making this dye the first synthetic drug used to treat malaria (Wiesner *et al.*, 2003, Schlitzer, 2007).

In 1925 chemists at Bayer, in Germany, developed a new synthetic drug called plasmochin by modification of methylene blue. Clinical evaluation, however, showed that there were many side effects associated to this drug. A better tolerated congeneric drug called primaquine was introduced in 1956 (Schlitzer, 2007).

Since the pathway for the synthesis of QN was not discovered until 1944 by Woodward and von Doering and the synthetic route was anyway too complex for commercial production, cinchona seeds were smuggled out from Peru and Cinchona plantations were established in Java, Indonesia by both the Dutch and the British. By 1918, 102,000 kg of quinine was produced annually (Foley & Tilley, 1998).

With the advent of World War I, and its campaigns in North Africa and Southern Europe, supplies of quinine were unable to meet the demands of the Allied and German armies. This situation had inspired further research in finding new antimalarials and in 1932 quinacrine was first introduced as an antimalarial drug (Schlitzer, 2007).

Later, during the Pacific war campaign, the Allies were completely cut off from supplies of quinine when Indonesia was captured by the Japanese and quinacrine became the main drug for prophylaxis and treatment for the allied troops (Foley & Tilley, 1998, Schlitzer, 2007). Nowadays the drug is no longer used for malaria, due to its substantial side effect, such as the yellow staining of the skin and eyes, but still used for treatment of *Giardia lamblia*.

A major success in the drug discovery happened in 1934 when resochin was found. Though after initial trials in Germany resochin was considered too toxic for human, resochin was later, after the war, re-evaluated and renamed as chloroquine (CQ)

(Schlitzer, 2007). CQ, then, largely replaced QN for prophylaxis and routine treatment.

1.2.2. Haemoglobin Degradation

During intraerythrocytic development, parasites degrade haemoglobin both to meet their nutrient demand and to counteract the osmotic imbalances caused by their own growth within the red blood cell (Lew *et al.*, 2003). Haemoglobin is shuttled from erythrocytes to the food vacuole (FV) with a mechanism that is not yet fully understood. Some suggests that the haemoglobin is transported primarily via cytostomes (Lazarus *et al.*, 2008), however some other mechanisms, such as internalisation of the host cell cytoplasm independent of actin polymerization, are also suggested recently (Elliott *et al.*, 2008) Either in the FV or already in the cytostomes, the protein component of haemoglobin is digested by the successive action of various proteolytic enzymes, aspartic proteases plasmepsin (Plm) I, II, IV and the closely related histoaspartic protease (HAP), cysteine proteases (falcipain-1,-2,-2', and -3), a metalloprotease falcilysin, and the recently discovered dipeptidyl aminopeptidase 1 (DPAP1) (Ersmark *et al.*, 2006).

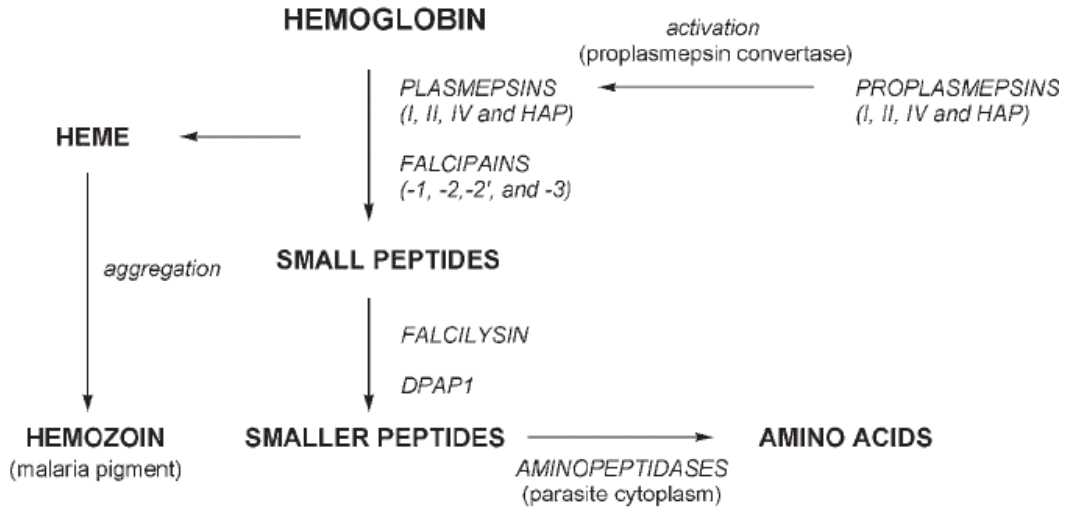

Figure 1.3. The general pathway for haemoglobin metabolism in *P. falciparum* (Ersmark *et al.*, 2006).

The precise sequence of events is still now a matter of controversy, especially whether a plasmepsin or a falcipain catalyzes the initial cleavage in the hinge region of the domain responsible for holding the native haemoglobin tetramer together. However, the general mechanism is shown in Figure 1.3. The cleavage unravels the protein, exposing it to subsequent cleavages into smaller peptides that can be

accomplished by both plasmepsins and falcipains. The metalloprotease falcilysin can only cleave small polypeptides, up to 20 amino acids, producing even shorter oligopeptides. DPAP1 was recently discovered to cleave off dipeptides from haemoglobin-derived oligopeptides in the food vacuole. Final hydrolysis to free amino acids is thought to occur in the parasite cytoplasm by aminopeptidases (Ersmark *et al.*, 2006).

The resulting small peptides and possibly free amino acids are transported across the vacuole membrane into the cytoplasm, leaving the haem part behind, leading to accumulation of large quantities of haem, which is toxic when accumulated at higher concentration in the FV, though the mechanisms of its toxicity remains unclear (Schlitzer, 2007). The parasite disposes this hazardous side product by biomineralising it to the inert haemozoin in the food vacuole (Egan *et al.*, 2002), which is also known as the malaria pigment.

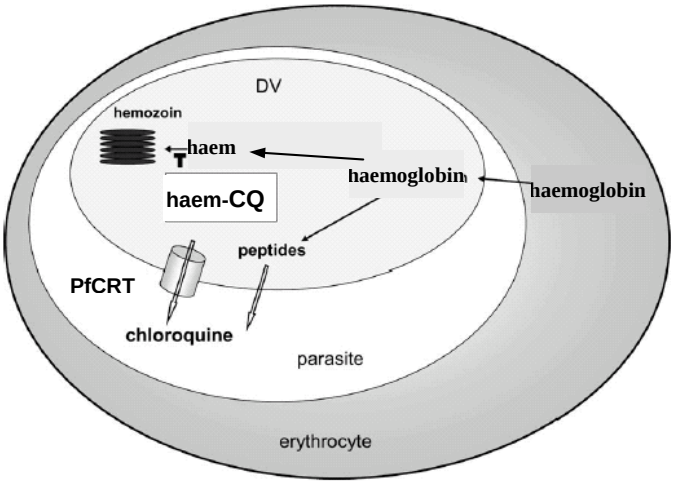

Figure 1.4. Large quantities of haemoglobin are degraded in the food vacuole, yielding peptides and haem (Schlitzer, 2007)
Haem, which is deposited as the insoluble polymer haemozoin, represents a harmful waste product to the parasite. CQ form complexes with FPIX which are toxic to the parasites. In chloroquine-resistant strains, the drug is expelled from the DV by the action of a membrane-bound transporter (PfCRT).

1.2.3. Chloroquine and Quinine – the Mechanism of Action

Despite the overwhelming importance and its being the first drug used for treatment of malaria, the mechanisms of action of QN is not well understood. It is generally believed that QN mechanism of action is similar to that of CQ. Just like CQ, QN can inhibit haem biomineralisation (Hawley *et al.*, 1998). Similar to CQ, incorporation of radiolabelled QN into the growing haemozoin polymers is almost completely arrested

in the presence of an inhibitor of plasmepsin I, an enzyme responsible for the initial cleavage of haemoglobin, suggesting that the interaction of both drugs with the haem monomer or polymer is central to activity (Mungthin *et al.*, 1998). In addition, quantitative trait loci (QTL) analysis showed that QN and CQ shared at least one inheritable resistance determinant (Ferdig *et al.*, 2004), despite QN being active against several CQ resistant *P. falciparum* strains.

CQ, QN and other quinolines are thought to inhibit haem biomineralisation by forming a complex with haem (Hawley *et al.*, 1998, Mungthin *et al.*, 1998). A more recent publication suggests that QN forms an intramolecular salt bridge with haem, interrupting formation of the haemozoin precursor dimmer (de Villiers *et al.*, 2008). The precise mechanism by which this toxic effect is exerted remains to be elucidated (Schlitzer, 2007). According to the new theory, the haem–CQ complex acts on a yet undefined membrane target, either impairing the membrane function directly, or triggering the release of Ca2+ ions resulting in the premature fusion of the transport vesicles shuttling haemoglobin to the FV. In these prematurely fused vesicles, haemoglobin is no longer properly degraded (Schlitzer, 2007).

In chloroquine sensitive (CQS) strains the concentration of CQ in FV can reach 20,000 times higher than that in the extracellular medium (Sanchez *et al.*, 2007). Since CQ presents in the FV as a diprotic, amphiphilic base, some early studies suggested that the drug was retained in the FV due to pH gradient between FV and parasite cytoplasmic pH (Yayon *et al.*, 1985), however a more recent publication shows that the FV pH in CQR and CQS strains are relatively comparable (Kuhn *et al.*, 2007).

1.2.4. Chloroquine and Quinine – the Resistance

The first signs of CQ resistance appeared almost simultaneously in southeast Asia and South America around 1960 (Hartl, 2004). Its continual use for treatment and prophylaxis increased the selection pressure for emergence of resistance, and since the first confirmed case CQ resistant *P. falciparum* malaria was reported in 1979 (Campbell *et al.*, 1979), more and more cases were reported subsequently from different parts of the world (Sansonetti *et al.*, 1985, Le Bras *et al.*, 1986, Weniger *et al.*, 1982) until it becomes a worldwide problem nowadays.

QN, on the other hand, has been spared from widespread or prolonged use that high level resistance to the drug has been very slow to develop (Foley & Tilley, 1998). Unfortunately, a decrease of QN dose responsiveness in *P. falciparum* infection in South East Asia, South America and Africa (Bloland, 2001, Pukrittayakamee *et al.*,

1994, Segurado *et al.*, 1997, Jelinek *et al.*, 1995) as well as the detection of field isolates with increased QN IC_{90} (Mayxay *et al.*, 2007) have been reported. This phenomena is very worrying since QN is up to now still the main medication used for the treatment of severe and complicated malaria (World Health Organisation, 2008).

QN and CQ were predicted to have similar, if not the same, mechanism of action (Mungthin *et al.*, 1998, Hawley *et al.*, 1998), although QN often remains active against some CQ resistant parasites. QTL analysis also shows that QN resistance shares at least one genetic determinant with CQ resistance, that is *pfcrt* (*P. falciparum* chloroquine resistant transporter), a gene located in chromosome 7 of *P. falciparum* genome (Ferdig *et al.*, 2004).

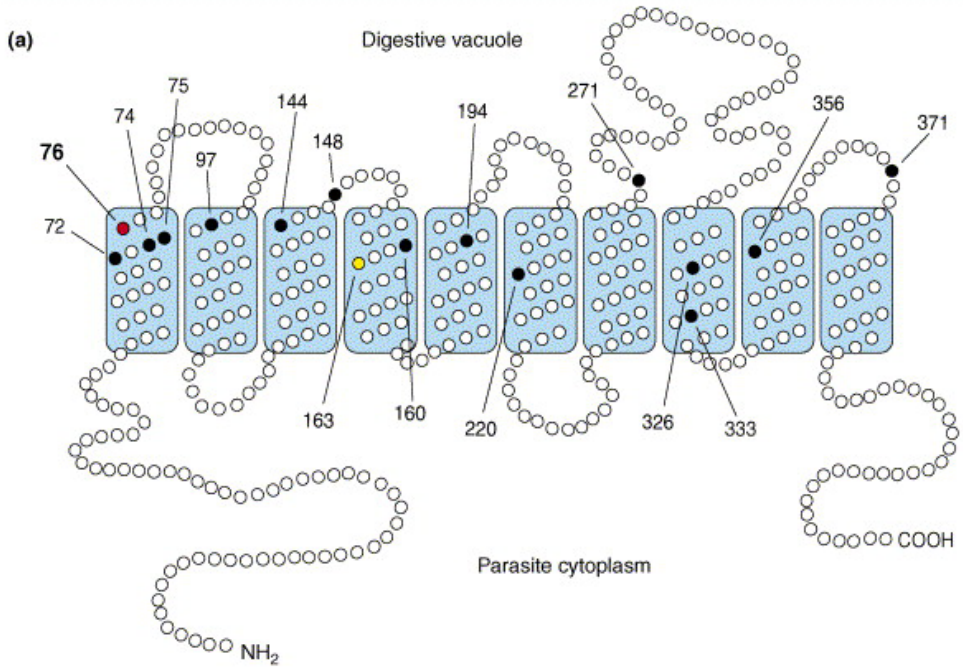

(b)

pfcrt allelic variants identified in *Plasmodium falciparum* field isolates and laboratory-adapted lines

		PfCRT position and encoded amino acid														
Region	Reference line (origin)	72	74	75	76	97	144	148	160	194	220	271	326	333	356	371
	Chloroquine-sensitive															
All	Wild type (HB3, Honduras)	C	M	N	K	H	A	L	L	I	A	Q	N	T	I	R
	Chloroquine-resistant															
Asia and Africa	Dd2 (Indochina)	C	I	E	T	H	A	L	L	I	S	E	S	T	T	I
Southeast Asia	734 (Cambodia)	C	I	D	T	H	F	I	L	T	S	E	N	S	I	R
Pacific region	2300 (Indonesian Papua)	C	I	K	T	H	A	L	L	I	S	E	S	T	I	I
	PH2 (Philippines)	S	M	N	T	H	T	L	Y	I	A	Q	D	T	I	R
South America and Pacific	7G8 (Brazil)	S	M	N	T	H	A	L	L	I	S	Q	D	T	L	R

Gray shading indicates residues that differ from the wild-type allele.

TRENDS in Pharmacological Sciences

Figure 1.5. Topology of PfCRT (Valderramos & Fidock, 2006)
Predicted structure and representative haplotypes of *P. falciparum* chloroquine resistance transporter. **(A)** PfCRT is predicted to have ten transmembrane domains (Bray *et al.*, 2005) **(B)** *pfcrt* allelic variants

PfCRT, the gene product of *pfcrt*, is a putative drug metabolite carrier having ten transmembrane domains (TMDs) (Figure 1.5.) (Bray *et al.*, 2005, Martin & Kirk, 2004) located at the FV membrane (Fidock *et al.*, 2000). It is unsure, however, whether the protein acts as a carrier (Sanchez *et al.*, 2007) or a pore (Bray *et al.*, 2006).

Mutations within *pfcrt* is associated with CQ resistance (Sidhu *et al.*, 2002, Fidock *et al.*, 2000, Lakshmanan *et al.*, 2005), altered susceptibility to CQ and QN (Cooper *et al.*, 2007, Lakshmanan *et al.*, 2005, Johnson *et al.*, 2004) and altered responsiveness to other antimalarial drugs (Johnson *et al.*, 2004). The most well studied mutation within the *pfcrt* gene is the K76T substitution. The K76T related CQ resistance is reversed by the presence of verapamil (Martin *et al.*, 1987, Wellems *et al.*, 1990) and removal of this mutation abolishes the CQ resistance and its verapamil reversibility (Lakshmanan *et al.*, 2005).

In comparison to the chloroquine sensitive (CQS) strains, the chloroquine resistant (CQR) strains of *P. falciparum* accumulate much less chloroquine (Bray *et al.*, 1998, Cooper *et al.*, 2007), keeping the intracellular concentration of CQ below toxic level. The reduced CQ accumulation has been genetically linked to *pfcrt* (Fidock *et al.*, 2000, Lakshmanan *et al.*, 2005, Sidhu *et al.*, 2002) and explained by a verapamil sensitive CQ efflux system (Wellems *et al.*, 1990, Martin *et al.*, 1987). In the case of QN, reduced accumulation of QN does not always correlate to increased QN resistance (Sanchez *et al.*, 2008b), however, all strains having K76T mutated *pfcrt* show increased verapamil-sensitive QN efflux (Sanchez *et al.*, 2008b).

In addition to *pfcrt*, there is another gene often associated with quinine resistance, that is *pfmdr1* (*Plasmodium falciparum* multi drug resistance 1)*,* which is located in chromosome 5. The *pfmdr1* gene encodes for a P-glycoprotein (P-gp) transporter called PfMDR1 or also known as Pgh-1, which is expressed during the intraerythrocytic stage. PfMDR1 consists of two homologous halves, each conataining six transmembrane domains (TMDs) (Figure 1.6.) (Peel, 2001). In bacteria and tumour cells, P-gp is often associated with verapamil-reversible multiple drug resistance (Valderramos & Fidock, 2006), since the protein is capable of extruding a wide range of structurally and functionally unrelated cytotoxic agents (Borges-Walmsley *et al.*, 2003). P-gp transporters belong to ABC (ATP Binding Cassette) transporter superfamily.

PfMDR1 is localised mainly in the food vacuolar membrane (FVM) (Cowman *et al.*, 1991), with its ATP binding site facing the cytoplasm (Karcz *et al.*, 1993). The protein is expressed at approximately equal levels in CQ resistant and sensitive isolates suggesting that over expression of PfMDR1 is not essential for CQ resistance (Cowman *et al.*, 1991). However, mutation of *pfmdr1* at amino acids 86, 184, 1034,

1042 and 1246 contribute to *in vitro* resistance to QN, mefloquine, chloroquine and artemisinin resistance (Sidhu *et al.*, 2005, Reed *et al.*, 2000), especially N1042D substitution that seems to play an important role in QN resistance (Sidhu *et al.*, 2005). Decreasing the copy number increases susceptibility to QN (Sidhu *et al.*, 2006) and *vice versa* (Cowman *et al.*, 1994), suggesting the involvement of the gene in QN resistance.

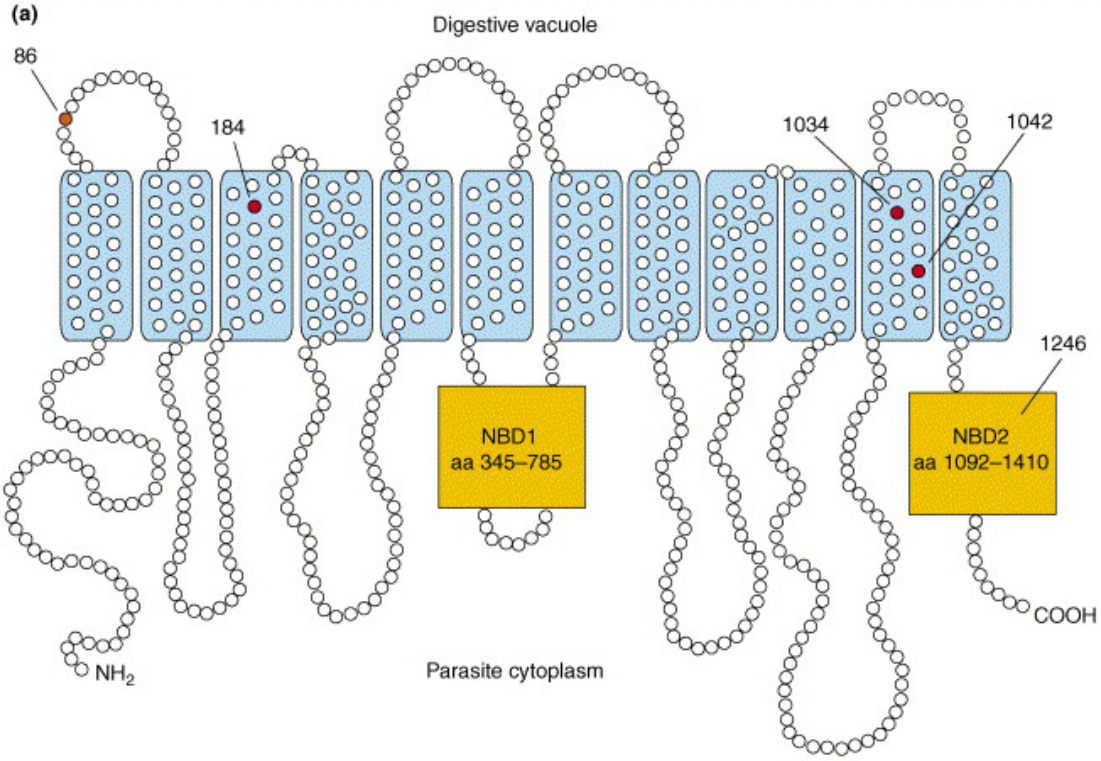

(b)

pfmdr1 variants identified in *Plasmodium falciparum* field isolates and laboratory-adapted lines

		PfMDR1 position and amino acid					Copy number
Region	Reference line (origin)	86	184	1034	1042	1246	
All	Wild type (3D7, Netherlands)	N	Y	S	N	D	1
Asia and Africa	FCB (Southeast Asia)	N	Y	S	N	D	≥2
	K1 (Thailand)	Y	Y	S	N	D	1
South America	7G8 (Brazil)	N	F	C	D	Y	1

Gray shading indicates residues that differ from the wild-type allele.

TRENDS in Pharmacological Sciences

Figure 1.6. Predicted structure of PfMDR1 (Valderramos & Fidock, 2006).

(a) PfMDR1 has two homologous halves, each with six predicted transmembrane domains and a nucleotide-binding pocket (Peel, 2001). The nucleotide-binding domains (NBD1 and NBD2; orange boxes) are each formed by large cytoplasmic domains. **(b)** Representative haplotypes, including the one most commonly associated with amplification of *pfmdr1* copy number.

On the contrary to the afore mentioned findings, QTL analysis of QN IC_{90} performed by Ferdig *et al.* (Ferdig *et al.*, 2004) showed no direct correlation between QN IC_{90}

and *pfmdr1*, neither in the primary, nor in the secondary scan. In addition, a recent finding also shows that *pfmdr1* polymorphism does not contribute to net QN accumulation (Sanchez *et al.*, 2008b).

Another group shows linkage between *pfmdr1* and the FV staining pattern of Fluo-4, a fluorescein acetoxymethyester (AM) derivative that have been used widely in imaging and in surrogate assay of P-gp function (Rohrbach *et al.*, 2006). In the same publication, it is also shown that several antimalarial drugs, including QN, can compete the Fluo-4 accumulation in the FV in chloroquine resistant strains but not in chloroquine sensistive strains (Rohrbach *et al.*, 2006).

1.3. Quantitative Trait Loci (QTL) Analysis

A complex, or quantitatively inherited trait, or a quantitative trait is a trait determined by numerous genes and might have complicated relationship with the environment (Wu *et al.*, 2007). Each gene involved gives a little but additive contribution to a trait and in most cases the genes effects are also influenced by the environment. Classical examples of such traits are human height variation, which is affected by health and diet as well as genetic potential.

The 'molecular dissection' of quantitative traits had been discussed even before the demonstration of DNA as the hereditary factor, due to the observation that many traits showed 'blending inheritance' accounted from combination of several Mendelian factors and environmental modifying effects (Paterson, 1995). Even in early 20^{th} century, association between a discrete trait or a marker with a continuously variable character was already noted (Sen & Churchill, 2001, Paterson, 1995).

The principle of QTL mapping is pretty simple; traits co-segregate with chromosomal regions carrying alternative alleles that influence the phenotype (Sen & Ferdig, 2004). Though not necessarily genes themselves, QTL are stretches of DNA closely linked to the genes underlying the respective trait. However, until the last decade the mapping principle has not been employed very extensively since most of genetic maps contained too few genetic markers to allow precise mapping of quantitative trait loci (QTL) to specific chromosomal locations (Paterson, 1995). Genetic markers are DNA sequence polymorphisms located at a specific location in the genome that show Mendelian inheritance (Wu *et al.*, 2007). The first genetic marker used for genomic mapping and population studies was the restriction fragment length polymorphisms (RFLP) (Wu *et al.*, 2007).

Genetic linkage occurs when particular genetic loci or alleles for genes are inherited jointly. Genetic loci on the same chromosome are physically connected and tend to stay together during meiosis, and are thus genetically linked. Because there are crossing overs of DNA when the chromosomes segregate, alleles on the same chromosome can be separated and go to different daughter cells.

QTL are mapped by linkage disequilibrium with molecular markers that do exhibit Mendelian segregation (Mackay, 2001). If a QTL is genetically linked to a marker locus, they will tend to be inherited together, that the frequency of the marker and the QTL inherited together in the offspring will be higher. The higher the percentage of descendants that does not show both traits, the further apart on the chromosome they are.

The distance between markers is expressed in centi Morgan (cM). When the distance between two loci, or two markers, or a locus and a marker, is 1 cM, then the recombination frequency (θ) between them is 1%, which means that in every 100 meiosis events, one recombination occurs between the two loci (or two markers, or between the marker and the locus). When two loci are not linked, or segregate independently, the θ value will be 50%. This is a consequence of independent assortment as described in the Mendel's second law (Wu *et al.*, 2007). Thus, linked genes have θ value less than 50% or are separated by a distance less than 50 cM.

Linkage between Mendelian traits (or between a trait and a marker, or two markers) is usually expressed as a LOD (Logarithm of Odds) score. The LOD score is the log base ten of the likelihood ratio comparing the likelihood of observing the phenotype when the two loci are linked and the likelihood of observing the phenotype when the two loci are not linked (Sen & Ferdig, 2004).

1.3.1. QTL Mapping of *P. falciparum*

The availability of *P. falciparum* Dd2xHB3 (Wellems *et al.*, 1990) genetic cross of through the Malaria Research and Reference Reagent Resource Center (MR4), and the segregation map of all progeny through the NCBI (http://www.ncbi.nlm.nih.gov/Malaria/Mapsmarkers/PfSegData/segdata.html) (Su *et al.*, 1999, Su *et al.*, 1997, Walker-Jonah *et al.*, 1992) provides tools for QTL analysis of the parasite. Since HB3 is a CQS strain with wild type *pfcrt* gene, whereas Dd2 is a CQR strain having mutated *pfcrt* gene, the availability of the progeny set allows closer analysis in the factors playing roles in drug, especially quinolines, accumulation, mechanism and resistance.

The presence of only small number of progeny (35 were published, but only 34 were available during this project), however, affects the sensitivity of the QTL analysis, allowing only for detection of small number of loci with large effects. Bringing down the threshold level, of course, will allow detection of more loci, but it will also compromise the stringency of the analysis (Sen & Ferdig, 2004).

Despite these drawbacks, there are advantages of the system, including the availability of completely sequenced genome (3D7 strain), small genome size (24 Mb; 1 gene/5kb) consisting of 14 nuclear chromosomes, and a fully genotyped, mapping population with corresponding MS linkage map demonstrating high, uniform recombination at an average resolution of one cross-over every 45 kb and one mapped marker approximately every 25 kb (Sen & Ferdig, 2004).

1.3.1.1. *P. falciparum* Genetics System

In almost all of its life, *P. falciparum* genome is haploid. Only within the mosquito midgut, when mature male and female gametes emerge from infected erythrocytes and fuse to form a zygote, commences the brief diploid phase of the parasite. Within three hours after fertilisation, meiosis occurs and the parasite develops into an ookinete that crosses the midgut wall and grows into oocyst. During the oocyst stage, mitotic division occurs, producing thousands of sporozoites that break out and travel by the haemolyph to the mosquito salivary gland. Together with the mosquito's saliva, the sporozoites are injected to the human bloodstream.

Due to its haploid genome, for mapping purpose, *P. falciparum* malaria cross can be treated like the backcross of two inbred line diploid organisms. As illustrated in Figure 1.7., in diploid organisms such as mouse, when two homozygous parental strains are crossed, identical F1 progeny will be produced. Due to crossing over events, the loci originating from the other parent (black bars) segregate when this F1 progeny is backcrossed to one of the parental strains (white bars).

In the parasite, diploid zygote produced by fertilisation grows into an ookinete, which then undergoes meiosis. Due to crossing over during meiosis, haploid recombinant oocysts, which eventually grow into sporozoites that infect humans, are produced. Thus, unlike diploid organisms that have to undergo two sexual generations before the segregating alleles can be observed, haploid parasites yields unique haploid recombinant in a single sexual generation.

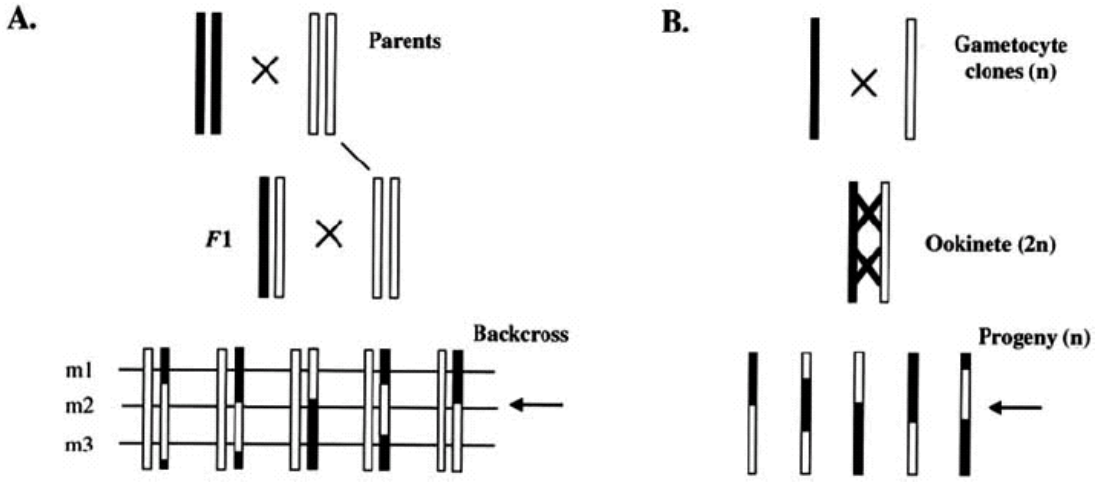

Figure 1.7. Genetic crossing schemes for generating mapping populations (Sen & Ferdig, 2004).
Unlike diploid organisms that have to undergo two sexual generations before the segregating alleles can be observed (**A**), haploid parasites yields unique haploid recombinant in a single sexual generation (**B**). In a mouse (**A**); parental strains (black and white bars) are crossed to produce genetically identical F_1 progeny which are crossed to one of the parental strains. Because of crossovers leading to the formation of the maternal gametes (black bars) the maternal alleles from the F_1 are segregating. Each scheme generates a mapping populations (arrows) with two genotype classes that segregate 1:1 at each marker (m1-m3).

1.3.1.2. More Than One Gene Involved in Quinoline Drug Responses

Reports of steady gradual decrease of antimalarial drugs sensitivity from all over the world suggest that the mechanism of quinoline resistance involves more than one factor affecting the sensitivity trait (van Vugt *et al.*, 1998, White *et al.*, 1999, Pukrittayakamee *et al.*, 1994). In addition, field studies also show that there are cross resistances between drugs in certain areas (Bloland, 2001) suggesting that the character shares molecular determinants (Sen & Ferdig, 2004).

The evidences from the laboratories also seem to support the clinical data. The hallmark of a quantitative trait is its continuous distribution in the population. Sen and Ferdig show in their publication that the distribution of CQ IC_{90} values of Dd2, HB3 and the F1 progeny of Dd2xHB3 cross illustrates the classical single gene Mendelian inheritance, with its typical bimodal distribution in the population (Sen & Ferdig, 2004), although obviously there are variations within CQS and CQR strains. The QN IC_{90}, on the other hand shows typical continuous distribution as observed in quantitative trait (Figure 1.8.).

In another publication, Ferdig *et al.* show by QTL analysis that CQ and QN share at least one determinant, *pfcrt* (Ferdig *et al.*, 2004). Resistance within this gene is known to alter susceptibility to CQ and QN (Cooper *et al.*, 2007, Lakshmanan *et al.*,

2005, Johnson *et al.*, 2004) and altered responsiveness to other antimalarial drugs (Johnson *et al.*, 2004). In addition to *pfcrt* as the common determinant, Ferdig *et al.* also suggested the involvement of other factors in chromosome 6, 9 and 13 in the QN resistance (Ferdig *et al.*, 2004).

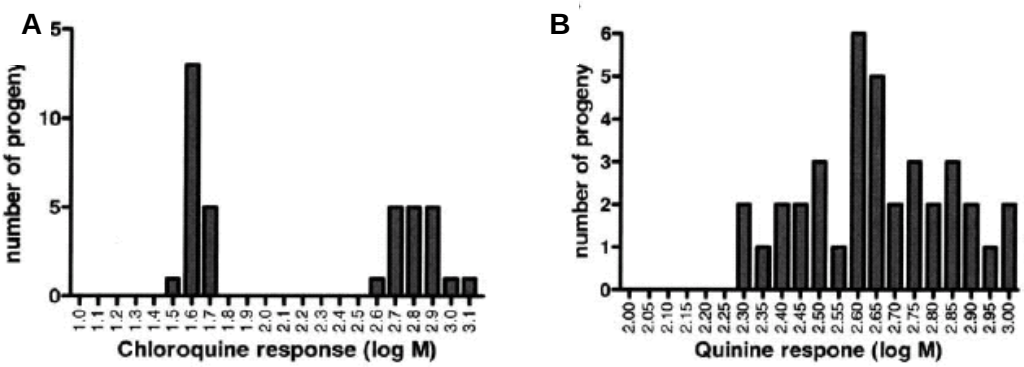

Figure 1.8. Drug response distributions in the HB3xDd2 cross (Sen & Ferdig, 2004).
Frequency histograms showing the number of clones (y-axis) and the quantitative dose responses (y-axis) to chloroquine (**A**) and quinine (**B**). The bimodal shape for CQ indicates a major gene is controlling the trait; the unimodal distribution for QN is typical of a quantitative, multi-gene trait.

1.3.2. Mapping of Quantitative Trait Loci (QTL) By Linear Regression Method

Several methods for QTL mapping have been described in the literature. Amongst them is the linear regression method (Haley & Knott, 1992), which was applied in this project. This method uses regression analysis, analysis of regression variance *(F-test)* and *t-test* of multiple markers. These statistical tests are performed solely on a single DNA information. Thus, basically in this test, linkage between a single DNA information and a phenotypic trait is analysed (Wu *et al.*, 2007). Calculation is performed based on phenotypic means and variances within each marker. Therefore, a complete genetic map is actually not essential for the analysis, though, as performed in this project, marker analysis can be extended to include all markers in the genome (Wu *et al.*, 2007).

In this project, QTL analysis was performed using progeny from Dd2xHB3 cross (Wellems *et al.*, 1990, Kirkman *et al.*, 1996), of which the markers are already published previously (Walker-Jonah *et al.*, 1992, Su *et al.*, 1999, Su *et al.*, 1997). Correlation between each marker to the QN accumulation or IC_{90} values of the 36 (34 progeny and 2 parental) strains was analysed.

When a phenotypic value *y* of an individual *i*, is affected by a locus *z*, then the relationship between the phenotypic character to a locus can be expressed in linear regression model as follows:

$$y_i = \mu + z_i \alpha + e_i,$$

where μ is the overall mean, α is the correlation coefficient, which determines the genetic effect of the locus to the phenotype and e_i is the random error (Wu *et al.*, 2007), which in this project was assumed to be 0. Applying this model, to the Dd2xHB3 cross segregation data, z_i was defined as:

z_i = 1 if *pfcrt* gene is inherited from Dd2

z_i = 0 if *pfcrt* gene is inherited from HB3

The correlation coefficient of a locus or α is then determined by Pearson regression (r) of the 0's and 1's of the locus against the phenotype of all strains, which is the measured values of uptake or IC_{90}, to yield the correlation coefficient for that locus.

If a QTL is linked to a marker, there will be a difference in the mean values of the quantitative trait amongst individuals having different alleles at the marker (Mackay, 2001). In this project, the significance of the locus genetic effect was tested by calculating, with the appropriate degrees of freedom, the regression variance (*F*) ratio, and hence the corresponding *p* value. The position giving the best fit gives the most likely position of a QTL and the best estimates of its effect (Haley & Knott, 1992).

The difference in trait phenotype between individuals having different alleles at a marker is larger, when the QTL is closer to the marker locus, and reaching maximum when the marker locus coincides exactly with the QTL (Mackay, 2001). To determine the most likely position of the QTL, a modification of likelihood ratio test as described previously by Lander and Botstein (Lander & Botstein, 1989) can be used to give the LOD score value. In this project, the likelihood ratio of a locus was calculated as the logarithm of the ratio between the *p* value of the corresponding locus with the mean of the *p* values of the entire markers used.

$$LOD\ score = -log_{10}(p_z/p_{ave}),$$

where p_z is the *p* value of locus *z* and p_{ave} is the mean of *p* values of the entire markers. The p_z value of 100 times less than p_{ave} was taken as being significant.

1.4. Aim of the Study

Parasites with reduced sensitivity to QN is an emerging problem for the world health authorities, since QN is up to now still the main medication used for the treatment of severe and complicated malaria (World Health Organisation, 2008). Although no real

QN resistant strains have been discovered so far, decreased QN dose responsiveness in *P. falciparum* infection in South East Asia, South America and Africa (Bloland, 2001, Pukrittayakamee *et al.*, 1994, Segurado *et al.*, 1997, Jelinek *et al.*, 1995) and discovery of field isolates with increased QN IC_{90} (Mayxay *et al.*, 2007) have been reported.

Many studies have been carried out to find genes involved in QN accumulation and resistance, although a recent publication shows that reduced accumulation of QN does not always correlate to increased QN resistance (Sanchez *et al.*, 2008b). Ferdig *et al.* had identified some loci contributing to quinine response variation using QTL analysis of QN IC_{90} data of the Dd2xHB3 cross progeny set (Ferdig *et al.*, 2004). These loci include *pfcrt*, which is located in chromosome 7, a loci in chromosome 5, which was thought to be linked to *pfmdr1*, and also a loci in chromosme 13, which was thought to be related to *pfnhe* (Ferdig *et al.*, 2004).

Although IC_{90} assay has been widely used to study drug response in *Plasmodium*, it is a measure of cell proliferation inhibition after 72 hours exposure to a drug. Thus, it may not only be affected by drug transport, but also other factors such as drug affinity to its target. Most cells, however, accumulate drugs within minutes of exposure to the drugs, thus, affected only by the transport mechanisms. Therefore, it was hypothesised that measuring the initial QN accumulation will lead to obtaining a readout defined by processes contributing to early quinine accumulation, whilst eliminating the effect of other processes causing cell death, such as inhibition of enzyme function. Thus, factors specifically affecting the transport of QN can be determined, hence complementing what have been found previously by Ferdig *et al.* (Ferdig *et al.*, 2004).

After several positive loci were located through the QTL analysis, mathematical analysis was also performed to investigate the interactions between some of these loci. In addition, bionformatics analysis was also carried out to find candidate genes lying within the positive loci.

2. Materials and Methods

2.1. Materials

2.1.1. Equipments

Analytical scales	Sartorius, Göttingen
Autoclave	Tuttnauer Systec 2540, Wettenberg
Camera, DC 120 Zoom digital	Kodak, New York
Centrifuges	
Biofuge fresco	Heraeus Instruments, Hanau
Biofuge pico	Heraeus Instruments, Hanau
J2-MC	Beckman, Krefeld
L-60 Ultracentrifuge	Beckman, Krefeld
Megafuge 1.0R	Heraeus Instruments, Hanau
Megafuge 2.0R	Heraeus Instruments, Hanau
RC5BPlus	Sorvall, Langenselbold
Computer-software	
Adobe Photoshop® 5.0	Adobe Systems Inc, USA
EndNote 8.0.2	ISI Research Soft, CA, USA
Internet Explorer	Microsoft Communication Corp., CA USA
MS Powerpoint	Microsoft Corporation, CA USA
MS Word 98	Microsoft Corporation, CA USA
SigmaPlot 9.01	Systat Software Inc.
DNA- electrophoresis apparatus	Biorad, München
Freezer -80ºC, UF85-300S	Heraeus GmbH, Hanau
Freezers -20ºC	Liebherr, Biberach
Fridges	Liebherr, Biberach
Gas burner gasprofi 1 micro	WLD-TEC
Ice machine AF 30	Scotsman, Milano, Italy
Incubator (P. falciparum)	Heraeus Instruments
Liquid nitrogen tank	Air Liquide, Ludwigshafen
TRI-CARB 2100 TR liquid scintillation counter	Packard
VarioMACS, MACS system	Miltenyi Biotec, Bergisch Gladbach
Magnetic stirrer	Heidolph, Schwabach

Microscopes:	
Light optical microscope Axiolab	Zeiss, Jena
Leica DMIL Light Microscope	Leica
Microwave oven	AEG, Nürnberg
Multipipette	Eppendorf, Germany
PCR-machines:	
T gradient Thermocycler	Biometra, Göttingen
GeneAmp PCR system 9700	AppliedBiosystems, CA USA
pH-meter pH 537	WTW, Weilheim
Pipetman Gilson P10; P20; P200; P1000	Abimed, Langenfeld
Pipetus- akku	Hirschmann Labortechnik, Eberstadt
pipetus® standard	Hirschmann Labortechnik, Eberstadt
Power supply: Power Pac 300	Biorad, München
Printer hp LaserJet 1300	Hewlett Packard, Heidelberg
Rotor JA20.1	Beckman instruments, Inc., Palo Alto, CA, USA
Spectrophotometer UVIKON 923	Kontron Instruments,
Sterile work bench Herasafe	Heraeus Instruments, Hanau
Stop watch	Roth, Karlsruhe
Thoma Counting Chamber	Marienfeld, Germany
UV-table UV-Transilluminator	Gibco BRL, Karlsruhe
Vortex Genie 2	Roth, Karlsruhe
Waterbath Julabo 7A	Julabo Labortechnik, Seelbach

2.1.2. Disposables

Aluminium foil	Roth, Karlsruhe
Centrifuge tubes, Polypropylen-18/95	Greiner Bio-one, Frickenhausen
Clingfilm Saran	Dow Chemical Company, Schwalbach
Coverslips for haemocytometer	Roth, Karlsruhe
Cryovials	Nalgene®, Wiesbaden
Cuvettes	Saarstedt, Nümbrecht, Germany
Eppendorf tubes	Saarstedt, Nümbrecht, Germany
Falcon tubes (15 ml; 50 ml)	Corning incorporation, Bodenheim

Gloves	Hartmann, Heidenheim
Immersion oil	Zeiss, Jena
Kimwipes lite 200	Kimberly Clark
MACS-columns CS	Miltenyi Biotec, Bergisch Gladbach
Object slides	Marienfeld, Lauda-Königshofen
Multipipette tips	
Eppendorf Combitips 1.25 ml	Eppendorf, Germany
Eppendorf Combitips 5 ml	Eppendorf, Germany
Parafilm	American International CanTM, USA
PCR softtubes 0.25 ml	Biozym Scientific, GmbH.
Petri dishes (10 ml diameter)	Greiner Bio-one, Frickenhausen
Petri dishes (25 ml diameter)	Greiner Bio-one, Frickenhausen
Pipette tips	Corning Inc., Bodenheim
Plastic pipettes (1 ml; 2 ml; 5 ml; 10 ml; 25 ml)	Corning Inc., Bodenheim
Radioactive Vials	
Mini PolyQ vials 6ml	Beckman Instruments Inc., USA
Saarstedt scintillation vials 20 ml	Saarstedt, Nümbrecht, Germany
Sterile filters (0,2 µm)	Millipore GmbH, Ashburn
Sterile filtration devices	Corning incorporation, Bodenheim
Thermo well PCR tubes	Corning incorporation, Bodenheim

2.1.3. Chemicals

2.1.3.1. Non Radioactive Chemicals

The non radioactive chemicals used in this study are from the firms Roth, Merck, Sigma, Serva and Applichem and were ordered directly or through the chemical facility of the University of Heidelberg medical faculty.

2.1.3.2. Radioactive Chemicals

The [^{3}H]-chloroquine and [^{3}H]-quinine (20.0 Ci mmol-1) used for this project were purchased from American Radiolabeled Chemicals.

2.1.4. Biological Materials

2.1.4.1. Parasite Strains

All parasite strains used in this study were received from the Malaria Research and Reference Reagent Resource Center (MR4), USA.

Dd2	chloroquine resistant (CQR) parental strain
HB3	chloroquine sensitive (CQS) parental strain
B1SD	progeny of Dd2 and HB3 cross
QC13	progeny of Dd2 and HB3 cross
QC01	progeny of Dd2 and HB3 cross
B4R3	progeny of Dd2 and HB3 cross
SC05	progeny of Dd2 and HB3 cross
TC08	progeny of Dd2 and HB3 cross
GC03	progeny of Dd2 and HB3 cross
3BA6	progeny of Dd2 and HB3 cross
1BB5	progeny of Dd2 and HB3 cross
3BD5	progeny of Dd2 and HB3 cross
SC01	progeny of Dd2 and HB3 cross
QC34	progeny of Dd2 and HB3 cross
QC23	progeny of Dd2 and HB3 cross
TC05	progeny of Dd2 and HB3 cross
GC06	progeny of Dd2 and HB3 cross
D43	progeny of Dd2 and HB3 cross
C188	progeny of Dd2 and HB3 cross
C408	progeny of Dd2 and HB3 cross
CH3-116	progeny of Dd2 and HB3 cross
CH3-61	progeny of Dd2 and HB3 cross
7C3	progeny of Dd2 and HB3 cross
7C7	progeny of Dd2 and HB3 cross
7C12	progeny of Dd2 and HB3 cross
7C16	progeny of Dd2 and HB3 cross
7C20	progeny of Dd2 and HB3 cross
7C46	progeny of Dd2 and HB3 cross
7C111	progeny of Dd2 and HB3 cross
7C126	progeny of Dd2 and HB3 cross

7C140	progeny of Dd2 and HB3 cross
7C159	progeny of Dd2 and HB3 cross
7C170	progeny of Dd2 and HB3 cross
7C183	progeny of Dd2 and HB3 cross
7C421	progeny of Dd2 and HB3 cross
7C424	progeny of Dd2 and HB3 cross

2.1.4.2. Enzymes and DNA Markers

ApoI Restriction enzyme	New England BioLabs, Schwalbach
EuroTaq DNA-polymerase	BioCat, Heidelberg
1 kb Plus DNA-ladder	GibcoBRL, Karlsruhe

2.1.4.3. Oligonucleotides

All primers were purchased from Thermo Electron GmbH (Ulm).

2.1.4.3.1. Fragment Length Polymorphisms

The primers used to determine fragment length polymorphisms were designed by Dr. J. Mu of NIH based on highly polymorphic microsattelite regions of *P.falciparum* genome. The microsattelites and primers sequences used to detect the polymorphisms were listed in Table 2.1.

Table 2.1. Microsattelites and primer sequences used to detect fragment length polymorphisms within the microsattelites.
The combinations of the fragment length polymorphisms were used to identify the progeny of Dd2xHB3 cross used in the project.

Microsattelites	Forward Primers	Reverse Primers
C1M4	5'-atatcctacaacggtaagca-3'	5'-ttctttttgaggagtaatgt-3'
C1M67	5'-acaggatttttgaagaaaaag-3'	5'-taggataaatgtagctttag-3'
C4M62	5'-gaattcacttaaatgtatttatttg-3'	5'-atgaagttatccattcgttt-3'
C13M13	5'-gttataagtatagcagacga-3'	5'-atacattacggtattttaaa-3'
C13M63	5'-agagatactatgattatttta-3'	5'-atattacaaagcttactacc-3'
C14M17	5'-acacaaagagaataggtata-3'	5'-tagtaattctagtttaccta-3'
B5M124	5'-taataagtgtaagaaatatgga-3'	5'-ataaaacagagcaaaataaag-3'
B5M5	5'-taaataatacaactactaatga-3'	5'-attgatccatatttatatctc-3'

2.1.4.3.2. Nested PCR of K76T PfCRT

Whenever the length polymorphisms were not sufficient for strain validation, nested PCR detection of K76T PfCRT (Djimde *et al.*, 2001) was employed. The primers used in the nested PCR reactions were listed in Table 2.2.

Table 2.2. Sequences of primers used in the nested PCR as described by Djimde and colleagues (Djimde *et al.*, 2001)

	Forward Primers	Reverse Primers
1st PCR	CRTP1: ccgttaataataaatacacgcag	CRTP2: cggatgttacaaaactatagttacc
2nd PCR	CRTD1: tgtgctcatgtgtttaaactt	CRTD2: caaaactatagttaccaattttg

2.1.5. Buffers, Media and Solutions

Cell culture medium	10% Human serum 0.2 µg/ml Gentamycin 0.1 mM Hypoxanthine in RPMI 25 mM HEPES L-Glutamine (Gibco)
Freezing Solution	28% Glycerol (v/v) 3% D-Sorbitol 0.65% NaCl in ddH2O filter sterilised, kept at 4ºC
Glucose solution for QN accumulation experiments	500 mM Glucose filter sterilised
MACS buffer	1x PBS 2 mM EDTA 0.5% BSA
Oil solution	Dibutylphtalate:Octylphtalate = 5:4
RPMI Media pH 7.4 at 4ºC and 37ºC for QN accumulation experiments	GIBCO Powder RPMI 1640 + L-Glutamine+ 25mM HEPES + $NaHCO_3$ pH to 7.4. at temperature 4ºC or 37ºC in 1000 ml H_2O filter sterilised

Sorbitol Solution	5% (w/v) D-sorbitol in ddH_2O filter sterilised
TAE	40 mM Tris-acetate 1 mM EDTA
TE Buffer	10 mM Tris/HCl pH 8.0 1 mM EDTA
Thawing solution I	12% NaCl, autoclaved
Thawing solution II	1.6% NaCl, autoclaved
Thawing solution III	0.9% NaCl / 0.2% glucose filter sterilised
TKM1 Solution	10 mM Tris pH 7.6 10 mM KCl 10 mM $MgCl_2$ 2 mM EDTA (pH 8.0)
TKM2 Solution	10 mM Tris pH 7.6 10 mM KCl 10 mM $MgCl_2$ 2 mM EDTA (pH 8.0) 0.4 M NaCl
Tissue solubiliser	50% (v/v) Tissue Solubiliser in Ethanol

2.2. Methods

2.2.1. Cell Culture

2.2.1.1. In Vitro Culture of Plasmodium falciparum

The erythrocytic stage of *P. falciparum* clones Dd2, HB3 and their 34 progeny (Ferdig *et al.*, 2004, Wellems *et al.*, 1990) were maintained in continuous blood culture as previously described (Trager & Jensen, 1976). The parasites were cultured in A^+ human erythrocytes of approximately 5% haematocrit in either 10 cm or 25 cm diameter petri dishes containing 15 ml or 35 ml HEPES buffered RPMI medium,

respectively, supplemented with 10% heat inactivated A^+ human serum, 200 µM hypoxanthine and 20 µg/ml gentamycin. The cultures were incubated in an atmosphere of 3% CO_2, 5 % O_2, 92 % N_2, and 95% humidity at 37°C. The medium was changed every other day and the parasitaemia was determined using Giemsa-stained blood smear. Whenever the parasitaemia reached 5-10%, the cultures were passaged to avoid parasites death due to lack of nutrient and accumulation of toxic metabolites in the medium.

2.2.1.2. Preparation of Human Serum and Erythrocytes

All erythrocytes and serum used in the project were received from the German Red Cross blood bank, Heidelberg. The human serum was aliquoted to 50 ml falcon tubes. 800 µl sterile 1 M $CaCl_2$ was added to each tube, and the tubes were incubated at 37ºC for 30 min and then at 4ºC overnight. The tubes were centrifuged (4000 rpm, 30min) on the following day to pellet the fibrin, and then incubated at 56ºC for 30 min to inactivate the serum. The serum was stored at -20ºC until needed. The concentrated erythrocytes were also aliquoted to 50 ml falcon tubes. To each tube 10 ml of RPMI medium was added, and the tubes were centrifuged (2300 rpm, 4 min, without break). The erythrocytes were then kept at 4ºC and used within 1-2 weeks.

2.2.1.3. Counting Erythrocyte with Thoma Counting Chamber

To determine the concentration of the enriched throphozoites cultures used in the QN accumulation experiments, a Thoma counting chamber was used. Before using the haemocytometer, the surfaces of the counting chamber and the coverslip had to be carefully cleaned with Kimwipes®. Then, a thin film of water vapour was formed on the surfaces by blowing wet air over them. The two surfaces were then pressed together to stick them, and then left to dry at room temperature. The culture used for counting had to be diluted enough not to allow the cells to be on top of one another that it might cause counting error. In addition, the cells had to be uniformly distributed. When the chamber was ready, the properly diluted sample of culture was introduced into it and the erythrocytes were counted using the 0.0025 mm^2 squares located in the middle of the counting grid. Counting was performed under microscope with 10x objective lens. Since there are two counting grids in the counting chamber,

the average of the counted number of erythrocytes in each grid was taken for calculation.

2.2.1.4. Calculating Erythrocyte Concentration

As mentioned above, the area of each tiny square in the counting grid is 0.0025 mm^2, whereas the depth of the chamber with the presence of a coverslip is 0.1 mm. So the volume of each square is $2.5x10^{-4}$ mm^3.

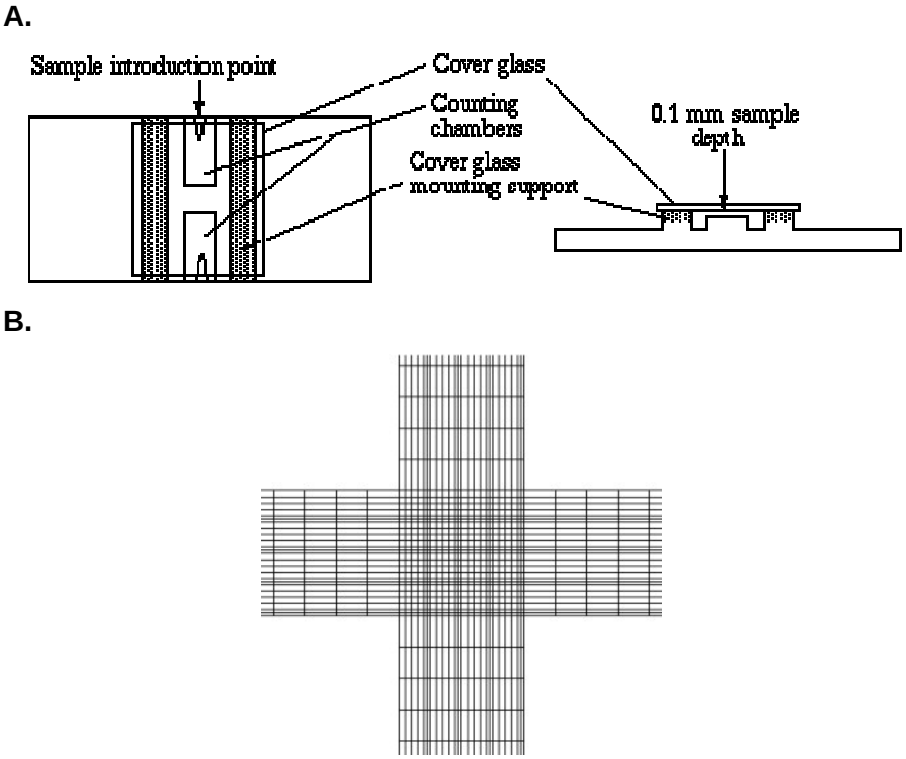

Figure 2.1. Thoma counting chamber (Rice University, 2007)
(A) Mounting a haemocytometer **(B)** The counting grid. The erythrocytes were counted using the 0.0025 mm^2 squares located in the middle of the counting grid.

In each Thoma counting chamber, there are two counting grids. Since there are 256 little squares in each counting grid, the number of erythrocytes per ml or mm^3 is determined as:

$$\frac{N \times 4000}{256}$$

where N is the average number of erythrocytes counted in each counting grid.

2.2.1.5. Preparing Giemsa-Stained Slide of *P. falciparum*

To determine culture's parasitaemia and parasite developmental stage, slide with thin film of blood culture was made by spreading 50 µl of culture evenly onto the surface of a clean microscope slide, air dried, fixed in 100% methanol for 30 sec, and then again air dried. Fixed cells were then stained for 5-10 min in a solution of 10% Giemsa, washed with water and allowed to dry.

2.2.1.6. Determining Parasitaemia

The parasitaemia is defined as the percentage of *P. falciparum* infected erythrocytes and is determined by examining Giemsa-stained blood slide under light microscopy with 100x objective using immersion oil. The numbers of infected and uninfected erythrocytes were counted in ten consecutive field, considering the multiple infection as a single parasite. The parasitaemia was then calculated with the formula:

(Number of parasites / Number of erythrocytes) X 100 = parasitaemia (%)

2.2.1.7. Freezing Parasites

Since the percentage of ring stage parasite will affect how fast the culture will revive after thawing, a culture containing at least 5% rings is normally used for freezing. First of all, most of the medium had to be removed from the plate. The culture was then centrifuged for 2 minutes at 1900 rpm and room temperature. The supernatant was then removed and the pellet was resuspended in equal volume of sterile freezing solution and mixed gently. Then, the 1 ml mixture was aliquoted into each of 2 ml cryotubes and snap frozen in ethanol/dry ice slurry for 15 minute before transferred to -80ºC freezer. For longer storage, the tubes were places in liquid nitrogen tank.

2.2.1.8. Thawing Parasites

After being removed from the liquid nitrogen, the cryotube containing parasites was warmed up for 2 min in a 37ºC water bath or in the palm of a hand to thaw the content. Then the content was transferred to a 15 ml falcon tube and 200 µl 12% NaCl per ml of blood was added to the tube at a rate of 2 drops per second, with constant, gentle mixing. Then, 9 ml 1.6% NaCl was added in the same way. The mixture was then centrifuged at 1900 rpm for 2 min, and the supernatant was decanted. Then, 7 ml 0.9% NaCl/0.2% glucose solution was added dropwisely to the pellet, whilst mixing it gently. Again the mixture was centrifuged at 1900 rpm for 2 min

and the supernatant was decanted. The pellet was then resuspended in complete 14 ml parasite medium and transferred to a small petri dish and 0.5 ml fresh blood was then added to the culture. The culture was then kept in parasite incubator for at least two days before the medium was changed to allow the newly thawed-parasite to revive. All solutions were pre-warmed to 37°C before starting the thawing procedure.

2.2.1.9. Synchronisation with Sorbitol

Sorbitol treatment causes osmotic lysis of late stage trophozoites (Lambros & Vanderberg, 1979) due to the presence of an induced transport pathway in the erythrocyte membrane that is permeable to sorbitol and absent in ring stage parasites. Whenever a synchronised throphozoite culture was required for an experiment, synchronisation was performed approximately 16-18 hours prior to the experiment. To start the synchronisation of 35 ml culture with 5% haematocrit, the medium was removed from the plate and the blood was resuspended in 10 ml pre-warmed, filter sterilised 5% D-Sorbitol solution and transferred to a 15 ml falcon tube. The tube was then incubated for 10 min at 37ºC before centrifuged for 2 min at 1900 rpm RT. The pellet was then washed with 10 ml complete medium before resuspended in 33 ml medium and returned to the plate.

2.2.1.10. Magnetic Cell Sorting (MACS) Purification

To obtain trophozoites culture with approximately 95-97% parasitaemia for QN accumulation experiment, 5% trophozoite infected-culture was passed through a magnetic column prior to being used for the experiment. This method makes use of the paramagnetic property of haemozoin in the parasite, in comparison to the dia-magnetic oxyhaemoglobin in red blood cell (Uhlemann *et al.*, 2000). During its intra-erythrocytic life cycle, *Plasmodium* parasite digests haemoglobin leaving haem, which is paramagnetic, as a by product. Haem is biomineralised into haemozoin in the food vacuole. Thus, when passed through magnetic column, trophozoites and schizonts stage infected erythrocytes were retained in the column, whereas uninfected and ring stage infected RBC passed unaffected. Prior to usage, the MACS column was fixed to the adapter and mounted to the magnetic field following the manufacturer's instruction. Then, the matrix was equilibrated with MACS buffer before the culture was applied. The stopcock at the bottom of the column had to be adjusted in such a way that it allowed slow steady flow of culture through the column.

Then, while still applying the magnetic field, the column was washed with approximately two column volumes of MACS buffer or until the effluent is colourless, to ensure washing out of non-paramagnetic cells. The trophozoites and schizonts stage infected RBC were obtained by eluting them with MACS buffer from the column while the magnetic field was released. The eluate was then centrifuged (1900 rpm for 2 min at room temperature) to harvest the cells and ready for the subsequent experiment.

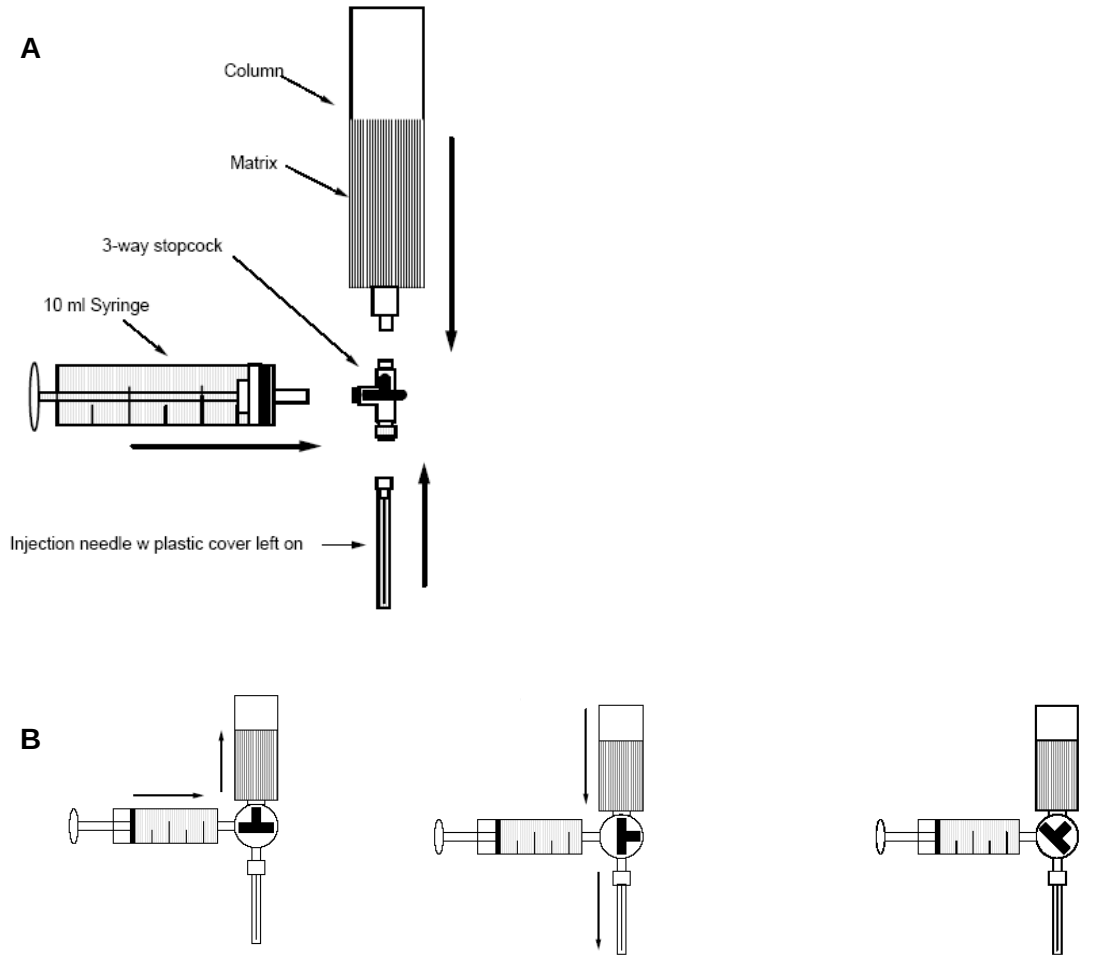

Figure 2.2. Magnetic Cell Sorting (MACS) Purification (Vogt, 2008)
(A) Assembly of MACS column **(B)** Three different positions of the stopcock: liquid flows from the syringe to the column (left), from the column to the needle (middle), and stop position (no flows of liquid) (right).

2.2.2. Strains Validations

2.2.2.1. Genomic DNA (gDNA) Isolation from *P. falciparum*

For the isolation of genomic DNA from *P. falciparum*, it was recommended to use a culture containing mature parasitic stages (trophozoites and schizonts), which would

give more DNA in comparison to ring stage parasites. The method described here was used to extract genomic DNA from 35 ml culture with 5% haematocrit.

2.2.2.1.1. Erythrocyte Lysis

Medium was removed by pipetting or centrifugation, then, the cells were resuspended with TKM1 solution to 30 ml. The suspension was then placed in 2x15 ml falcon tubes. 150 µl 10% Saponin was added to each of the tube. The mixtures were mixed by gently inverting the tubes repeatedly until erythrocyte lysis occured. Once lysis had occurred, tubes were placed for 5 min on ice. Then the tubes were centrifuged for 8 min at 3800 rpm 4ºC in a pre-cooled centrifuge. The supernatants were then decanted and pellets were redissolved in TKM1 (equal volume used as before). The tubes were then re-centrifuged as previously, then the supernatants were decanted and the pellets were kept in -20ºC until required.

2.2.2.1.2. gDNA Extraction

150 µl TKM1 was added to a frozen parasite pellet. The mixture was vortexed to ensure pellet was properly dissolved, then 2.4 ml TKM2 was added and the mixture was further vortexed before the addition of 150 µl 20% SDS. The mixture was again vortexed before incubated for 15 min at 56ºC. Transfer mixture to 12 ml centrifuge tube (Greiner Polypropylen-12/75 centrifuge tube), then 1.35 ml 4 M NaCl was added and suspension was mixed properly by inverting the tube repeatedly. Then, the tube was centrifuged (Beckman JA20.1 rotor) for 10 min at 4ºC 11500 rpm. The supernatant was transferred to a new tube and two volumes of 100% ethanol was added. The solution was mixed thoroughly by inverting the tube before the tube was kept overnight at -20ºC. On the following day, the tube was centrifuged (Beckman JA20.1 rotor) for 30 minute at 4ºC 11500 rpm to pellet the DNA. The supernatant was then decanted, whereas the pellet was washed with 500 µl 70% ethanol and centrifuged for 5 min. The DNA pellet was then dried and resuspended in water or TE buffer.

2.2.2.2. Detection of Fragment Length Polymorphisms

The genome of *P. falciparum* contains highly polymorphic regions that may be PCR amplified and used to identify the strains (Anderson *et al.*, 1999, Su *et al.*, 1999, Su & Wellems, 1996). In the progeny of Dd2xHB3 cross, these regions were inherited from either one of the parents and the polymorphism patterns were used for strains

validation. Eight different primer pairs (sequences provided by Dr. Mu, MR4) were used for the PCR amplifications. The annealing temperatures used in the PCR reactions differ from one primer pairs to the other. The amplicons were run either in 3% normal agarose gel or 2% MetaPhor® gel.

PCR of Microsatellites for Detection of Fragment Length Polymorphisms

25 µl PCR reaction

Euro-Taq buffer (10x)	2.5	µl
dNTPs (10 mM)	0.5	µl
Forward primer (50 µM)	0.5	µl
Reverse primer (50 µM)	0.5	µl
$MgCl_2$ (50 mM)	1.25	µl
Template gDNA	1	µl
Euro-Taq DNA-Polymerase	0.25	µl
H_2O	18.5	µl

Primers	**Anneling Temperature**	**PCR Reaction**		
C1M4	59ºC	95ºC	4’	
C1M67	55°C	95ºC	45“	
C4M62	59ºC	55°C or 59ºC	45“	
C13M13	55°C	68ºC	45“	**35x**
C13M63	55°C	68ºC	10’	
C14M17	55°C			
B5M124	55°C			
B5M5	55°C			

2.2.2.3. Nested PCR Detection of K76T PfCRT

Lysine substitution to threonine in PfCRT amino acid 76 is a common feature found in most chloroquine resistant (CQR) parasites. In the progeny of Dd2xHB3 cross, the substitution is inherited from the CQR parent, Dd2, whereas those progeny inheriting the *pfcrt* gene from the chloroquine sensitive (CQS) parent, HB3, retains the wild-type K76. Therefore, whenever the length polymorphisms not sufficient for strains validation nested PCR detection of K76T PfCRT was employed to identify the strains (Djimde *et al.*, 2001).

2.2.2.3.1. Nested PCR

The first pair of primers used in the reaction consists of the flanking primers CRTP1 and CRTP2, which amplify a 537 base pair region around the mutation K76T. The second reaction was performed with the internal primers flanking the K76T mutation, CRTD1 and CRTD2, producing a 145 base pair amplicon (Djimde *et al.*, 2001). The first reaction was performed for ten cycles, then the thermocycler was stopped and 0.5 µl PCR products was taken and transferred to second PCR mixture. The thermocycler was restarted and run for 35 cycles.

Nested PCR of K76T PfCRT

First PCR Mixture (25 µl)			**Second PCR Mixture (25 µl)**		
Euro-Taq buffer (10x)	2.5	µl	Euro-Taq buffer (10x)	2.5	µl
dNTPs (10 mM)	0.5	µl	dNTPs (10 mM)	0.5	µl
CRTP1 primer (50 µM)	0.5	µl	CRTD1 primer (50 µM)	0.5	µl
CRTP2 primer (50 µM)	0.5	µl	CRTD2 primer (50 µM)	0.5	µl
$MgCl_2$ (50 mM)	1.25	µl	$MgCl_2$ (50 mM)	1.25	µl
Template gDNA	1	µl	First PCR Amplicon	0.5	µl
DNA-Polymerase (1u/ µl)	0.25	µl	DNA-Polymerase (1u/ µl)	0.25	µl
H_2O	18.5	µl	H_2O	19	µl

PCR Reactions

First PCR Reaction			**Second PCR Reaction**		
94ºC	4’		95ºC	45“	
94ºC	45“		59°C	45“	
59°C	45“		68ºC	1’	**35x**
68ºC	1’	**10x**	68ºC	10’	

Thermocycler was stopped and 0.5 µl amplicon was transferred to the second PCR mixture

2.2.2.3.2. Restriction Digests

The nested PCR amplicon was digested with restriction enzyme ApoI. The enzyme digests only the sensitive type allele, resulting in a size reduction of 34 base pairs, but does not digest the resistant allele (Djimde *et al.*, 2001). The digest product was run on 2% agarose gel at 120 V for at least 30 minute before checking.

Digest Reaction

The second PCR amplicon	8	µl
NEB Buffer 3	1	µl
BSA (10x)	1	µl
ApoI Enzyme	0.5	µl

Incubation at 50ºC for 6 hours

2.2.2.4. Agarose Gel Electrophoreses

In this project analytical agarose gel electrophoresis was employed to for size determination of PCR fragments. Two types of gels were used, the 2 or 3% normal agarose and 2% Metaphor® gel electrophoreses. MetaPhor® is an analytical special agarose with intermediate melting temperature 75ºC with twice the resolution capabilities of the finest-sieving agarose product (Cambrex Bio Science Rockland, 2003). In this project, 2% Metaphor® agarose in TAE buffer was used to distinguish PCR products with very small size differences during strains validation. To make the electrophoresis gel, an appropriate quantity of agarose was added to TAE and the mixture was boiled until the agarose was completely dissolved. Ethidium bromide was added to a final concentration of 1 µg/ml. Ethidium bromide intercalates with the DNA allowing visualization by UV irradiation. DNA samples were mixed with loading buffer (1:5, v/v) and loaded on the gel. As a size marker, the 1 Kb Plus DNA Ladder™ was used. Electrophoresis was performed at a constant voltage of 120 V in TAE. The result was photographed using a DC120 Zoom Digital Camera (Kodak).

2.2.3. Measurement of Drugs Accumulation

Accumulations of CQ and QN were measured in throphozoites culture with very high parasitaemia (approximately 95-97%). To obtain the required concentration and parasitaemia, the culture had to undergo several treatments, starting with sorbitol synchronisation approximately 16-18 hours prior to experiment and followed by MACS column purification before the cells were eventually diluted to the right concentration. The amount of drug presents in the cell and medium was obtained by measuring the radioactivity of the labelled drugs used in the experiment. The method was already previously fully described (Sanchez *et al.*, 2003, Sanchez *et al.*, 2008b).

2.2.3.1. Preparation of Culture

MACS purified trophozoite-infected RBC was reconstituted in prewarmed RPMI 1640 (pH7.4 at 37°C) to a cell concentration of 25000-32000 cells/µl. The exact concentration was determined using a Thoma counting chamber. The parasite's trophozoite stage was confirmed with light microsopic examination of Giemsa-stained blood smears.

2.2.3.2. Accumulation Experiment

In the parental strains (Dd2 and HB3) QN accumulation was measured at full time course, that is, accumulation was measured periodically starting from 30 seconds after the drug was added until the accumulation reached stationary phase. In the progeny, a time point corresponding to the drug initial uptake state and another one corresponding to the steady state were selected and drug accumulation at these time points only were measured.

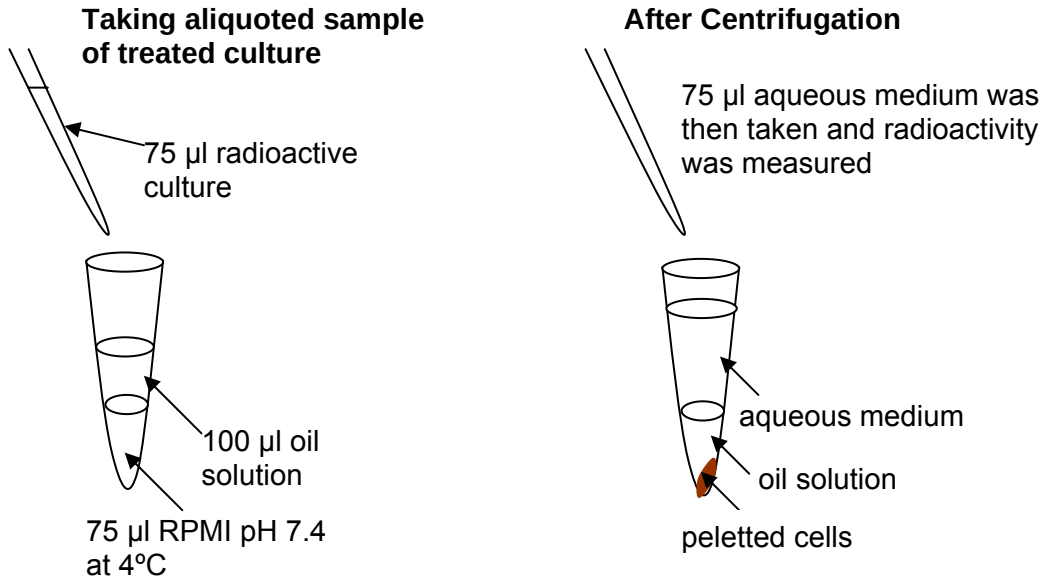

Figure 2.3. Accumulation Experiment
(A) 75 µl duplicated aliquot of radioactive culture were each placed in a prepared tube containing oil solution and cold RPMI medium. The tubes were then centrifuged (15000 g, 1 min) to separate the cells from the aqueous medium **(B)** After centrifugation cells were separated from the aqueous medium. The pelleted cells were isolated by cutting the tip of the tube.

Trophozoite culture (25000-32000 cells/µl, 95-97% parasitemia) in RPMI 1640 (pH7.4 at 37°C) was pre-incubated for 2 min at 37°C. [^{3}H]-drug was added to the pre-incubated culture to a concentration of 40 nM, and then the treated culture was

mixed and incubated in a waterbath set at 37ºC. 75 µl aliquot of the radioactive treated-culture was taken in duplicate at each corresponding time point after the addition of the drug. Each aliquot was diluted with equal volume of ice-cold RPMI 1640 (pH7.3 at 4°C). The ice-cold medium should stop any active transport of the drug. These aliquot-cold medium mixtures were immediately spun through a layer of oil solution containing 5:4 mixture of dibutyl phthalate and dioctyl phthalate (15000 g, 1 min) to separate the cells from the aqueous medium containing the unincorporated labelled drug, hence preventing further entry of the drug to the cells.

2.2.3.3. Estimation of Drug Level by Radioactivity Measurement

The cell pellets that had been separated from the medium was placed in a 1.5 ml Eppendorf tube and incubated with 66 µl of ethanol and 33 µl of tissue solubiliser overnight at 55°C. The lysate was then decolorised by the addition of 25 µl of 30% H_2O_2 and acidified by the addition of 25 mL of 1 N HCl. The lysate was transferred to a scintillation vial, and the radioactivity was measured. The amount of radioactivity in the known volume of aqueous medium was also measured. The intracellular drug concentration was calculated from the amount of labelled drug taken up by the cells and by assuming that the volume of a trophozoite-infected erythrocyte is 75 fL (Saliba *et al.*, 1998). Drug accumulation was then expressed as the ratio of the intracellular to the extracellular drug concentration ($drug_{in}/drug_{out}$) (Sanchez *et al.*, 2008b).

2.2.4. QTL Analysis

In this project, the QTL analysis was performed using an Excel sheet calculation designed by Prof. W. Stein from the Department of Biological Chemistry, Hebrew University of Jerussalem, Israel. The calculation was performed based on the simple regression method QTL analysis as described by Haley and Knott (Haley & Knott, 1992). A table provided as an Excel file at NCBI (National Center for Biotechnology Information) website (National Center for Biotechnology Information, 2000) provides a full listing of the parental (Dd2 or HB3) origin of each of the 900 microsatellite markers mapped by Su *et al.* (Su *et al.*, 1999), with their location in cMs along each chromosome.

Of these 900 microsatellite markers, only 818 of these markers were used on this project, removing 82 markers where the information was incomplete. The markers

were arranged as rows in the table. For each of the 36 strains, arranged in columns, the appropriate drug accumulation value was inserted. For the comparable analysis of the IC_{90} values, the QN IC_{90} values were taken from the publication of Ferdig *et al.* (Ferdig *et al.*, 2004). If, from the NCBI data, a marker for a particular strain was derived from the Dd2 strain, a 1 was entered into the table at the appropriate intersection, whereas if the origin was from the HB3 strain, a 0 was entered. This then gave a matrix of 818 x 36 numbers in 0 and 1. For each marker (each row), a Pearson regression of the 0's and 1's were performed against the measured accumulation or the IC_{90}, to yield the Pearson r for the marker. (The Pearson r for a marker is a measure of how well the pattern of 0 and 1 values across the strains, for that marker, predicted the measured values of accumulation or IC_{90}). The probability p was determined with the appropriate degrees of freedom. For the entire 818 markers, the p value was divided by the mean of p values. This ratio showed whether the p value was higher or lower than the mean. The logarithm of this ratio gave the LOD (logarithm of odd) score. Therefore, when a marker had a negative LOD score, its p value was lower than the mean, and *vice versa*. A p value of 100 times less than the mean ($p<0.01$) was taken as being the significance limit and a line at this level was drawn in all the LOD score figures, hence the peak positions of LOD scores, chromosome by chromosome, were readily determined.

The sign of the regression coefficients used to derive the LOD scores indicated whether or not an increase or a decrease in a measured quantity was being reported. When a marker had a negative Pearson r value, it had decreasing effect to the measured quantity, and *vice versa*.

The QTL primary scan was performed by regression analysis across all 36 strains, thus aiming to find factors affecting major variations between the strains. The QTL secondary scans were performed by regression analysis within either the 17 strains inheriting *pfcrt* locus from Dd2 (CQR strains) or the 19 strains inheriting the locus from HB3 (CQS strains), taking the appropriate degrees of freedom. The secondary scan should have pointed at factors affecting phenotypic variations within the groups.

2.2.5. Mathematical Analysis of Loci Interactions

The mean of QN accumulation and IC_{90} levels of strains were calculated at different combinations of loci. *P* values were calculated to determine whether there were significant differences between the means. Strains were analysed whether the significance in the difference of means is correlated to allelic difference in the analysed loci.

2.2.6. Bioinformatics Analysis

Bioinformatics analysis was performed on the chromosomal areas under the peaks to find candidate genes. After determining the peaks positions by QTL analysis, molecular markers located under peaks were identified by comparing the NCBI microsattelites marker map with the Sequence Tagged Site (STS) and gene maps as published in NCBI gene bank . Then, genes located within and directly adjacent to these markers were identified and selected using online databases PlasmoDB (PlasmoDB, 2008a) and NCBI gene bank (National Center for Biotechnology Information, 2008).

The selected genes were analysed further for their putative functions, the presence of polymorphisms in the parental strains, and the presence of transmembrane domains (TMD).

Some of the genes had their putative functions already annotated in PlasmoDB and NCBI gene bank. Whenever the functions of the genes were not accessible from PlasmoDB or NCBI gene bank, Basic BLAST (Basic Local Alignment Search Tool) search hosted by the Swiss Institute for Bioinformatics (EMBNet, 2008) was performed to predict the putative functions of the gene products by comparing the sequence to find similarity with other genes in the database.

Since the annotated genes in PlasmoDB and NCBI were all based on 3D7 genomic sequence, the selected genes had to be further analysed for the presence of polymorphisms between Dd2 and HB3 by BLAST search on Dd2 and HB3 sequence databases in Broad Institute MIT (BROAD, 2009).

Polymorphisms within transporters have long been associated with altered quinoline drug sensitivity (Sanchez *et al.*, 2008, Sidhu *et al.*, 2002, Fidock *et al.*, 2000, Lakshmanan *et al.*, 2005). Therefore, finding transporters is one of the targets in this analysis. For this purpose, analysis was performed to look for genes expressing protein with TMD, as the presence of TMD is a prerequisite of a membrane transporter (Busch & Saier, 2002). The prediction of TMD was performed based on hidden Markov model (Krogh *et al.*, 2001), using TMHMM (Transmembrane domain Hidden Markov Model) Server (CBS, 2007). The number of TMDs were double checked by comparing it to the annotated data in PlasmoDB, which were also determined the Hidden Markov Model (HMM) using a different software called HMMPfam (PlasmoDB, 2008b).

3. Results

3.1. Validation of Strains Used in the Accumulation Experiments

From the 35 progeny of the Dd2xHB3 cross performed by Wellems (Wellems *et al.*, 1990), 34 were used in this project. One of them, the C101, was not available from the MR4 during the time of the project, and therefore had to be excluded. Prior to being used for the accumulation experiment, these strains, the progeny as well as the parents, had to be genetically checked to validate. The validation was performed by comparing the fragment length polymorphisms of certain microsatellites and K76T mutation (Djimde *et al.*, 2001) patterns in these strains with the known segregation patterns as published at the NCBI home page (National Center for Biotechnology Information, 2000). The microsatellites and *pfcrt* segregation patterns can be seen in Table 3.1.

For the microsatellite fragment length polymorphisms, a selection of microsatellites and their primer sequences were kindly provided by Dr. J. Mu of the NIH, whereas the K76T mutation was detected by nested PCR as described previously by Djimde *et al.* (Djimde *et al.*, 2001). All strains used in this project had been tested and proven that the genetic components met the segregation pattern as described in Table 3.1., prior to being used in the drug accumulation experiments.

Table 3.1. Strains used in the project and their patterns of microsatellite polymorphisms and pfcrt inheritance

H: originated from HB3, D: originated from Dd2, CQR: Chloroquine Resistant, CQS: Chloroquine Sensitive, R: Resistant, S: Sensitive

Parental strains

Progeny

Markers	Dd2	HB3	B1SD	QC13	QC01	B4R3	SC05	TC08	GC03	3BA6	1BB5	3BD5	SC01	QC34	QC23	TC05	GC06	D43	C188
C1M4	D	H	D	D	D	H	H	H	D	H	D	D	H	D	D	H	D	D	H
C1M67	D	H	H	H	D	H	D	H	D	D	D	D	D	H	H	H	D	H	H
C4M62	D	H	D	D	H	H	H	H	D	H	D	D	D	D	H	D	D	D	D
C13M13	D	H	D	H	D	H	D	H	H	D	H	H	H	D	D	D	D	D	D
C13M63	D	H	D	H	D	H	H	H	H	D	H	H	H	D	D	D	D	D	D
C14M17	D	H	H	H	D	D	H	H	D	H	D	H	D	H	D	H	D	H	H
B5M124	D	H	D	D	D	H	H	H	H	D	H	H	H	H	D	H	H	H	D
B5M5	D	H	D	D	H	H	H	D	D	H	D	H	D	H	H	D	D	H	H
***pfcrt* origin**	D	H	H	H	H	H	H	H	H	D	D	D	D	D	D	D	D	D	H
CQR/CQS	R	S	S	S	S	S	S	S	S	R	R	R	R	R	R	R	R	R	S

Markers	C408	CH3-116	CH3-61	7C3	7C7	7C12	7C16	7C20	7C46	7C111	7C126	7C140	7C159	7C170	7C183	7C421	7C424
C1M4	**H**	**D**	**H**	**D**	**D**	**H**	**D**	**D**	**D**	**D**	**D**	**H**	**D**	**H**	**D**	**D**	**H**
C1M67	**D**	**H**	**D**	**D**	**H**	**D**	**H**	**H**	**H**	**D**	**H**	**H**	**D**	**H**	**H**	**H**	**H**
C4M62	**D**	**D**	**D**	**H**	**H**	**D**	**H**	**H**	**D**	**D**	**H**	**D**	**D**	**H**	**H**	**H**	**D**
C13M13	**D**	**D**	**D**	**D**	**D**	**D**	**H**	**H**	**H**	**H**	**H**	**D**	**D**	**D**	**H**	**H**	**H**
C13M63	**D**	**D**	**D**	**D**	**D**	**D**	**H**	**H**	**H**	**H**	**H**	**H**	**D**	**D**	**D**	**H**	**H**
C14M17	**H**	**D**	**D**	**H**	**D**	**D**	**H**	**D**	**D**	**H**	**H**	**D**	**D**	**D**	**D**	**D**	**H**
B5M124	**H**	**D**	**H**	**D**	**H**	**D**	**H**	**H**	**H**	**D**	**D**	**D**	**D**	**H**	**D**	**H**	**D**
B5M5	**D**	**D**	**D**	**H**	**H**	**D**	**D**	**H**	**H**	**D**	**D**	**H**	**D**	**H**	**H**	**H**	**D**
pfcrt origin	**D**	**H**	**H**	**H**	**H**	**D**	**H**	**H**	**D**	**D**	**H**	**H**	**H**	**H**	**D**	**D**	**D**
CQR/CQS	**R**	**S**	**S**	**S**	**S**	**R**	**S**	**S**	**R**	**R**	**S**	**S**	**S**	**S**	**R**	**R**	**R**

3.2. Quinine Accumulation

3.2.1. Determination of Initial Steady State Time Point from the Full Time Course Quinine Accumulation of Dd2 and HB3

At the beginning of the project, QN accumulation was measured periodically in Dd2 and HB3 to understand the pattern of full time course QN accumulation (Figure 3.1.). To ensure robustness of the assay at least five independent measurements were carried out for each time point, therefore each time point in this graph represents the mean of these measurements, and the error bar represents the standard error calculated from these multiple measurements. From this full time course graph, two time points were selected, one at the initial uptake state (at 5 min) and the other during the steady state (at 20 min). In the progeny, QN accumulation was only measured at these two time points, excluding other time points measured in the full time course.

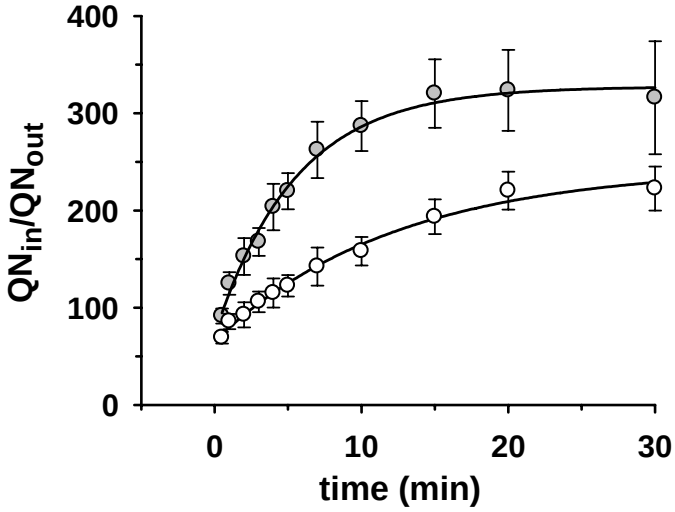

Figure 3.1. Full time course accumulation of quinine in Dd2 and HB3
(● HB3; ○ Dd2) Based on this full time course graph, a time point during the initial uptake stage was selected (5 min). QN accumulation in the progeny was measured only at this particular time point.

3.2.2. Quinine Initial Accumulation of Dd2, HB3 and their Progeny

The QN accumulation levels of Dd2, HB3 and the 34 progeny are represented in Figure 3.2. As in the parental strains, the accumulation levels in the progeny were

also determined from the mean of at least five measurements and each error bar represents the standard error of these measurements.

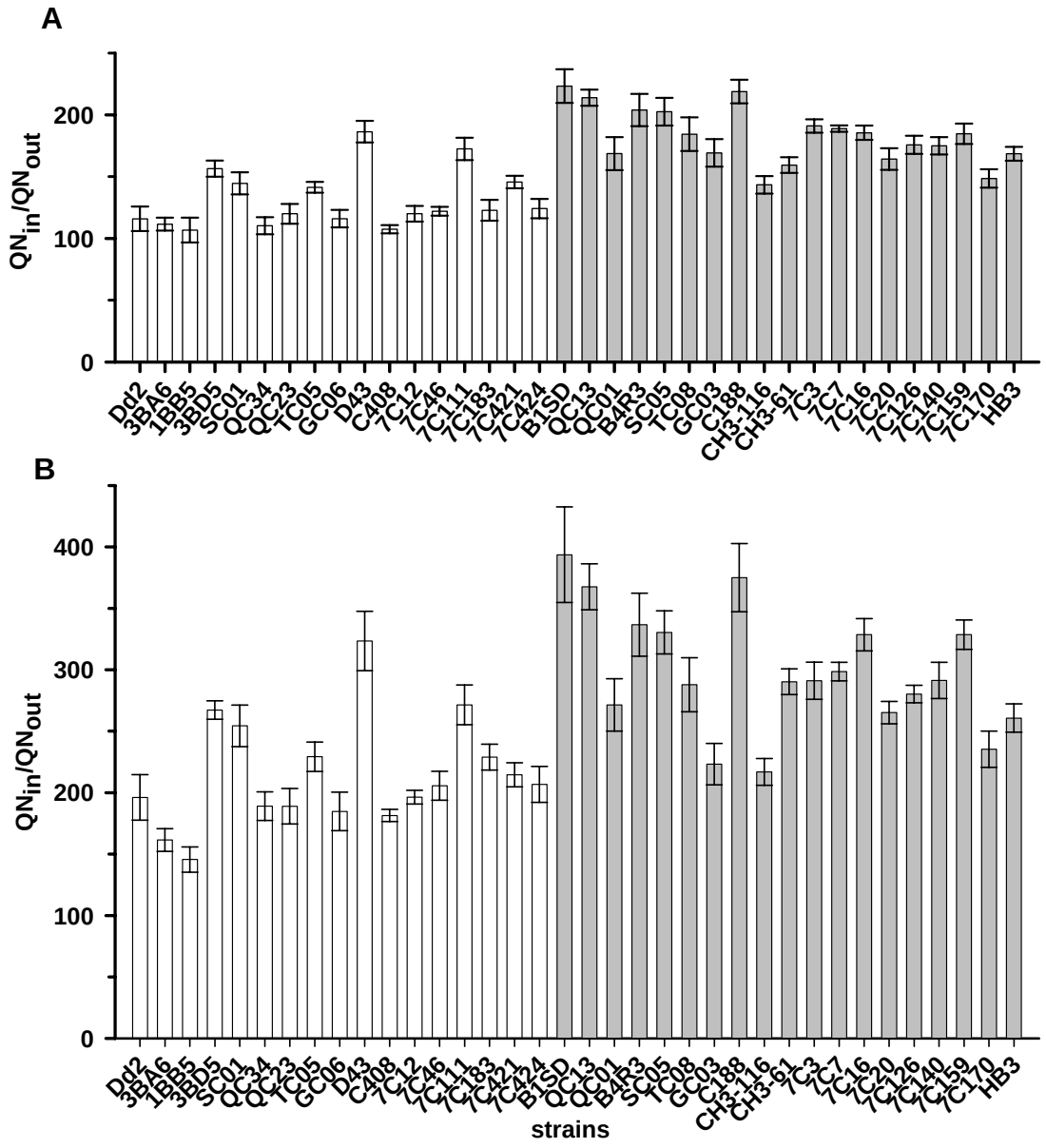

Figure 3.2. Quinine initial and steady state accumulation level of Dd2, HB3 and their progeny

QN accumulation levels **(A)** at 5 min and **(B)** at 20 min after treatment of the culture with radioactive QN. (▭ strains with *pfcrt* from HB3; □ strains with *pfcrt* from Dd2).

Although [^{3}H]-Quinine accumulation was measured at two different time points, only accumulation during the initial state was used later for QTL analysis. As indicated in the graph (Figure 3.2.), the measurements at the two different time points showed very similar patterns. The only difference between the two sets of data was the error bars, which were smaller in the early steady state, indicating that at initial state the measurements gave more consistent results than at the early steady state. This

might have been caused by saturation of the drug to the transport machinery of the parasites instead of reduction of cell viability, since Trypan Blue treatment and visualisation under light microscope showed no difference in the cells viability after 5 and 20 minutes treatment with QN (data not shown).

Figure 3.2. showed that the CQR parental strain (Dd2) accumulated a low amount of QN, whereas the CQS parental strain (HB3) accumulated higher amount of QN. Amongst the progeny, however, there are variations in the accumulation levels. Some progeny accumulated as much QN as the resistant parent (Dd2), whereas others accumulated QN to the level comparable to that of HB3. In addition to these two phenotypes, there are also progeny accumulating intermediate level of QN, such as TC05 and CH3-116, and those accumulating even higher level than the sensitive strains, such as B1SD and C188. This phenotypic pattern implies that more than one factor might be involved in QN accumulation.

3.2.3. Multifactorial Inheritance of Quinine Accumulation as Indicated by the Accumulation Pattern

The 17 columns on the left side of both parts of Figure 3.2. depicted QN accumulation in the strains having mutated *pfcrt* gene and showing CQR character, while the remaining 19 columns (on the right of each sub-figure) were data from the strains having wild-type *pfcrt* and showing sensitivity to CQ. Variation between strains having the same *pfcrt* gene further suggests that *pfcrt* is not a single factor affecting QN accumulation.

During this project, parallel to measuring the QN accumulation, CQ accumulation was also measured (in collaboration with Sybille Mayer) at early uptake state (4 min) in all strains (Mayer, 2009). This was intended to be a control, since it had been shown by QTL analysis that *pfcrt* was the single major determinant of CQ resistant (Ferdig *et al.*, 2004, Bray *et al.*, 2005) and that the CQR strains having mutated *pfcrt* accumulated less CQ than the CQS strains with wild-type *pfcrt* (Cooper *et al.*, 2007, Sidhu *et al.*, 2002). This pattern, where CQR strains with mutated *pfcrt* accumulated less CQ than CQS strains with wild-type *pfcrt* was also observed (Mayer, 2009), hence proving the validity of the method used.

The continuous variation as shown by the QN accumulation level (Figure 3.2.) was typical of the multifactorial phenotype, and in contrast to the classical single gene Mendelian inheritance, with typical bimodal distribution in the population (Sen & Ferdig, 2004). The results indicated that there was no clear distinction between

strains having wild-type (QN accumulation = 182.6 ± 5.2 units) or mutant *pfcrt* (QN accumulation = 130.8 ± 5.7 units), suggesting that QN accumulation is a quantitative trait. The means for QN accumulation for the two groups were, however, still highly significantly different at $p<0.0001$. Thus, *pfcrt,* though not a single determinant, is a major factor affecting QN accumulation.

3.3. QTL Analysis

3.3.1. QTL Analysis of Quinine Accumulation

Using quantitative trait loci (QTL) analysis based on IC_{90} data, Ferdig *et al.* demonstrated that *pfcrt* is a common determinant in QN and CQ resistance (Ferdig *et al.*, 2004), in addition to other factors involved in QN resistance present in chromosomes 6, 9 and 13 (Ferdig *et al.*, 2004).

Although IC_{50} and IC_{90} assays have been widely used to study drug response in *Plasmodium*, these assays are indicators for cell viability and cell death after 72 hours exposure to the drug and, therefore, several factors might influence them, including affinity of the drug to its target and intracellular drug concentration, which may be affected by the carrier systems. On the contrary, the assay used in this project measured the drug accumulation in the parasite within minutes of exposure to the drug, which was likely to be determined only by the transport mechanisms. Thus, genetic factors found to be linked to the QN accumulation phenotypes by the QTL analysis were likely to affect or be involved in the QN transport mechanisms.

QTL analysis was also performed on CQ accumulation data (Mayer, 2009) as a mean of proving the validity of the method, since the CQ system was the one most thoroughly studied.

3.3.1.1. Primary Scan

The QTL primary scan was performed by regression analysis of QN accumulation across all 36 strains and aimed to find major factors affecting QN accumulation. Figure 3.3. shows the LOD score of QTL analysis primary scan on QN accumulation. The horizontal dotted line in this (and all subsequent figures) defines the confidence level of $p<0.01$ (see Methods), so that all peaks arising above this line can be considered as well-supported by the data. It should also be noted that a peak in the QTL analysis corresponded in general to one or more chromosome markers. This number might vary from 1 to 11 in the various peaks, since several markers might

share the same position in centiMorgan (cM). Where there were more than one marker within a peak, the name of the marker located in the middle of the peak, as provided in the NCBI list of markers (see Method), was assigned as the name of the peak. The regression data on these peaks were listed in Table 3.2., 3.3. and 3.4., where in each case a central chromosome marker present in that peak, was recorded.

In the primary scan, a major double peak was readily seen in chromosome 7. One of the major peaks, positioned at *pfcrt*. The presence of *pfcrt* as a major peak here was not surprising since the gene has often been associated with QN resistance (Ferdig *et al.*, 2004) and accumulation (Sanchez *et al.*, 2008b). The peak on the left, assigned to the marker B5M12, however, is novel. The Pearson regression showed that both peaks had negative correlation to QN accumulation (Table 3.2.), meaning that they both work in synergy in reducing the QN accumulation level.

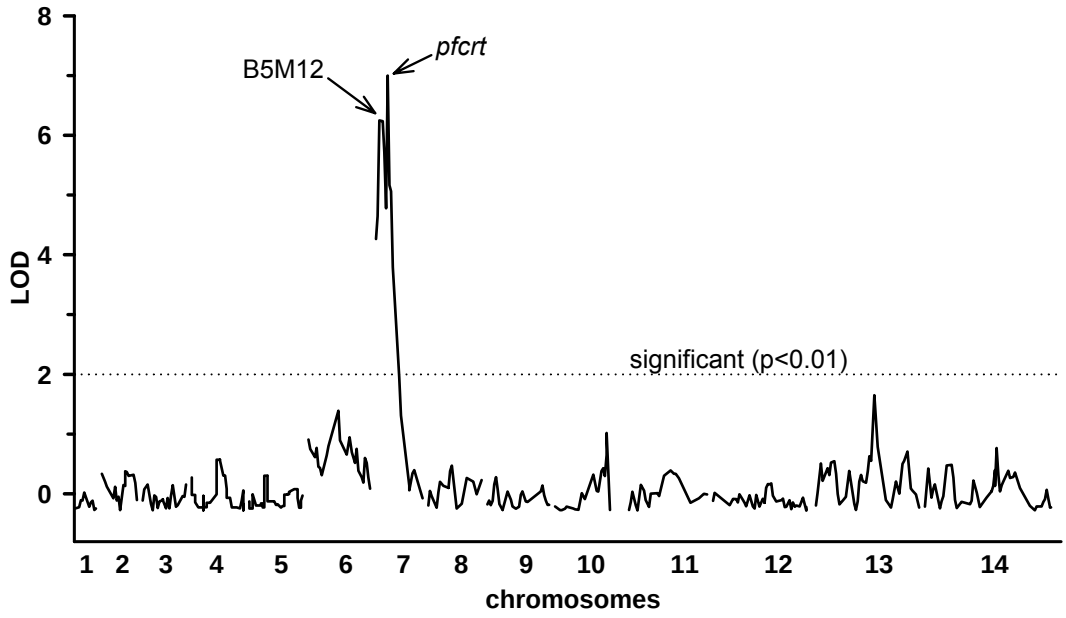

Figure 3.3. QTL analysis primary scan of quinine accumulation
A double peak is observed in the primary scan, one located on pfcrt, whereas the other one is novel and assigned to the marker B5M12 (—— QN Accumulation; ····· significant threshold p<0.01)

3.3.1.2. Secondary Scan

The QTL secondary scan was performed separately on the 17 mutant *pfcrt*-containing strains and the 19 wild-type *pfcrt*-containing strains. Figure 3.4. **(A)** depicts the QTL analysis across the chromosomes of only the 17 mutant *pfcrt*-

containing strains, whilst Figure 3.4.**(B)** shows the QTL analysis across the chromosomes of only the 19 wild-type *pfcrt*-containing strains.

Some markers in chromosome 7 were excluded from the secondary scans. These markers are located around and segregated with *pfcrt*. Thus within CQR or CQS group, there is no variation of the parental origin of these markers, that is, all CQR strains and all CQS strains have inherited the markers from Dd2 and HB3, respectively. Therefore, by excluding these markers from the analysis, the major effect of *pfcrt* was removed. In the graph, the excluded markers are represented as a gap in chromosome 7.

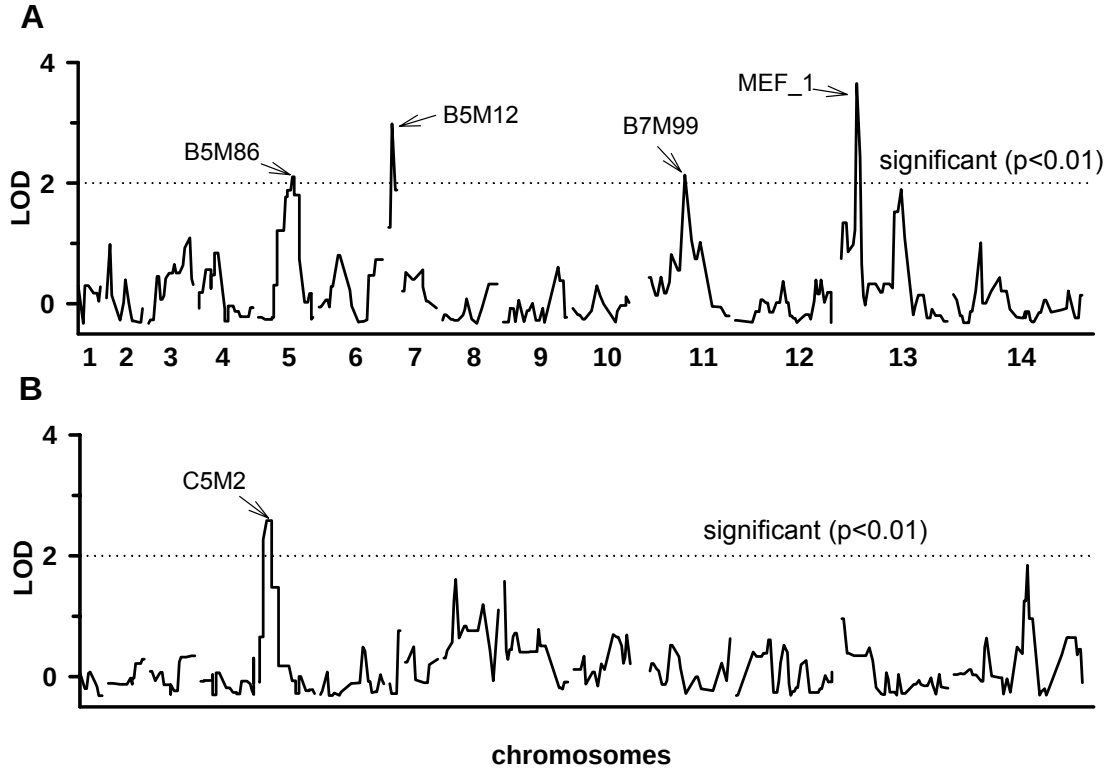

Figure 3.4. QTL analysis secondary scan of quinine accumulation
(**A**) LOD score of secondary scan on 17 CQR strains (**B**) LOD score of secondary scan on 19 CQS strains (—— QN Accumulation; ····· significant threshold p<0.01)

3.3.1.2.1. Secondary Scan on CQR Strains

The secondary scan on CQR strains showed significant peaks in chromosome 5, 7, 11, and 13 (Figure 3.4. **(A)**).

The peak in chromosome 5 resides on the marker B5M86, which Ferdig *et al.* also found in his QTL analysis secondary scan on QN IC_{90} (Ferdig *et al.*, 2004). Only 4.3 cM away from the B5M86 marker, lies the MDR1 marker containing *pfmdr1* gene. Although not at the top of the peak, the MDR1 marker is located within the B5M86

peak. B5M86 appeared only in the secondary scan, but not in the primary scan. The Pearson regression showed that B5M86 peak had a positive correlation to QN accumulation, meaning that the peak contributes positively to QN accumulation.
In chromosome 7, the B5M12 peak appeared again. The peak had a negative correlation to QN accumulation. However, this peak was not present in the secondary scan on CQS strains (Figure 3.4. **(B)**).
The peak in chromosome 11 is located on marker B7M99 at 83.3 cM, whereas in chromosome 13, there was a peak found on MEF_1 marker, located at 32.6 cM. However, this peak nowhere near the *pfnhe* gene, which is often associated with QN resistance (Bennett *et al.*, 2007). The *pfnhe* gene is positioned in the vicinity of the TA46 marker (at 173.1 cM).

3.3.1.2.2. Secondary Scan on CQS Strains

Only one peak was observed in the QTL secondary scan on CQS strains, that is the C5M2 peak located in chromosome 5. Pearson regression showed that the peak contributed positively to QN accumulation (Figure 3.4. **(B)**).

3.3.2. QTL Reanalysis of Ferdig's Quinine IC_{90} Data with and without Verapamil

In their publication, Ferdig *et al.* (Ferdig *et al.*, 2004) published QTL analysis data of CQ and QN IC_{90}, and QN IC_{90} in the presence of verapamil (QN-VP IC_{90}). Verapamil is an L-type calcium channel blocker known to be able to reverse CQ resistance (Martin *et al.*, 1987, Martiney *et al.*, 1995). In this project, Ferdig's data of QN IC_{90} and QN-VP IC_{90} were reanalysed.
There were two major double peaks, located in chromosome 7 and 13, observed in the primary scan of QN IC_{90}. Although the LOD score is not as high as in QN accumulation QTL analysis, the dominant peak in chromosome 7 again correlated to *pfcrt*. In agreement with its negative contribution to accumulation, the regression coefficient showed that *pfcrt* had a positive correlation to IC_{90}. Plotting the QN IC_{90} and QN-VP IC_{90} data sets in the same graph showed that this *pfcrt* peak was verapamil-sensitive (Figure 3.5. **(B)**).
The B5M12 peak, which appeared pronouncedly as the left peak of chromosome 7 in the QN accumulation QTL analysis, was not readily visible in QN IC_{90}. Despite its significant LOD score, B5M12 appeared only as a small protrusion to the left of the *pfcrt* peak in the QTL analysis of QN IC_{90}. The presence of B5M12 in the primary

scans of both QN accumulation and IC_{90} can be seen in Figure 3.5. **(B)**. B5M12 peak is also VP sensitive.

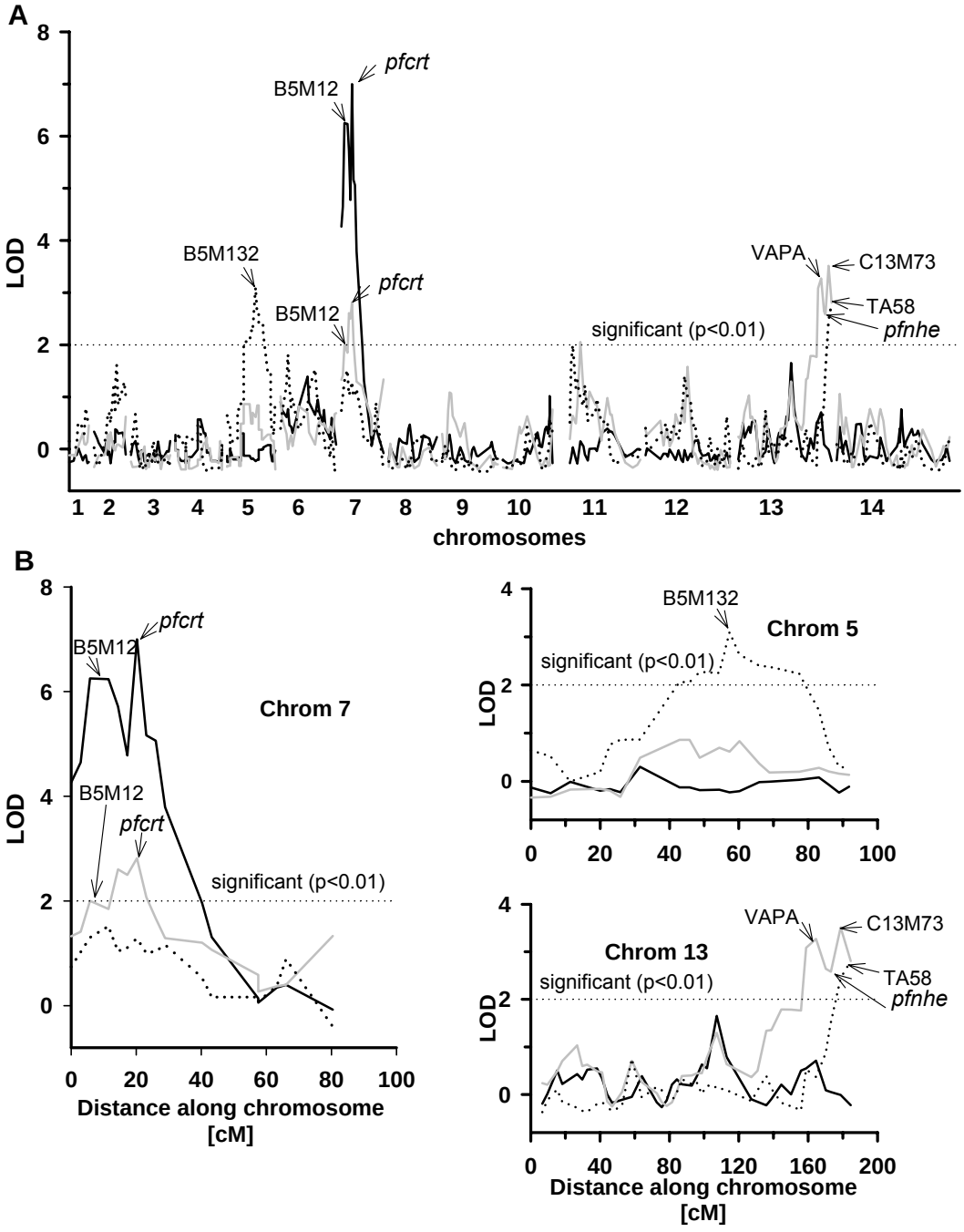

Figure 3.5. Comparing the QTL analysis primary scan of QN accumulation with the QTL reanalysis of Ferdig's QN IC_{90} and QN-VP IC_{90}
(**A**) Scan across all 14 chromosomes (**B**) Peaks in chromosomes 7, 5 and 13
(——— QN Accumulation; ——— QN IC_{90}; ••••••• QN-VP IC_{90}; ····· significant threshold p<0.01)

In the QTL analysis of QN IC_{90}data, there were two clearly separated peaks in chromosome 13, which were only small or even absent in the QN accumulation data set. The left peak, VAPA, is located at 3.27 cM, whereas the right peak, C13M73, is

located at 178.8 cM. C13M73 is exactly at the same position in cM as the C13M56 peak published by Ferdig's group. Despite their hypothesis that *pfnhe* might be present within the peak they found in chromosome 13 (Ferdig *et al.*, 2004) and a more recent publication suggesting involvement of PfNHE in QN resistance (Bennett *et al.*, 2007, Nkrumah *et al.*, 2009), the reanalysis of Ferdig's IC_{90} data showed that *pfnhe* was not located in either of the two peaks in chromosome 13. Instead, the gene, which was positioned within TA46 marker, was located in the valley between the two peaks.

The regression coefficient showed that both VAPA and C13M73 peaks in chromosome 13 had positive contribution to IC_{90}, hence reducing sensitivity to QN. Superimposing the QTL analysis data of QN IC_{90} with and without verapamil showed that the presence of verapamil affected the C13M73 peak only slightly whilst completely diminishing the VAPA peak. A peak, TA58, lying within the shoulder of the C13M73 peak, was found in QN-VP IC_{90} data. The presence of TA58 peak further proved that C13M73 peak was not greatly affected by the presence of verapamil.

Table 3.2. List of QTL primary scan peaks

peak with negative correlation | peak with positive correlation
not a peak, negative correlation | not a peak, positive correlation

Chr.	Marker Name	Marker Number	Position [cM]	LOD Scores		
				QN Acc.	QN IC_{90}	QN-VP IC_{90}
5	**B5M132**	214	57.3	-0.23	0.62	3.10
7	**B5M12**	297	5.8	6.25	2.00	1.30
7	**PfCRT**	310	20.2	7.00	2.82	1.29
11	**TA31**	507	43.1	0.15	2.05	0.97
13	**VAPA**	705	164.5	0.71	3.27	0.37
13	**C13M73**	717	178.8	-0.01	3.51	2.44
13	**TA58**	719	184.5	-0.23	2.81	2.80

In the primary scan of the QN-VP IC_{90} there was a quite pronounced peak (B5M132) on chromosome 5, which was not apparent when verapamil is absent. The regression coefficients show that the B5M132 peak contributed negatively to IC_{90}, hence increasing sensitivity. Verapamil is known to have intrinsic antiplasmodial activity independent to its capability in reversing CQR (Adovelande *et al.*, 1998). It was also reported previously that mutations in *pfmdr1* modulated *P. falciparum* sensitivity to the intrinsic antiplasmodial activity of verapamil (Hayward *et al.*, 2005).

Therefore, it is interesting to see that this peak, B5M132, is located in chromosome 5, around 8.6 cM away from *pfmdr1.*

3.3.2.1. Secondary Scan

In the secondary scan of QN IC_{90} and QN-VP IC_{90} reanalysis several peaks were found and listed in Tables 3.3. and 3.4. As mentioned previously, the secondary scans aim to find factors affecting variations within the CQR or CQS strains, since the scans were performed on either the wild-type or mutant *pfcrt* carrying strains.
As with the secondary scan of QN accumulation, *pfcrt* and markers located close to and segregated with *pfcrt* were also excluded from the secondary scans performed on QN IC_{90} and QN-VP IC_{90} data to remove the effects of *pfcrt.* The excluded markers were represented as gaps in chromosome 7 (Figure 3.6. **(A)** and **(B)**).

3.3.2.1.1. Secondary Scan on CQR Strains

For the first time, the analysis showed MDR1, the marker where *pfmdr1* resides, as a significant, verapamil sensitive peak located in chromosome 5 in the secondary scan on CQR strains of QN IC_{90}. The regression coefficient showed that the peak contributed negatively to QN IC_{90}.

Table 3.3. QTL secondary scan on CQR strains peaks

peak with negative correlation
not a peak, negative correlation
peak with positive correlation
not a peak, positive correlation

Chromosome Number	Marker Name	Marker Number	Position [cM]	LOD Scores		
				QN Accumulation	QN IC90	QN-VP IC90
2	BM41	60	57.5	-0.31	0.57	2.37
5	B5M86	217	60.2	2.10	1.79	0.52
5	MDR1	222	65.9	1.80	2.28	0.77
6	BM75	266	31.7	0.80	2.43	0.64
6	BM103	289	100.5	0.73	2.00	-0.03
7	B5M12	297	5.8	2.98	0.33	-0.16
11	B7M99	521	83.3	2.13	-0.20	-0.29
12	Y588M4	557	71.6	0.02	1.18	2.50
12	Y812M3	565	88.8	0.02	1.18	2.50
13	MEF_1	632	32.6	3.65	0.90	0.16

As mentioned previously, MDR1 is located close to B5M86, a peak which appeared in the secondary scan of QN accumulation data. Again, as in the secondary scan of QN accumulation data, scanning the QN IC_{90} data showed that both markers were located within the same peak (Table 3.3. and Figure 3.6. **(B)**). It is very probable, therefore, that the effect shown by these markers corresponded to the same locus or gene.

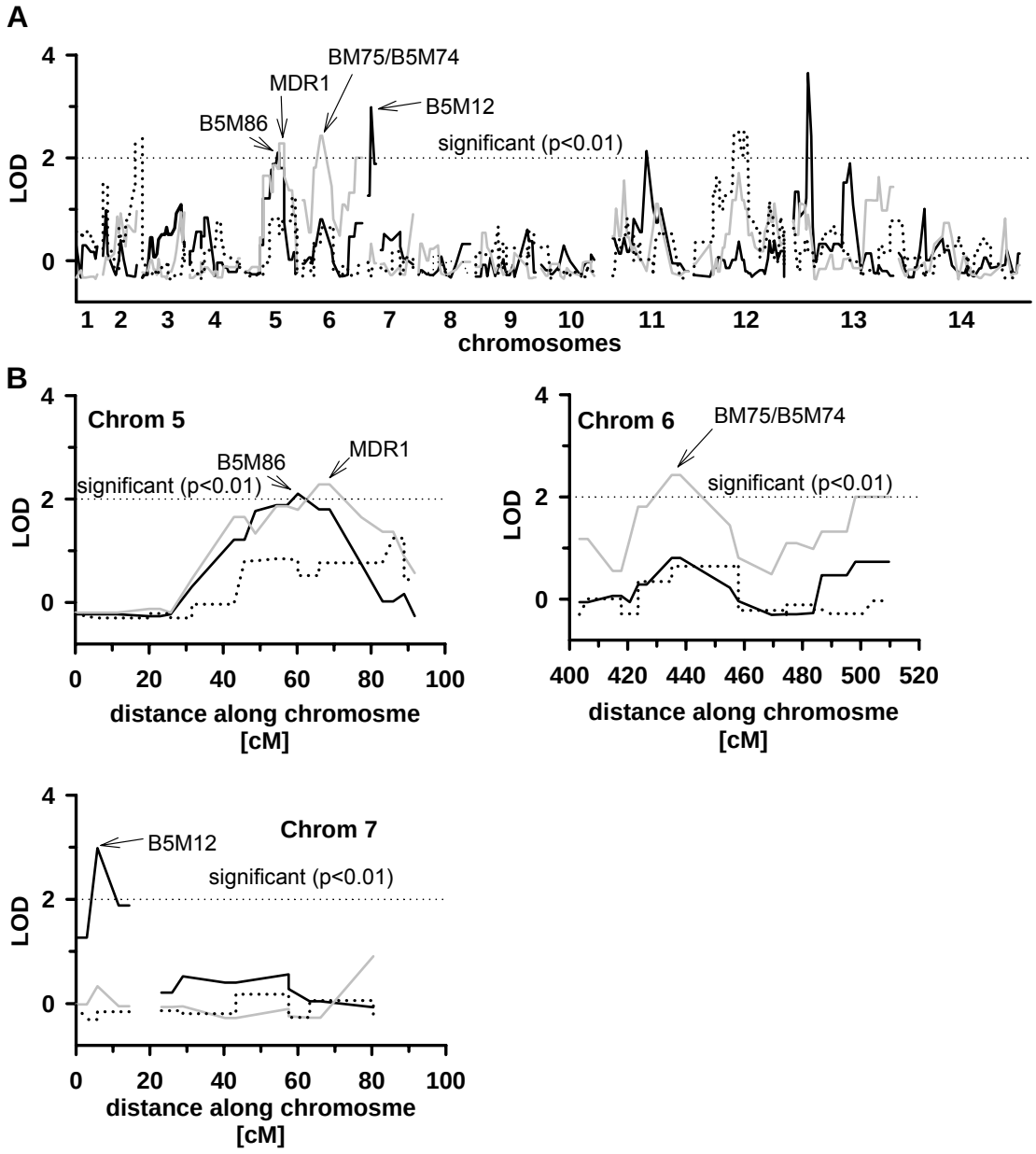

Figure 3.6. Comparing the QTL analysis secondary scans on CQR strains of QN accumulation and QTL reanalysis of Ferdig's QN IC90

(**A**) Scan across all 14 chromosomes (**B**) Peaks in chromosomes 5, 6 and 7
(——— QN Accumulation; ——— QN IC_{90}; ••••••• QN-VP IC_{90}; ····· significant threshold p<0.01)

In chromosome 6, a peak located on the marker BM75 appeared in QC IC_{90}. The regression coefficient shows that BM75 contributes positively to QN IC_{90} but does not seem to affect QN accumulation. This peak is also abolished by the presence of verapamil.

BM75 is located at the same cM position as a peak called B5M74 mentioned in the work of Ferdig and colleagues (Ferdig *et al.*, 2004). The paper mentioned that B5M74 interacted with *pfcrt* and B5M74 originated from Dd2 increased the positive effect of *pfcrt* to IC_{90}. It seems that both BM75 and B5M74 corresponded to the same gene located in that area.

3.3.2.1.2. Secondary Scan on CQS Strains

Several peaks appeared in the secondary scan of QN IC_{90} data on CQS strains. The largest peak was the VP-resistant C13M73, which is located in chromosome 13. This peak was also present in the QN IC_{90} primary scan but not present in the secondary scan on CQR strains, suggesting that the peak found in the primary scan were solely contributed by the CQS strains (Figure 3.7. **(B)**).

The C5M2 peak, which appeared significantly in the secondary scan of QN accumulation, was not present at all in QN IC_{90} (Figure 3.7. **(B)**).

Unlike in the secondary scans on CQR strains, in this secondary scan on CQS strains MDR1 and B5M86 peaks were no longer significant (Figure 3.7. **(B)**).

Another peak, readily seen in the secondary scan on CQS strains was B5M4, located in chromosome 6. The presence of this peak was not affected by VP.

Table 3.4. QTL secondary scan on CQS strains peaks

peak with negative correlation
not a peak, negative correlation
peak with positive correlation
Not a peak, positive correlation

Chromosome Number	Marker Name	Marker Number	Position [cM]	LOD Scores		
				QN Acc.	QN IC90	QN-VP IC90
5	C5M2	194	20	2.58	0.29	0.14
6	B5M4	263	23.1	-0.27	2.02	2.29
13	C13M73	717	178.8	-0.18	3.14	3.68

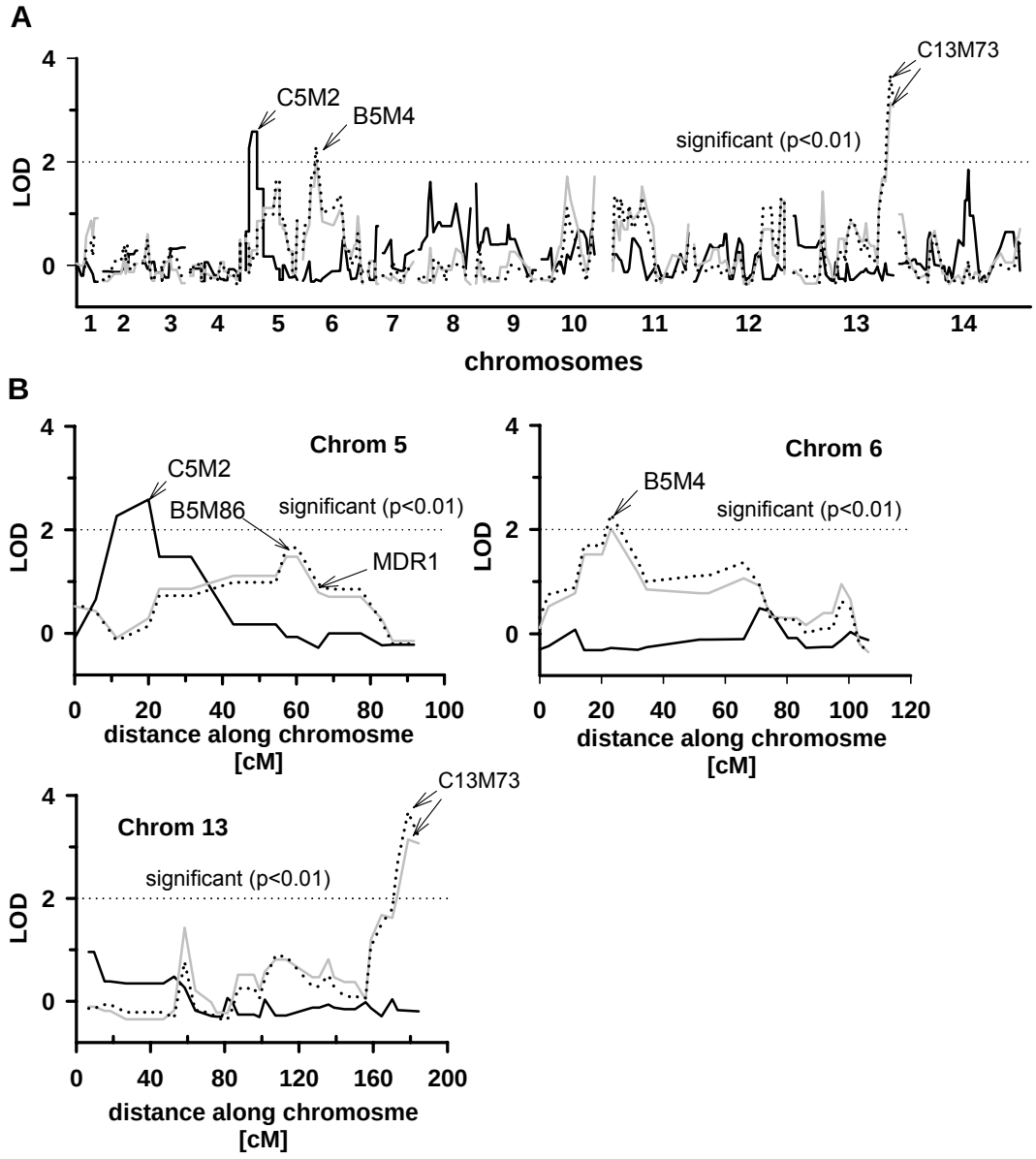

Figure 3.7. Comparing the QTL analysis secondary scans on CQS strains of QN accumulation and QTL reanalysis of Ferdig's QN IC_{90}
(**A**) Scan across all 14 chromosomes (**B**) Peaks in chromosomes 5, 6 and 13 (━━ QN accumulation; ━━ QN IC_{90}; ┅┅ QN-VP IC_{90}; ┈┈ significant threshold p<0.01)

3.4. Mathematical Analysis of Selected Peaks

Mathematical analyses were performed to an assorted number of positive loci to determine the effects of these loci to the phenotype, i.e. the QN accumulation or IC_{90}, and whether some of these loci interact with one another.

3.4.1. Only Dd2 Version of B5M12 Present in CQR Strains Affects the QN Accumulation and IC_{90}

The observation of B5M12 peak was novel. The peak was not observed by Ferdig in his QTL analysis of QN IC_{90} (Ferdig *et al.*, 2004) (See Appendix 1 **(A)**). This might have been caused by lower LOD score that they obtained, affecting the resolution of the peak. Nevertheless, in the reanalysis of Ferdig's data performed in this project, a small, not so obvious protrusion correlated to B5M12 appeared to the left of the *pfcrt* peak in the primary scan. This peak had positive contribution to IC_{90}.

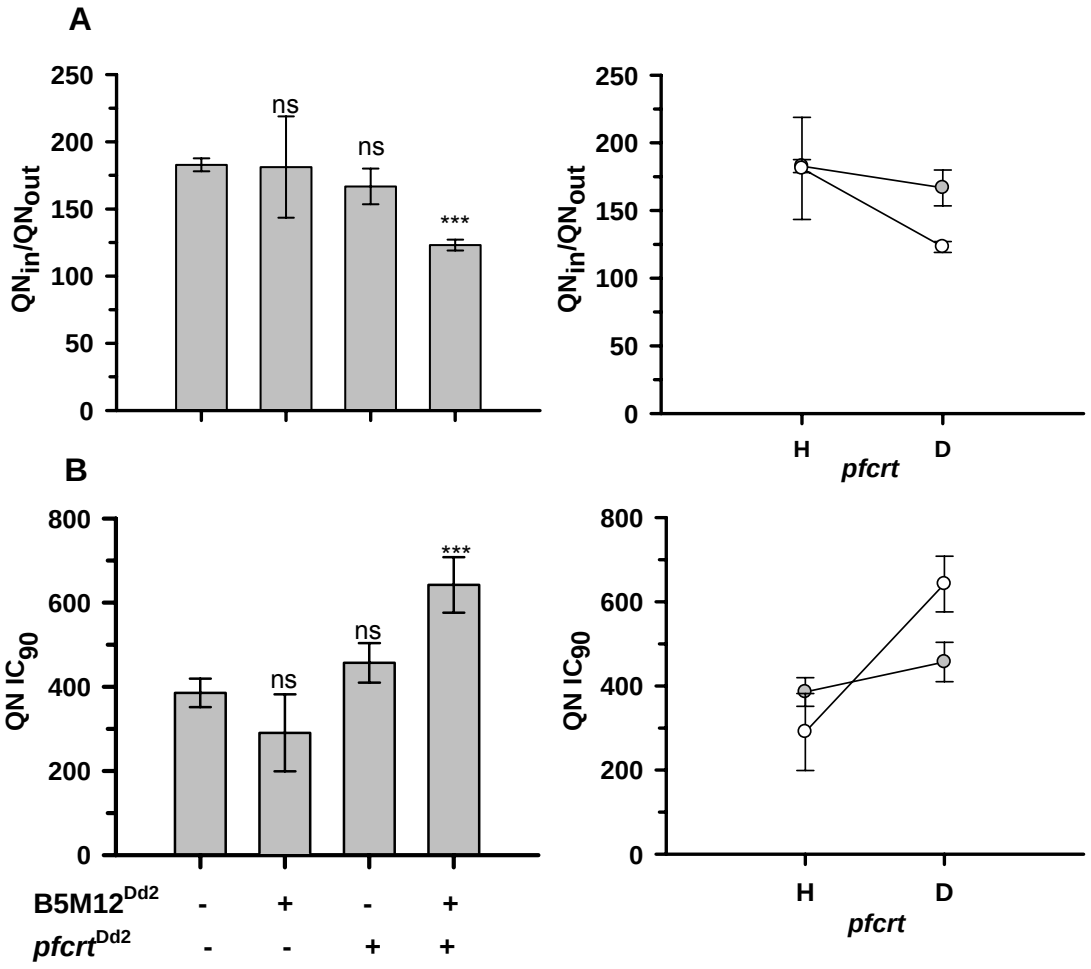

Figure 3.8. The effects of B5M12 and *pfcrt* origins to quinine accumulation and IC_{90}

The means of (**A**) QN accumulation and (**B**) QN IC_{90} levels when different B5M12 alleles coming from Dd2 and HB3 were tested to see whether the origins of B5M12 and *pfcrt* significantly affect the levels. The results showed that Dd2 allele of B5M12 significantly affected both QN accumulation and IC90 only when *pfcrt* was also inherited from Dd2, i.e. in CQR strains. (○ B5M12 from Dd2; ● B5M12 from HB3)

In addition to its manifestation in the primary scan of QN accumulation, the B5M12 peak also appeared in the secondary scan on strains having mutated *pfcrt*, but not in the secondary scan on strains having wild-type *pfcrt*. Thus, suggesting that the presence of B5M12 peak in QN accumulation was contributed solely by CQR strains.
To prove this hypothesis, the effect of B5M12 and *pfcrt* origins to the levels of QN accumulation and IC_{90} was tested. The mean of QN accumulation and IC_{90} levels of strains having different combinations of loci were calculated. *P* values were calculated to determine whether there was significant difference between the means, when both loci came from HB3 or otherwise.
Bearing in mind that all CQR strains inherited *pfcrt* from Dd2 and all CQS strains have inherited *pfcrt* from HB3, the results showed that CQS strains with Dd2-like B5M12 and CQR strains with Dd2-like *pfcrt* did not give significantly different levels of QN accumulation and IC_{90} in comparison to CQS strains with B5M12 from HB3. However, CQR strains with B5M12 from Dd2 showed significantly different level of QN accumulation and IC_{90} compared to CQS strains with B5M12 from HB3. Therefore it seemed that B5M12 had a major effect over QN accumulation and IC_{90} only when it came from Dd2 and was present in strains having Dd2-like *pfcrt*, or in other words, in CQR strains. Thus, as clearly depicted in Figures 3.8. **(A)** right and **(B)** right, the Dd2 alleles of B5M12 and B5M47, which contain *pfcrt*, act synergistically increasing IC_{90} and reducing accumulation.

3.4.2. Dd2 Alleles of VAPA and C13M73 are Associated with Higher QN IC_{90} but not Accumulation

C13M73 was one of the major peaks appearing in the primary scan of Ferdig's QN IC_{90} data reanalysis. This peak is located at the same cM position as C13M56 peak discovered by Ferdig (Ferdig *et al.*, 2004), and thus very likely to correspond to the same gene. This peak was, however, absent in the QTL analysis of QN accumulation.
In this project, the effects of Dd2 allele at C13M73 locus to QN IC_{90} and accumulation were tested, using *pfcrt* effect as a background. The result showed that Dd2 allele of C13M73 had an additive effect to QN IC_{90}. The value of QN IC_{90} was significantly increased in the presence of Dd2 allele of C13M73, regardless of the origins of *pfcrt* (Figure 3.9. **(A)** and **(B)** middle) or B5M12 (Figure 3.9. **(A)** and **(B)** lower). Thus, indicating that the C13M73 effect is independent of *pfcrt* and B5M12. There was, however, no effect of the C13M73 locus to QN accumulation observed (Figure 3.9. **(B)**).

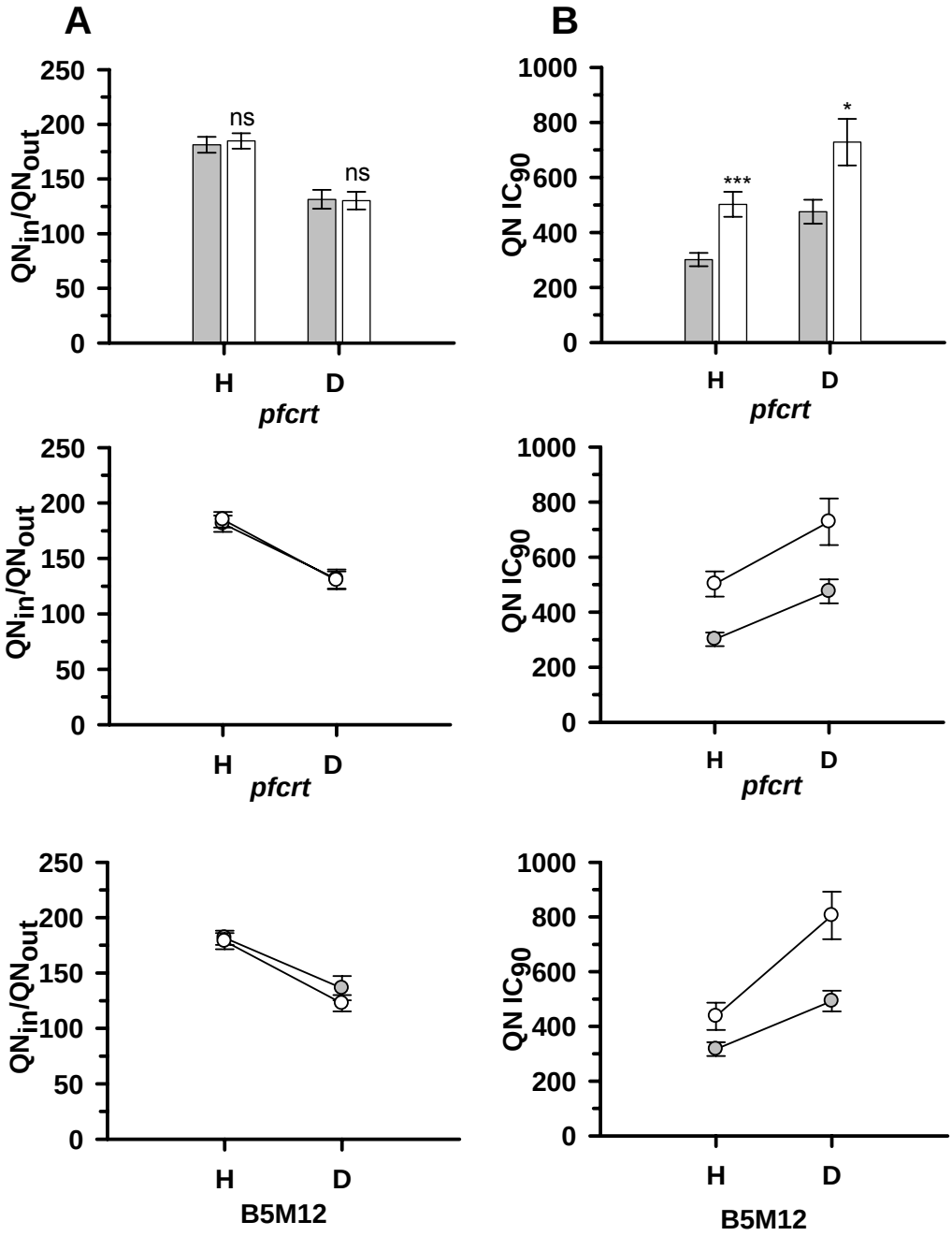

Figure 3.9. The effect of C13M73 to quinine accumulation and IC_{90}
The means of (**A**) QN accumulation and (**B**) QN IC_{90} levels when different C13M73 alleles coming from Dd2 and HB3 were tested to see whether the origins of C13M73 and *pfcrt* significantly affect the levels. The results showed that Dd2 allele of C13M73 was associated with higher QN IC_{90}. However, neither HB3 nor Dd2 allele of C13M73 affected QN accumulation. Adding BM12 added no influence the effect of C13M73.
○ □ C13M73 from Dd2 ● ▭ C13M73 from HB3

The same test was also applied to the VAPA peak, which is the other major peak in chromosome 13 appearing only in the primary scan of Ferdig's QN IC_{90} data reanalysis. Just like the C13M73 peak, VAPA had no effect to QN accumulation

(Figure 3.10. **(B)**). The Dd2 allele of this of this peak again showed an additive effect, significantly increasing QN IC_{90} value (Figure 3.10. **(A)**), independent of the origins of *pfcrt* and B5M12.

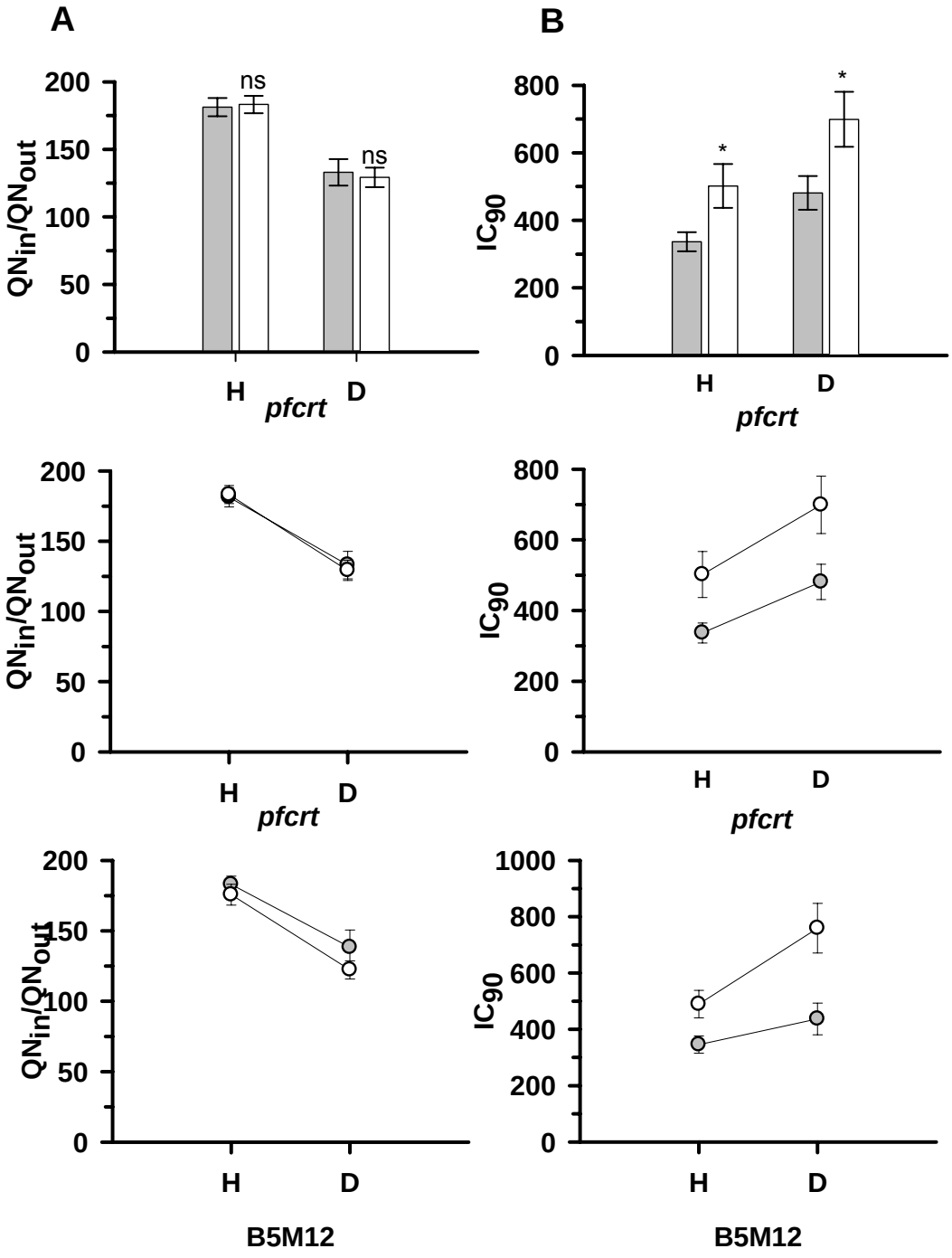

Figure 3.10. The effect of VAPA to quinine accumulation and IC_{90}
The means of (**A**) QN accumulation and (**B**) QN IC_{90} levels when different VAPA alleles coming from Dd2 and HB3 were tested to see whether the origins of VAPA and *pfcrt* significantly affect the levels. It was shown in the results that just like C13M73, Dd2 allele of VAPA significantly affected QN IC_{90}, but had no effect at all to QN accumulation.
○ □ VAPA from Dd2 ● ■ VAPA from HB3

3.4.3. MDR1 and B5M86 Showed the Same Effect on Both Quinine Accumulation and IC_{90}

Peaks correlated to MDR1 and B5M86 appeared in the secondary scans only. Since these peaks were found only in the secondary scans and not in the primary scans, their contribution should not be major.

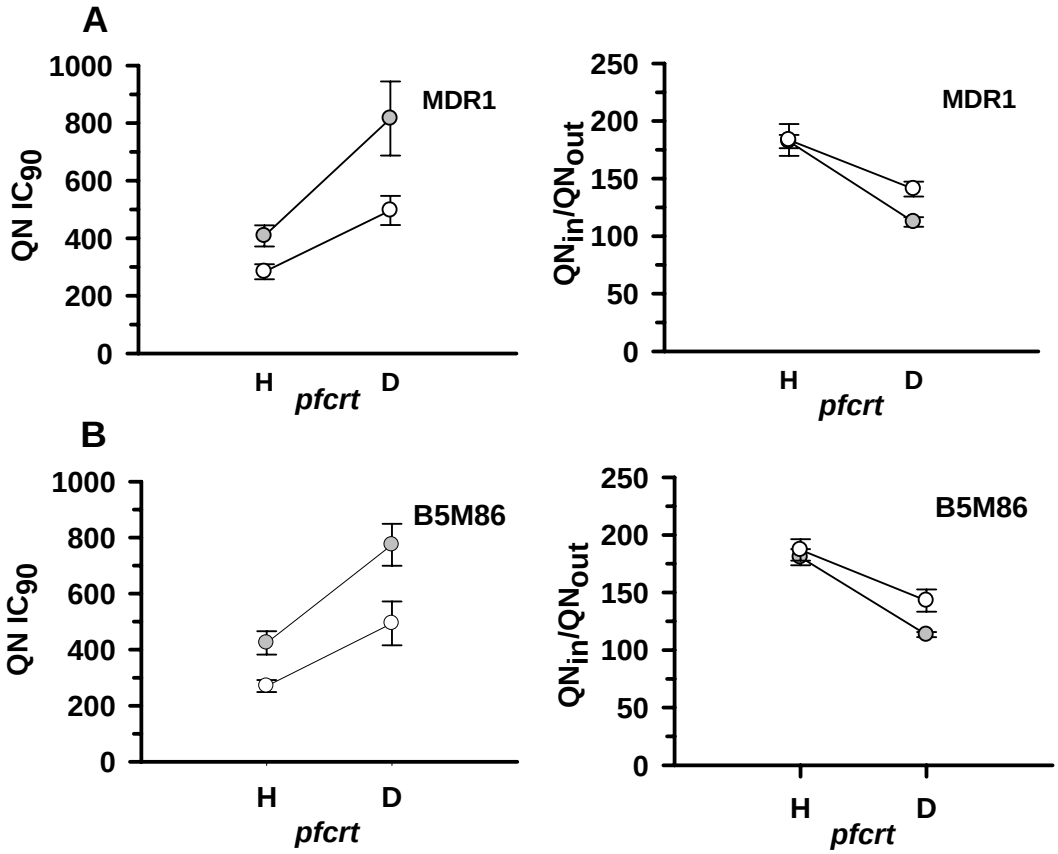

Figure 3.11. The effect of MDR1 and B5M86 to quinine accumulation and IC90

The means of QN accumulation and QN IC_{90} levels when different (**A**) MDR1 and (**B**) B5M86 alleles coming from Dd2 and HB3 were tested to see whether the origins of the loci significantly affect the levels. The two loci seemed to have exactly the same effects to QN IC_{90}. HB3 alleles of both loci were associated with higher QN IC_{90}.
○ from Dd2 ● from HB3

Within the MDR1 marker, resides the *pfmdr1* gene. PfMDR1 is often associated with increased *in vitro* QN resistance (Sidhu *et al.*, 2005, Sidhu *et al.*, 2006), although a recent publication by Sanchez *et al.* shows that there was no difference in the level of accumulated QN in *Xenopus laevis* oocytes expressing HB3 and Dd2 types *pfmdr1* (Sanchez *et al.*, 2008).

The mathematical analysis of QN accumulation showed that MDR1 marker had almost no effect to accumulation in CQS strains and only a slight, though significant

positive effect to accumulation in CQR strains seemed to be contributed by the Dd2 allele (Figure 3.11. **(A)** right). This is consistent with the result of the QTL analysis, where the significant MDR1 peak only appeared in the secondary scan on CQR strains but not on CQS strain.

The analysis of Ferdig's IC_{90} data showed that the Dd2-type MDR1 was associated with decreased QN IC_{90} regardless of the origin of *pfcrt* (Figure 3.11. **(A)** left), suggesting that this allele had additive effect to the phenotype.

As mentioned previously, the secondary scans of both QN accumulation and IC_{90} on CQR strains showed overlapping peaks containing both B5M86 and MDR1 markers, although not necessarily as the marker with the highest LOD score (Figure 3.6. and Table 3.3.). Since the two markers are located in close proximity to one another and showed the same effects to both accumulation and IC_{90} (Figure 3.11. **(A)** and **(B)**), it is very likely that the effect of the two peaks corresponded to the same loci or gene. In addition, since *pfmdr1* is located within these peaks, then the possibility that *pfmdr1* is the underlying gene responsible for the effect is not unlikely.

3.4.4. The Inheritance of Dd2 Alleles at both BM75 and *pfcrt* Results in Higher Quinine IC_{90} but Has no Effect on Quinine Accumulation

BM75 was a peak found only in the secondary scan on CQR strains of QN IC_{90} and did not appear at all in QN accumulation. The peak was located at the same cM position as B5M74, mentioned in Ferdig's paper as a locus interacting with *pfcrt*. In the paper they mentioned that the inheritance of Dd2 alleles in both *pfcrt* and B5M74 had increased substantially QN IC_{90} value in comparison to other possible allelic combinations at these loci (Ferdig *et al.*, 2004).

As Ferdig's result showed that B5M74 interact with *pfcrt* increasing the QN IC_{90} value, the BM75 locus increased the QN IC_{90} level significantly only when there was Dd2 allele at the *pfcrt* locus, indicating that the presence of Dd2 alleles at the two loci act synergistically (Figure 3.12. **(B)**) increasing the IC_{90} value. Thus, this observation supported the previous finding by Ferdig, which mentioned interaction between the two loci (Ferdig *et al.*, 2004).

On the other hand, the analysis on QN accumulation failed to show any significant difference in QN accumulation level resulted from different allelic combinations at the BM75 and *pfcrt* loci (Figure 3.12. **(A)**).

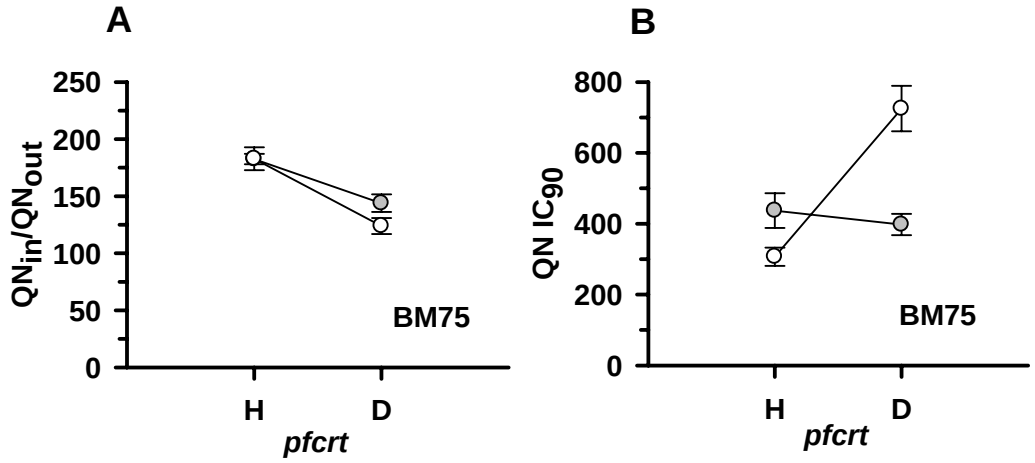

Figure 3.12. The effect of BM75 to quinine accumulation and IC_{90}
The means of QN accumulation (**A**) and QN IC_{90} (**B**) levels when different alleles coming from Dd2 and HB3 were tested to see whether the origins of the loci significantly affect the levels. Mathematical analysis showed that the the presence of Dd2 alleles at both *pfcrt* and BM75 act synergistically increasing the QN IC_{90} value (**B**).
○ from Dd2 ◍ from HB3

3.4.5. HB3-Allele of C5M2 Affects Accumulation in Chloroquine Sensitive Strains Only

C5M2 was the only locus appeared in the secondary scan QTL analysis of QN accumulation on CQS strains, which did not appear in the QTL analysis of QN accumulation on CQR strains nor in the QTL analysis of QN IC_{90}. The locus was also not observed in the primary scans of both QN accumulation and IC_{90}. Thus, the QTL analysis results suggested that this locus has a minor effect on QN accumulation only, and it affects variation within the CQS strains.

In consistence with the prediction arisen from the QTL analysis results, analysing the locus further revealed that the HB3-allele of the locus is associated with lower QN accumulation only in strains containing wild type *pfcrt*, i.e. CQS strains (Figure 3.13. **(A)**), whilst having no effect at all in strains having mutated *pfcrt*, i.e. CQR strains (Figure 3.13. **(B)**).

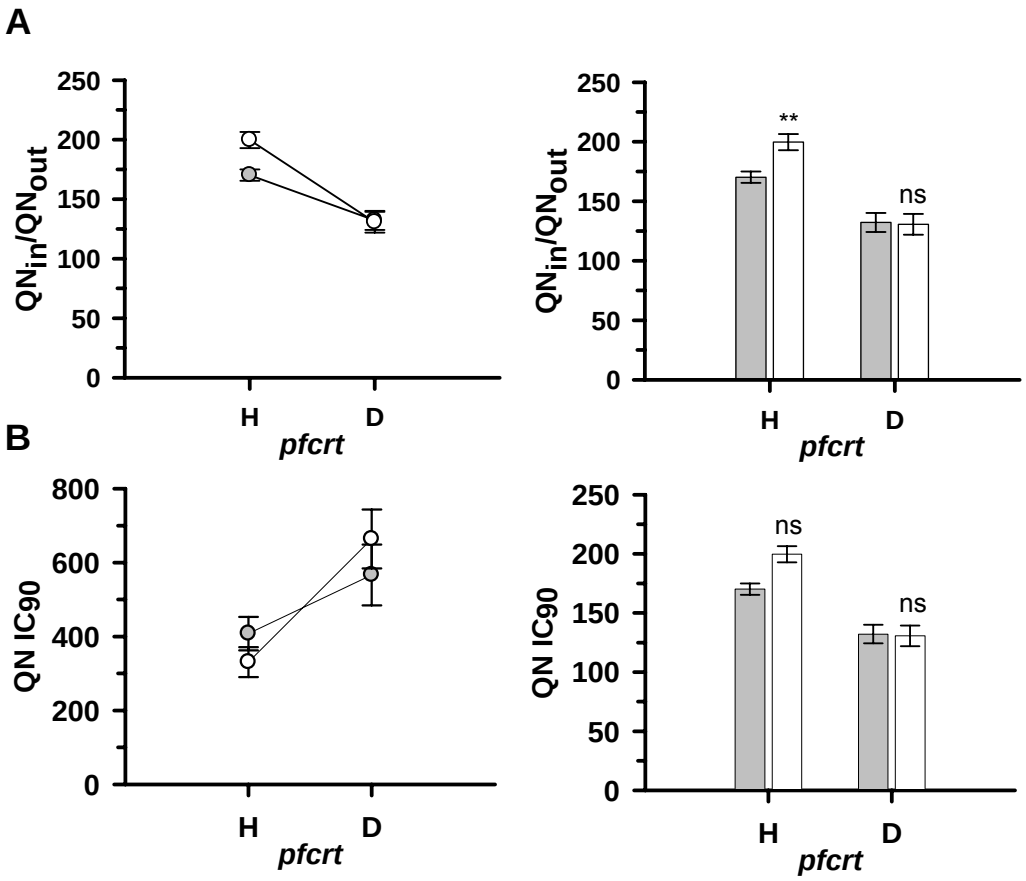

Figure 3.13. The effect of C5M2 on quinine accumulation and IC_{90}
The means of QN accumulation (**A**) and QN IC_{90} (**B**) levels when different alleles coming from Dd2 and HB3 were tested to see whether the origins of the loci significantly affect the levels. Analysis showed C5M2 has no effect to QN IC_{90} (**B**) and that HB3-allele of C5M2 is associated with lower QN accumulation in CQS strains only (**A**).
○ □ from Dd2 ○ ▭ from HB3

3.5. Bioinformatics Analysis of Positive Loci with Major Effects on Quinine Accumulation and IC_{90}

Since the target of this project is to find factors affecting QN accumulation and (or) resistance, the bioinformatics analysis was performed to find candidate genes located within the peaks that might play roles in QN accumulation and (or) resistance.

Two major peaks were selected from the QTL primary scans of QN accumulation and IC_{90}. These are the B5M12 peak in chromosome 7, which appeared in QTL analysis of QN accumulation, and the VAPA peak in chromosome 13, which appeared in the QTL analysis of QN IC_{90}.

After identifying molecular markers located under the peaks by comparing the NCBI microsattelites marker map with the Sequence Tagged Site (STS) and gene maps as published in the NCBI gene bank , genes located within and directly adjacent to these markers were identified and selected by analysis using online databases PlasmoDB and NCBI gene bank. Several genes could already be excluded early during the bioinformatic analysis, since their annotated functions in the NCBI and PlasmoDB showed that they were not likely to be involved in accumulation or resistance. The examples of these genes were tRNA genes present in B5M12 peak. Those with no annotated functions in PlasmoDB or NCBI were analysed further by sequence similarity alignment with known gene sequences using Basic BLAST . The genes were also analysed for the presence of TMD using TMHMM2 Server and for the presence of polymorphisms between Dd2 and HB3 by BLAST search on Dd2 and HB3 sequence databases in Broad Institute MIT .

3.5.1. Analysis of B5M12 Peak

The B5M12 peak spanned over six markers (four markers lying within area with the highest LOD score plus two flanking markers). Within this area 41 genes were annotated in PlasmoDB and NCBI gene bank. From these 41 genes, four tRNA genes and three genes with no polymorphism between Dd2 and HB3 were excluded, leaving 34 genes to analyse.

Many drug transporters, such as human and bacterial MDR proteins, are members of ABC transporter superfamily. ABC transporter might function as dimers or even tetramers. Typical ABC transporters contain two intracellular nucleotide binding domains (NBDs) and two multiple membrane spanning domains (MSDs) (Kerr, 2002), each consisting of 6-11 TMDs.

Transporters that have been associated with drugs resistance in *P. falciparum*, such as PfCRT and PfMDR1, have 10 (Bray *et al.*, 2005) and 11 TMDs (Peel, 2001), respectively. PfMDR1 has two homologous halves, each with predicted six TMDs (Peel, 2001). Considering that many transporters act as dimers or tetramers, genes encoding proteins with at least two predicted TMDs were particularly interesting. Annotations in PlasmoDB mentioned that 11 of the 34 genes to analyse had transmembrane domains. Of these 11 genes, seven were particularly interesting since the putative protein expressed by these genes had at least two predicted transmembrane domains. The five genes were MAL7P1.16, MAL7P1.17, PF07_0016, MAL7P1.19, PF07_0018, MAL7P1.340, and MAL7P1.205 (Table 3.5.). MAL7P1.19 was annotated in PlasmoDB as putative ubiquitin transferase and

MAL7P1.340 as ATP synthase subunit c, putative. The functions of the others, though, were still unknown. Basic BLAST search to find sequence similarity between the genes with unknown function with functionally understood genes also failed to give satisfactory results with the appropriate S and E values.

For most of the five putative proteins, apart from MAL7P1.19, the number of TMDs determined by TMHMM method (Krogh *et al.*, 2001) were in agreement with the number annotated at PlasmoDB. For this MAL7P1.19 protein, PlasmoDB showed only four TMDs, whereas the TMHMM method predicted the presence of six TMDs.

Table 3.5. Candidate genes having TMD that are located within B5M12 peak.
All of them are expressed during the trophozoite stage
ER: Early Rings; LR: Late Rings; ET: Early Trophozoites; LT: Late Trophozoites; ES: Early Schizonts; LS: Late Schizonts; M: Merozoites; *: as annotated in PlasmoDB

Gene	Expression Pattern*	Annotated Name/Function*	TMDs
MAL7P1.16	Expressed in ER, ET, and LT	conserved *Plasmodium* membrane protein, unknown function	8
MAL7P1.17	from LT onwards	conserved Plasmodium membrane protein, unknown function	7
PF07_0016	Expressed throughout intra-erythrocytic stage	conserved Plasmodium membrane protein, unknown function	4
MAL7P1.19	Expressed throughout intra-erythrocytic stage	putative ubiquitin transferase	4 (K&D) 6 (TMHMM)
PF07_0018	Expressed throughout intra-erythrocytic stage	conserved Plasmodium membrane protein, unknown function	7
MAL7P1.340	Unknown	putative ATP synthase subunit c	2
MAL7P1.205	Expressed at the same level throughout the intraerythrocytic stage (Dd2) Expressed throughout the intraerythrocytic stage, with peak in ET (HB3)	conserved Plasmodium protein, unknown function	3

Database analysis showed that MAL7P1.16 and MAL7P1.17 were expressed during trophozoite stage of the parasite, whereas the other three were expressed constitutively during intraerythrocytic life cycle. These expression patterns were in

agreement with the common belief that quinoline drugs act by interfering with haem detoxification in the food vacuole (Hawley *et al.*, 1998), which presents only from trophozoite stage onwards.

Searching for polymorphisms of these candidate genes in Dd2 and HB3 though productive was not reliable. The Dd2 sequence was incomplete at the time of the analysis that it was difficult to decide whether the polymorphisms found were genuine or due to poor sequencing.

3.5.2. Analysis of VAPA Peak

The verapamil sensitive VAPA peak located in chromosome 13 was present specifically in the primary scan of QN IC_{90}. This part of the chromosome did not seem to affect QN accumulation, since the peak did not come out in QTL analysis on the drug accumulation.

The peak spanned over seven markers (five markers lie within area with the highest LOD score plus two flanking markers). According to NCBI data base, there were 71 genes located within these markers. However, newer annotation by PlasmoDB showed that eight of these genes were in fact located elsewhere in the chromosome whereas two others did not exist at all, thus leaving only 61 genes positioned within these markers.

BLAST analysis of these 61 genes using Broad Institute MIT Database led to the finding that 14 of these genes were completely conserved in Dd2 and HB3, thus excluding them from possible candidates. In addition to that, the BLAST search showed that there were three genes where a small part of either Dd2 or HB3 sequences were incomplete, but showing no polymorphism at all in the part that had been sequenced. The absence of polymorphisms in these genes, however, had to be further proven by thoroughly re-sequencing the genes. There was also a gene named MAL13P1.45, where the only polymorphism between Dd2 and HB3 was a deletion of an asparagine (N) residue from position 661 in Dd2. This residue, however, lies in an N-rich area, that the apparent deletion might be a mere sequencing error. Apart from this gene, there was also PF13_0070 gene, which only polymorphism between Dd2 and HB3 was an R429P substitution at the last amino acid. Since this amino acid position is prone to sequencing error, it would probably be necessary to perform new sequencing to ensure whether this polymorphism was real or merely an artefact.

The number of candidate genes was further reduced when analysing the expression pattern of these genes as annotated in PlasmoDB, since some genes were only

expressed in late schizont (LS) and gametocyte (G) stages. Some others were not expressed at all during intraerythrocytice cycle. Bearing in mind that QN, like other quinoline drugs, acts by interfering with haem detoxification in the food vacuole (Hawley *et al.*, 1998), these genes could not have affected the QN IC_{90}.

Analysis of TMDs led to 6 proteins with 2, 6 and 14 transmembrane domains. PlasmoDB also annotated the same number of TMD in these proteins (listed in Table 3.6.). From these genes only PF13_0077 was annotated with a known function. The other four genes, MAL13P1.49, MAL13P1.50, PF13_0078 and MAL13P1.70 were Basic Blast searched to find sequence similarities with genes of known functions. However, the search failed to find any hits with suitable S and E values.

Table 3.6. Candidate genes located within VAPA peak.
All of them are expressed during the trophozoite stage
ER: Early Rings; LR: Late Rings; ET: Early Trophozoites; LT: Late Trophozoites; ES: Early Schizonts; LS: Late Schizonts; M: Merozoites

Gene	Expression Pattern*	Annotated Name/Function*	TMDs
MAL13P1.49	constitutively expressed, peak in ES and LS	hypothetical protein, conserved	2
MAL13P1.50	constitutively expressed, peak at LT and ES	hypothetical protein, conserved	2
PF13_0077	From LR to LS	DEAD box helicase, putative	2
PF13_0078	LR, LT, ES, LS, M	hypothetical protein, conserved	14
MAL13P1.70	ET, LT	hypothetical protein, conserved	6

4. Discussions

In this project, QTL analysis based on QN accumulation data showed that the initial accumulation of QN is genetically linked to two major factors, *pfcrt* and a factor located within the area of B5M12 peak as shown in Figure 3.5. The factor located in B5M12 seems to act synergistically with *pfcrt* in reducing QN accumulation (Figure 3.8.). The reanalysis of the published Ferdig's QN IC_{90} data indicated that both of these loci also synergistically increased QN IC_{90} (Figure 3.8.), hence reducing the drug sensitivity. In addition, the reanalysis of the QN IC_{90} also indicated the involvement of two QTL on chromosome 13 (Figure 3.5.), which were already reported previously (Ferdig *et al.*, 2004). These QTL do not seem to affect QN accumulation, thus, might encode for a target of QN.

Unlike CQ, the mechanisms of QN accumulation, action and resistance are not well understood, despite the numbers of research and discovery related to it. Studies have also shown that QN and CQ resistances share the same factor, that is *pfcrt* (Ferdig *et al.*, 2004), and mutation within this gene results in reduced sensitivity in CQ and QN (Cooper *et al.*, 2007, Lakshmanan *et al.*, 2005, Johnson *et al.*, 2004). However, in their publication Sen and Ferdig pointed out that unlike CQ resistance, which is determined by only a single factor (Sen & Ferdig, 2004), *pfcrt* (Ferdig *et al.*, 2004), QN sensitivity shows a pattern typical of that of a multifactorial trait (Sen & Ferdig, 2004).

Due to its multifactorial determinants, QTL analysis has been used to understand QN mechanisms. Ferdig *et al.* used QTL analysis of Dd2xHB3 cross QN IC_{90} data to determine loci related to QN sensitivity levels (Ferdig *et al.*, 2004). The results of Ferdig's study identified two major QTL in the primary scan, the *pfcrt* locus on chromosome 7 and a locus in chromosome 13, closed to *pfnhe.* In the secondary scan, they identified a locus located close to *pfmdr1* on chromosome 5.

Despite the association between several loci with QN resistance as shown by Ferdig *et al.* in their publication (Ferdig *et al.*, 2004), a recent publication shows that reduced accumulation of QN is not always accompanied with increased QN resistance (Sanchez *et al.*, 2008b). Since IC_{90} is a measure of cell proliferation inhibition after 72 hours of exposure to a drug, it might be influenced by other factors in addition to those affecting only the initial drug accumulation property. Whilst initial drug accumulation is affected by only partitioning and transport processes, IC_{90} might also be influenced by mutation and availability of the drug target, or even the combination of both mutation at the target and the transport machinery. Thus, measuring initial

QN accumulation leads to obtaining a readout defined by only transport mechanism, whilst eliminating the effect of other processes causing cell death.

In this study, Ferdig's IC_{90} data were reanalysed using the same QTL method to ensure the comparability of the different sets of data. In parallel to measuring and performing QTL analysis on QN accumulation, CQ accumulation was also measured and the QTL analysis of its initial accumulation was also performed as a mean of proving the validity of the method (Mayer, 2009). As predicted, QTL analysis of CQ initial accumulation was linked to a single factor affecting CQ accumulation (Mayer, 2009), hence proving the validity of the approach.

In this study, three stages of QTL analysis were performed. In the primary scan, major factors affecting the phenotypic trait were investigated. Loci obtained in the primary scans greatly affect the accumulation or IC_{90}. The secondary scans, on the other hand, explored factors affecting variations within two different groups of strains, the CQR and CQS strains. These factors might not have significant effect to the overall variation of the strains, and therefore might not be obvious in the primary scans, since their effect might be masked by the presence of the major factors. The third stage of QTL analysis performed in this study is mathematically analysing the interaction between positive loci found in the primary and secondary scans.

In addition to reanalysing Ferdig's QN IC_{90} data, Ferdig's data on QN IC_{90} with the presence of verapamil (Ferdig *et al.*, 2004) was also reanalysed. Verapamil is known to reverse CQ resistance caused by *pfcrt* mutation (Wellems *et al.*, 1990, Martin *et al.*, 1987). Although reduced accumulation of QN does not always correlate to increased QN resistance (Sanchez *et al.*, 2008b), all strains having K76T mutated *pfcrt* show increased verapamil-sensitive QN efflux (Sanchez *et al.*, 2008b). Thus comparing the data of QN IC_{90} QTL analyses with and without the presence of verapamil should lead to discovering factors affecting QN IC_{90} other than *pfcrt*, if any, which effect is reversed by verapamil.

This study shows that reduced initial quinine accumulation is genetically linked to both *pfcrt* and a novel QTL corresponding to B512 marker in chromosome 7 (Figure 3.5.). Both loci have negative effect to QN accumulation. The reanalysis of Ferdig's QN IC_{90} data indicated that both loci also contribute to the increased QN IC_{90} value, hence reducing the sensitivity. Lower LOD score obtained in the original study of QN IC_{90} performed by Ferdig's group (Ferdig *et al.*, 2004), leading to poor resolution of the two loci, is the underlying reason why they had failed to observe the significant effect of B5M12 locus.

The mathematical analysis shows that Dd2 allele of B5M12 only affects the QN accumulation and IC_{90}, when *pfcrt* is also from Dd2, that is, in CQR strains but not in

CQS strains (Figure 3.8.), suggesting that the presence of Dd2 alleles at both loci act synergistically reducing accumulation and increasing IC_{90}.

A

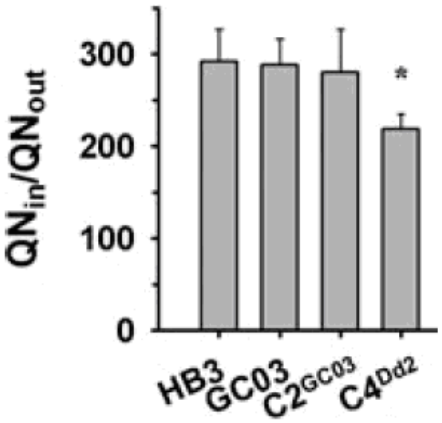

B

	Accumulation	IC_{90}
Dd2	115.89	925
HB3	168.49	382

Origin of B5M12	Origin of *pfcrt*	Accumulation (mean ± SE)	IC90 (mean ± SE)
H	H	182.8±4.8	385.4±33.8
D	H	181.1±37.7	290.5±91.5
H	D	166.8±13.3	456.7±46.8
D	D	123.1±4.1	642.1±66.1

Figure 4.1. Some allelic exchange mutants, with the genetic background of GC03 strain and having Dd2 *pfcrt* allele introduced to them, exhibited a decreased QN IC_{50} values, in comparison to GC03 (Sanchez *et al.*, 2008b) (A) and the presence of Dd2 allele at *pfcrt* locus is not the only prerequisite of acquiring QN accumulation and IC_{90} levels comparable to that of Dd2 (B).
$C2^{GC03}$ has GC03 background with autologous HB3-like *pfcrt* allele. $C4^{Dd2}$ has GC03 background with Dd2-like *pfcrt* allele.

Ferdig's QN IC_{90} data demonstrated that several F1 progeny of the Dd2xHB3 cross having Dd2 *pfcrt* displayed QN IC_{90} values comparable to that of HB3, the QN sensitive parent (see Apendix 3) (Ferdig *et al.*, 2004). In addition, Sanchez *et al.* demonstrated in their publication that some allelic exchange mutants having Dd2 *pfcrt* allele introduced to them with the genetic background of GC03 strain exhibited a decreased QN IC_{50} values, in comparison to GC03 (Figure 4.1.) (Sanchez *et al.*, 2008b). Originally, GC03 has inherited both its *pfcrt* and B5M12 from HB3 (Su *et al.*, 1999). The phenomena observed by Ferdig's and Sanchez's groups can be explained partly by the involvement of B5M12 as a major factor affecting QN accumulation and IC_{90} and the synergistic effect of *pfcrt* and B5M12. The analysis performed in the current study demonstrated that the presence of Dd2 allele at *pfcrt* locus is not the only prerequisite of acquiring QN accumulation and IC_{90} levels comparable to that of Dd2. The average QN accumulation and IC_{90} values of strains with different combinations of *pfcrt* and B5M12 are tabulated in Figure 4.1.

Despite the database search performed, the responsible gene lying within the B5M12 locus is not yet identified. Within the locus, 41 genes were annotated in PlasmoDB

and NCBI gene bank, of which four were tRNA genes, leaving 34 genes possible candidates. A comparison of the corresponding genomic sequences from HB3 and Dd2 identified putative polymorphisms in 32 of the genes. Seven of these genes encode for proteins with at least two TMDs (Table 3.5.). Physical interaction between PfCRT and a protein encoded within the B5M12 is a possibility, since there are examples of interaction between different subunits of plant transporters (Reinders *et al.*, 2002), mammalian transporters (Sun *et al.*, 2007), and bacteria (Ames, 1976). Yet, unavailability of complete sequences within the region had rendered it impossible to point specifically at certain candidates. Further sequencing revealing polymorphisms within this region should be attempted to be able to answer the question.

In the primary scan reanalysis of Ferdig's QN IC_{90} data, two additional positive loci were found in chromosome 13 (Figure 3.5.), which LOD scores were almost as high as those of B5M12 and *pfcrt*. The positive loci are correlated to markers VAPA and C13M73. Despite their high LOD scores for QN IC_{90}, these loci showed no influence to QN accumulation. This specific character of the loci would not have been revealed had the QTL analysis based on QN accumulation data not been performed.

Ferdig's group had considered the two significant peaks in chromosome 13 as only one QTL called C13M56 and that the putative *pfnhe* gene, which had been implicated in altered QN responsiveness (Bennett *et al.*, 2007), might be present within the area (Ferdig *et al.*, 2004). In the reanalysis, however, it was clear that these two peaks corresponded to two functionally separable loci with different responsiveness to verapamil. The left hand VAPA peak was completely diminished by the presence of verapamil, whereas the right hand C13M73 peak was relatively verapamil insensitive (Figure 3.5.).

In addition, the reanalysis also revealed that the TA46 marker, which contains the putative *pfnhe* gene, is located in neither of these two peaks. Instead, the marker mapped to the valley between the two peaks, clearly outside of the two QTL (Figure 3.5.).

The involvement of extended repeat polymorphisms within PfNHE in increased QN resistance, as reported previously (Ferdig *et al.*, 2004, Bennett *et al.*, 2007, Nkrumah *et al.*, 2009), might therefore be mediated by mechanisms at later time point than the commencement of the initial QN accumulation.

The facts that the two loci (VAPA and C13M73) involved only in QN IC_{90} but not in QN accumulation suggested that they were targeted by QN, instead of affecting QN transport. Mathematical analysis showed that the presence of Dd2 allele at these loci is associated with higher QN IC_{90} value (Figures 3.11. **(B)** and 3.12. **(B)**),

independent of the origins of the *pfcrt* and B5M12. Thus, it seemed that the Dd2 alleles at these loci have additive effect to the QN IC_{90}.

So far, verapamil ability to reverse CQ and QN resistance has been attributed to the reversal of the K76T mutation of *pfcrt* (Lakshmanan *et al.*, 2005). However, the discovery of the verapamil sensitive VAPA peak, which could be targeted by QN, might lead to understanding an additional role of verapamil in reducing the IC_{90}. It was, however, published previously that quinine and verapamil showed synergistic chemosensitisation of multidrug resistant tumour cells (Lehnert *et al.*, 1991), that it is tempting to speculate whether they could compete for the same target.

The genes encoding for this putative QN target remain to discover. Exploration of databases reveals 61 genes lying within the VAPA peak, of which 14 showed no polymorphisms between Dd2 and HB3. Incomplete data available at the online database had been a real obstacle that had yet to be overcome by thorough sequencing of the area under the peak.

The secondary scan revealed the association of peaks with minor effect to the phenotypes. These peaks were not obvious in the primary scan because their presence were overshadowed by the effects of the major peaks found in the primary scan.

The secondary scans showed association between the peaks containing *pfmdr1* to both QN accumulation and IC_{90}. Interestingly, the Dd2 allele of the locus seemed to contribute to an increase in initial QN accumulation and to the decrease of QN IC_{90}.

The involvement of PfMDR1 as well as its role in drug resistance has been much studied, however, how the protein works remains obscure. PfMDR1 resides in the FVM, with its ATP binding domains facing the parasite cytosol (Karcz *et al.*, 1993), and thus might allow import of solutes from the cytosol to the FV. A publication by Rohrbach *et al.* showed that subcellular distribution of a fluorescent indicator consistent with the view that the PfMDR1 indeed imported solutes into the FV and the import function is influenced by *pfmdr1* polymorphisms that affect antimalarial drug sensitivity (Rohrbach *et al.*, 2006). The protein also seems to transport a range of solutes across the FVM (Saliba *et al.*, 2008). Sanchez *et al.* used *pfmdr1*-expressing *Xenopus laevis* oocytes to show that polymorphisms at this gene brought about substantial differences in the transport of pharmaceuticals, including quinine (Sanchez *et al.*, 2008a). Thus, it is not improbable that it is, indeed, the *pfmdr1* gene on chromosome 5 that in the Dd2 version pumps QN into the FV, this bringing about the increased sensitivity to quinine.

Another positive locus found in the secondary scan of QN IC_{90} was BM75. The locus was located in chromosome 7. This locus is located at the same cM position as

B5M74 locus, which is described in Ferdig's publication as interacting with *pfcrt* and that the inheritance of the Dd2 alleles at both B5M74 and *pfcrt* loci resulted in substantially higher QN IC_{90} values than inheritance of other possible allele combinations (Ferdig *et al.*, 2004).

Analysis of BM75 demonstrated that the presence of Dd2 allele at both *pfcrt* and BM75 loci was a must for the significant increased of QN IC_{90}, indicating that these allele have synergistic effect to the IC_{90} phenotype. Since BM75 peak was not present in the secondary scan of QN accumulation, it make sense that the locus showed no significant difference in QN accumulation level with all allelic combinations at the BM75 and *pfcrt* loci (Figure 3.12. **(A)**).

C5M2 was another locus appeared in the secondary scan. This locus is the only accumulation specific locus discovered in the secondary scan on CQS strains. As predicted by the QTL analysis and confirmed by further analysis mathematically, the locus seemed to affect QN accumulation variation in CQS strains only, without showing any observable effect to IC_{90} (Figure 3.13.).

In conclusion, the study has proven that the strain specific variation of initial QN accumulation and degree of resistance are clearly controlled by multiple genetic factors. The analysis of QN accumulation has managed to reveal novel loci linked to initial QN accumulation level, which were not previously identified by QTL analysis using QN IC_{90} data. Having obtained better LOD scores from the reanalysis of QN IC_{90} data, peaks with better resolution than the ones originally published by Ferdig (Ferdig *et al.*, 2004) were obtained. In addition to *pfcrt*, B5M12 seems to be a major factor in both QN accumulation and IC_{90} and act synergistically with *pfcrt*.

Two other loci, VAPA and C13 M73, which are located in chromosome 13 seem to have major roles in QN IC_{90}, but not accumulation. These loci were not likely to be resolved from factors affecting QN accumulation, had no QTL analysis of QN accumulation been performed. These two loci act independently from the major loci in chromosome 7 and have additive effect related to the Dd2-alleles.

The secondary scans performed separately on CQR and CQS strains managed to reveal minor factors affecting the phenotypes. Peaks containing *pfmdr1* gene were found to be associated to both QN accumulation and IC_{90}. It was really intriguing, however, to find that the Dd2 allele of the locus seemed to contribute to an increase in initial QN accumulation and to the decrease of QN IC_{90}. However, the phenomenon that PfMDR1 imports solute into the FV was also observed previously (Rohrbach *et al.*, 2006).

Although the study has discovered various loci linked to QN accumulation and resistance, detailed investigation, locus by locus, separately or in combination to one

another, is essential to find the specific underlying gene responsible for the phenotypes and to understand the exact mechanisms of the accumulation and its relation to resistance.

Some of the minor loci revealed in the secondary scans, for example BM75, seemed to interact with major loci such as *pfcrt*. It would be interesting, had time permitted it to study, locus-by-locus, the interactions of the positive loci to one another.

So far, the major obstacle in finding specifically the responsible genes in the loci is the unavailability of complete sequences of Dd2 and HB3, let alone the progeny, in the databases. Thus, following the *in silico* dissection of the positive loci by searching available databases in order to find candidate genes, *in vitro* sequencing of the parental strains (Dd2 and HB3), especially within the areas under the positive loci, should be performed followed by analysis of the presence of polymorphisms within the area. Polymorphisms within these areas might be related to the different phenotypes expressed by the strains. Prediction of protein conformation and presence of transmembrane domains in the putative proteins might lead to discovery of new transport proteins related to the accumulation of the drugs. Functional studies of the putative proteins can then be performed by expressing the mRNA of the putative gene in *Xenopus laevis* oocytes to see the activity of the putative proteins. Generation of mutants with knocked-out the candidate genes might be a useful approach to see what the effects and the functions might be.

In short, plenty of works await still to be done before the thorough understanding of the complete mechanisms behind QN accumulation and resistance might be acquired.

5. References

Plasmodium falciparum Database. http://www.broad.mit.edu/annotation/genome/plasmodium_falciparum_spp/MultiHome.html BROAD MIT Institute

Clinical Manifestations: General Features. http://www.malaria.am/eng/manifest.php Malaria In Armenia

PlasmoDB: Methods. http://plasmodb.org/plasmo/showXmlDataContent.do?name=XmlQuestions.Methods PlasmoDB

WHO Programs and Projects: Child and Adolescent Health and Development, Data Statistics, and Epidemiology. http://www.who.int/child_adolescent_health/data/child/en/index.html World Health Organisation

Adovelande, J., J. Delèze & J. Schrével, (1998) Synergy between two calcium channel blockers, verapamil and fantofarone (SR33557), in reversing chloroquine resistance in Plasmodium falciparum. *Biochemical Pharmacology* **55**: 433-440.

Ames, G. F.-L., (1976) Protein-protein interaction in transport. *Journal of Cellular Physiology* **89**: 543.

Baruch, D. I., (1999) Adhesive receptors on malaria-parasitized red cells. *Best Practice & Research Clinical Haematology* **12**: 747-761.

Bennett, T. N., J. Patel, M. T. Ferdig & P. D. Roepe, (2007) Plasmodium falciparum Na+/H+ exchanger activity and quinine resistance. *Mol Biochem Parasitol* **153**: 48-58.

Bloland, P. B., (2001) *Drug resistance in malaria*. WHO.

Borges-Walmsley, M. I., K. S. McKeegan & A. R. Walmsley, (2003) Structure and function of efflux pumps that confer resistance to drugs. *Biochem J* **376**: 313-338.

Bray, P. G., R. E. Martin, L. Tilley, S. A. Ward, K. Kirk & D. A. Fidock, (2005) Defining the role of PfCRT in Plasmodium falciparum chloroquine resistance. *Mol Microbiol* **56**: 323-333.

Bray, P. G., M. Mungthin, I. M. Hastings, G. A. Biagini, D. K. Saidu, V. Lakshmanan, D. J. Johnson, R. H. Hughes, P. A. Stocks, P. M. O'Neill, D. A. Fidock, D. C. Warhurst & S. A. Ward, (2006) PfCRT and the trans-vacuolar proton electrochemical gradient: regulating the access of chloroquine to ferriprotoporphyrin IX. *Molecular Microbiology* **62**: 238-251.

Bray, P. G., M. Mungthin, R. G. Ridley & S. A. Ward, (1998) Access to Hematin: The Basis of Chloroquine Resistance. *Mol Pharmacol* **54**: 170-179.

BROAD, (2009) *Plasmodium falciparum* Database. http://www.broad.mit.edu/annotation/genome/plasmodium_falciparum_spp/MultiHome.html BROAD MIT Institute

Busch, W. & M. H. Saier, (2002) The Transporter Classification (TC) System, 2002. *Critical Reviews in Biochemistry and Molecular Biology* **37**: 287 - 337.

Cambrex Bio Science Rockland, I., (2003) *MetaPhor® Agarose Product Information*.

Campbell, C. C., W. Chin, W. E. Collins, S. M. Teutsch & D. M. Moss, (1979) Chloroquine-resistant Plasmodium falciparum from East Africa: cultivation and drug sensitivity of the Tanzanian I/CDC strain from an American tourist. *Lancet* **2**: 1151-1154.

CBS, (2007) TMHMM Server v. 2.0 Prediction of transmembrane helices in proteins. http://www.cbs.dtu.dk/services/TMHMM/ Center for Biological Sequence Analysis

Chen, Q., M. Schlichtherle & M. Wahlgren, (2000) Molecular aspects of severe malaria. *Clin Microbiol Rev* **13**: 439-450.

Cooper, R. A., K. D. Lane, B. Deng, J. Mu, J. J. Patel, T. E. Wellems, X. Su & M. T. Ferdig, (2007) Mutations in transmembrane domains 1, 4 and 9 of the *Plasmodium falciparum* chloroquine resistance transporter alter susceptibility to chloroquine, quinine and quinidine. *Molecular Microbiology* **63**: 270-282.

Cowman, A. F. & B. S. Crabb, (2002) The Plasmodium falciparum Genome-- a Blueprint for Erythrocyte Invasion. *Science* **298**: 126-128.

Cowman, A. F., D. Galatis & J. K. Thompson, (1994) Selection for mefloquine resistance in Plasmodium falciparum is linked to amplification of the pfmdr1 gene and cross-resistance to halofantrine and quinine. *Proc Natl Acad Sci U S A* **91**: 1143-1147.

Cowman, A. F., S. Karcz, D. Galatis & J. G. Culvenor, (1991) A P-glycoprotein homologue of Plasmodium falciparum is localized on the digestive vacuole. *J. Cell Biol.* **113**: 1033-1042.

Cox-Singh, J., TimothyÂ M. Â E. Davis, K. S. Lee, SunitaÂ S. Â G. Shamsul, A. Matusop, S. Ratnam, HasanÂ A. Rahman, DavidÂ J. Conway & B. Singh, (2008) Plasmodium knowlesi Malaria in Humans Is Widely Distributed and Potentially Life Threatening. *Clinical Infectious Diseases* **46**: 165-171.

Cox, F. E. G., (2002) History of Human Parasitology. *Clin. Microbiol. Rev.* **15**: 595-612.

de Villiers, K. A., H. M. Marques & T. J. Egan, (2008) The crystal structure of halofantrine-ferriprotoporphyrin IX and the mechanism of action of arylmethanol antimalarials. *Journal of Inorganic Biochemistry* **102**: 1660-1667.

Djimde, A., O. K. Doumbo, J. F. Cortese, K. Kayentao, S. Doumbo, Y. Diourte, A. Dicko, X. Z. Su, T. Nomura, D. A. Fidock, T. E. Wellems, C. V. Plowe & D. Coulibaly, (2001) A molecular marker for chloroquine-resistant falciparum malaria. *N Engl J Med* **344**: 257-263.

Egan, T. J., J. M. Combrinck, J. Egan, G. R. Hearne, H. M. Marques, S. Ntenteni, B. T. Sewell, P. J. Smith, D. Taylor, D. A. van Schalkwyk & J. C. Walden, (2002) Fate of haem iron in the malaria parasite Plasmodium falciparum. *Biochem J* **365**: 343-347.

Elliott, D. A., M. T. McIntosh, H. D. Hosgood, 3rd, S. Chen, G. Zhang, P. Baevova & K. A. Joiner, (2008) Four distinct pathways of hemoglobin uptake in the malaria parasite Plasmodium falciparum. *Proc Natl Acad Sci U S A* **105**: 2463-2468.

EMBNet, (2008) EMBnet Basic BLAST. http://www.ch.embnet.org/software/bBLAST.html Swiss Institute of Bioinformatics

Ersmark, K., B. Samuelsson & A. Hallberg, (2006) Plasmepsins as potential targets for new antimalarial therapy. *Medicinal Research Reviews* **26**: 626-666.

Ferdig, M. T., R. A. Cooper, J. Mu, B. Deng, D. A. Joy, X. Z. Su & T. E. Wellems, (2004) Dissecting the loci of low-level quinine resistance in malaria parasites. *Mol Microbiol* **52**: 985-997.

Fidock, D. A., T. Nomura, A. K. Talley, R. A. Cooper, S. M. Dzekunov, M. T. Ferdig, L. M. Ursos, A. B. Sidhu, B. Naude, K. W. Deitsch, X. Z. Su, J. C. Wootton, P. D. Roepe & T. E. Wellems, (2000) Mutations in the P. falciparum digestive vacuole transmembrane protein PfCRT and evidence for their role in chloroquine resistance. *Mol Cell* **6**: 861-871.

Foley, M. & L. Tilley, (1998) Quinoline Antimalarials: Mechanisms of Action and Resistance and Prospects for New Agents. *Pharmacology & Therapeutics* **79**: 55-87.

Gallup, J. L. & J. D. Sachs, (2001) The economic burden of malaria. *Am J Trop Med Hyg* **64**: 85-96.

Greenwood, B. M., K. Bojang, C. J. Whitty & G. A. Targett, (2005) Malaria. *Lancet* **365**: 1487-1498.

Gregson, A. & C. V. Plowe, (2005) Mechanisms of resistance of malaria parasites to antifolates. *Pharmacol Rev* **57**: 117-145.

Guerra, C. A., P. W. Gikandi, A. J. Tatem, A. M. Noor, D. L. Smith, S. I. Hay & R. W. Snow, (2008) The limits and intensity of Plasmodium falciparum transmission: implications for malaria control and elimination worldwide. *PLoS Med* **5**: e38.

Haley, C. S. & S. A. Knott, (1992) A simple regression method for mapping quantitative trait loci in line crosses using flanking markers. *Heredity* **69**: 315-324.

Hartl, D. L., (2004) The origin of malaria: mixed messages from genetic diversity. *Nat Rev Micro* **2**: 15-22.

Hawley, S. R., P. G. Bray, M. Mungthin, J. D. Atkinson, P. M. O'Neill & S. A. Ward, (1998) Relationship between antimalarial drug activity, accumulation, and inhibition of heme polymerization in Plasmodium falciparum in vitro. *Antimicrob Agents Chemother* **42**: 682-686.

Hayward, R., K. J. Saliba & K. Kirk, (2005) Mutations in pfmdr1 modulate the sensitivity of Plasmodium falciparum to the intrinsic antiplasmodial activity of verapamil. *Antimicrob Agents Chemother* **49**: 840-842.

Hyde, J. E., (2007) Drug-resistant malaria- an insight. *FEBS Journal* **274**: 4688-4698.

Jelinek, T., P. Schelbert, T. Loscher & D. Eichenlaub, (1995) Quinine resistant falciparum malaria acquired in east Africa. *Trop Med Parasitol* **46**: 38-40.

Johnson, D. J., D. A. Fidock, M. Mungthin, V. Lakshmanan, A. B. Sidhu, P. G. Bray & S. A. Ward, (2004) Evidence for a central role for PfCRT in conferring Plasmodium falciparum resistance to diverse antimalarial agents. *Mol Cell* **15**: 867-877.

Karcz, S. R., D. Galatis & A. F. Cowman, (1993) Nucleotide binding properties of a P-glycoprotein homologue from Plasmodium falciparum. *Mol Biochem Parasitol* **58**: 269-276.

Kerr, I. D., (2002) Structure and association of ATP-binding cassette transporter nucleotide-binding domains. *Biochimica et Biophysica Acta (BBA) - Biomembranes* **1561**: 47-64.

Kirkman, L. A., X.-z. Su & T. E. Wellems, (1996) Plasmodium falciparum:Isolation of Large Numbers of Parasite Clones from Infected Blood Samples. *Experimental Parasitology* **83**: 147-149.

Krogh, A., B. Larsson, G. von Heijne & E. L. L. Sonnhammer, (2001) Predicting transmembrane protein topology with a hidden markov model: application to complete genomes. *Journal of Molecular Biology* **305**: 567-580.

Kuhn, Y., P. Rohrbach & M. Lanzer, (2007) Quantitative pH measurements in Plasmodium falciparum-infected erythrocytes using pHluorin. *Cell Microbiol* **9**: 1004-1013.

Kwiatkowski, D., J. G. Cannon, K. R. Manogue, A. Cerami, C. A. Dinarello & B. M. Greenwood, (1989) Tumour necrosis factor production in Falciparum malaria and its association with schizont rupture. *Clin Exp Immunol* **77**: 361-366.

Lakshmanan, V., P. G. Bray, D. Verdier-Pinard, D. J. Johnson, P. Horrocks, R. A. Muhle, G. E. Alakpa, R. H. Hughes, S. A. Ward, D. J. Krogstad, A. B. Sidhu & D. A. Fidock, (2005) A critical role for PfCRT K76T in Plasmodium falciparum verapamil-reversible chloroquine resistance. *EMBO J* **24**: 2294-2305.

Lambros, C. & J. P. Vanderberg, (1979) Synchronization of Plasmodium falciparum erythrocytic stages in culture. *J Parasitol* **65**: 418-420.

Lander, E. S. & D. Botstein, (1989) Mapping Mendelian Factors Underlying Quantitative Traits Using RFLP Linkage Maps. *Genetics* **121**: 185-199.

Lazarus, M. D., T. G. Schneider & T. F. Taraschi, (2008) A new model for hemoglobin ingestion and transport by the human malaria parasite Plasmodium falciparum. *J Cell Sci* **121**: 1937-1949.

Le Bras, J., I. Hatin, P. Bouree, O. Coco-Cianci, J. P. Garin, M. Rey, G. Charmot & R. Roue, (1986) Chloroquine-resistant falciparum malaria in Benin. *Lancet* **2**: 1043-1044.

Lehnert, M., W. S. Dalton, D. Roe, S. Emerson & S. E. Salmon, (1991) Synergistic inhibition by verapamil and quinine of P-glycoprotein- mediated multidrug resistance in a human myeloma cell line model. *Blood* **77**: 348-354.

Lew, V. L., T. Tiffert & H. Ginsburg, (2003) Excess hemoglobin digestion and the osmotic stability of Plasmodium falciparum-infected red blood cells. *Blood* **101**: 4189-4194.

Mackay, T. F., (2001) The genetic architecture of quantitative traits. *Annu Rev Genet* **35**: 303-339.

Maitra, N., M. Joshi & M. Hazra, (1993) Maternal manifestations of malaria in pregnancy: a review. *Ind J Matern Child Health* **4**: 4.

Makler, M. T., R. C. Piper & W. K. Milhous, (1998) Lactate Dehydrogenase and the Diagnosis of Malaria. *Parasitology Today* **14**: 376-377.

Malaria In Armenia, (2002) Roll Back Malaria: Clinical Manifestations - General Features. http://www.malaria.am/eng/manifest.php Malaria In Armenia

Martin, R. E. & K. Kirk, (2004) The Malaria Parasite's Chloroquine Resistance Transporter is a Member of the Drug/Metabolite Transporter Superfamily. *Mol Biol Evol* **21**: 1938-1949.

Martin, S. K., A. M. Oduola & W. K. Milhous, (1987) Reversal of chloroquine resistance in Plasmodium falciparum by verapamil. *Science* **235**: 899-901.

Mayer, S., 2009, *Biochemische und genetische Analyse von Chinolin-Resistenzen in Plamodium falciparum*, Doctoral Thesis

Mayxay, M., M. Barends, A. Brockman, A. Jaidee, S. Nair, D. A. N. Sudimack, T. Pongvongsa, S. Phompida, R. Phetsouvanh, T. I. M. Anderson, N. J. White & P. N. Newton, (2007) *In Vitro* Antimalarial Drug Susceptibility and *pfcrt* Mutation Among Fresh *Plasmodium falciparum* Isolates from the Lao PDR (Laos). *Am J Trop Med Hyg* **76**: 245-250.

Meier, B., H. Döbeli & U. Certa, (1992) Stage-specific expression of aldolase isoenzymes in the rodent malaria parasite Plasmodium berghei. *Molecular and Biochemical Parasitology* **52**: 15-27.

Miller, L. H., D. I. Baruch, K. Marsh & O. K. Doumbo, (2002) The pathogenic basis of malaria. *Nature* **415**: 673-679.

Moody, A., (2002) Rapid Diagnostic Tests for Malaria Parasites. *Clin. Microbiol. Rev.* **15**: 66-78.

Mota, M. M., G. Pradel, J. P. Vanderberg, J. C. R. Hafalla, U. Frevert, R. S. Nussenzweig, V. Nussenzweig & A. Rodriguez, (2001) Migration of Plasmodium Sporozoites Through Cells Before Infection. *Science* **291**: 141-144.

Mungthin, M., P. G. Bray, R. G. Ridley & S. A. Ward, (1998) Central Role of Hemoglobin Degradation in Mechanisms of Action of 4-Aminoquinolines, Quinoline Methanols, and Phenanthrene Methanols. *Antimicrob. Agents Chemother.* **42**: 2973-2977.

National Center for Biotechnology Information, (2000) Malaria Genetics and Genomics: *P. falciparum* HB3xDd2 Cross Segregation Data. http://www.ncbi.nlm.nih.gov/Malaria/Mapsmarkers/PfSegData/segdata.html NCBI

National Center for Biotechnology Information, (2008) NCBI Map Viewer: Plasmodium falciparum genome view. http://www.ncbi.nlm.nih.gov/projects/mapview/map_search.cgi?taxid=5833 NCBI

Nkrumah, L. J., P. M. Riegelhaupt, P. Mourac, D. J. Johnsona, J. Patel, K. Haytone, M. T. Ferdig, T. E. Wellems, M. H. Akabas & D. A. Fidock, (2009) Probing the multifactorial basis of Plasmodium falciparum quinine resistance: Evidence for a strain-specific contribution of the sodium-proton exchanger PfNHE *Molecular and Biochemical Parasitology* **165**: 10.

Patel, D. N., P. Pradeep, M. M. Surti & S. B. Agarwal, (2003) Clinical Manifestations of Complicated Malaria – An Overview. *J Ind Acad Clin Med* **4**: 9.

Paterson, A. H., (1995) Molecular dissection of quantitative traits: progress and prospects. *Genome Research* **5**: 321-333.

Peel, S. A., (2001) The ABC transporter genes of Plasmodium falciparum and drug resistance. *Drug Resistance Updates* **4**: 66-74.

PlasmoDB, (2008a) PlasmoDB: The Plasmodium Genome Resource. http://plasmodb.org/plasmo/ PlasmoDB

PlasmoDB, (2008b) PlasmoDB: Methods. http://plasmodb.org/plasmo/showXmlDataContent.do?name=XmlQuestions.Methods PlasmoDB

Pukrittayakamee, S., W. Supanaranond, S. Looareesuwan, S. Vanijanonta & N. J. White, (1994) Quinine in severe falciparum malaria: evidence of declining efficacy in Thailand. *Transactions of the Royal Society of Tropical Medicine and Hygiene* **88**: 324-327.

Rasti, N., M. Wahlgren & Q. Chen, (2004) Molecular aspects of malaria pathogenesis. *FEMS Immunology and Medical Microbiology* **41**: 9-26.

Reed, M. B., K. J. Saliba, S. R. Caruana, K. Kirk & A. F. Cowman, (2000) Pgh1 modulates sensitivity and resistance to multiple antimalarials in Plasmodium falciparum. *Nature* **403**: 906-909.

Reinders, A., W. Schulze, C. Kuhn, L. Barker, A. Schulz, J. M. Ward & W. B. Frommer, (2002) Protein-Protein Interactions between Sucrose Transporters of Different Affinities Colocalized in the Same Enucleate Sieve Element. *Plant Cell* **14**: 1567-1577.

Retief, F. & L. Cilliers, (2006) Periodic pyrexia and malaria in antiquity. *S Afr Med J* **96**: 684, 686-688.

Rice University, (2007) Experimental Biosiences: Using a Counting Chamber. http://www.ruf.rice.edu/~bioslabs/methods/microscopy/cellcounting.html Rice University

Rock, E. P., K. Marsh, A. J. Saul, T. E. Wellems, D. W. Taylor, W. L. Maloy & R. J. Howard, (1987) Comparative analysis of the Plasmodium falciparum histidine-rich proteins HRP-I, HRP-II and HRP-III in malaria parasites of diverse origin. *Parasitology* **95 (Pt 2)**: 209-227.

Rohrbach, P., C. P. Sanchez, K. Hayton, O. Friedrich, J. Patel, A. B. Sidhu, M. T. Ferdig, D. A. Fidock & M. Lanzer, (2006) Genetic linkage of pfmdr1 with food vacuolar solute import in Plasmodium falciparum. *EMBO J* **25**: 3000-3011.

Sachs, J. & P. Malaney, (2002) The economic and social burden of malaria. *Nature* **415**: 680-685.

Saliba, K. J., H. A. Horner & K. Kirk, (1998) Transport and metabolism of the essential vitamin pantothenic acid in human erythrocytes infected with the malaria parasite Plasmodium falciparum. *J Biol Chem* **273**: 10190-10195.

Saliba, K. J., A. M. Lehane & K. Kirk, (2008) A polymorphic drug pump in the malaria parasite. *Mol Microbiol* **70**: 775-779.

Sanchez, C. P., A. Rotmann, W. D. Stein & M. Lanzer, (2008a) Polymorphisms within PfMDR1 alter the substrate specificity for anti-malarial drugs in Plasmodium falciparum. *Mol Microbiol* **70**: 786-798.

Sanchez, C. P., W. Stein & M. Lanzer, (2003) Trans Stimulation Provides Evidence for a Drug Efflux Carrier as the Mechanism of Chloroquine Resistance in Plasmodium falciparum&#x2020. *Biochemistry* **42**: 9383-9394.

Sanchez, C. P., W. D. Stein & M. Lanzer, (2007) Is PfCRT a channel or a carrier? Two competing models explaining chloroquine resistance in Plasmodium falciparum. *Trends Parasitol* **23**: 332-339.

Sanchez, C. P., W. D. Stein & M. Lanzer, (2008b) Dissecting the components of quinine accumulation in Plasmodium falciparum. *Mol Microbiol* **67**: 1081-1093.

Sansonetti, P. J., C. Lebras, F. Verdier, G. Charmot, B. Dupont & C. Lapresle, (1985) Chloroquine-resistant Plasmodium falciparum in Cameroon. *Lancet* **1**: 1154-1155.

Schlitzer, M., (2007) Malaria Chemotherapeutics Part I: History of Antimalarial Drug Development, Currently Used Therapeutics, and Drugs in Clinical Development. *ChemMedChem* **2**: 944-986.

Segurado, A. A., S. M. di Santi & M. Shiroma, (1997) In vivo and in vitro Plasmodium falciparum resistance to chloroquine, amodiaquine and quinine in the Brazilian Amazon. *Rev Inst Med Trop Sao Paulo* **39**: 85-90.

Sen, Å. & M. Ferdig, (2004) QTL Analysis for Discovery of Genes Involved in Drug Responses. *Current Drug Targets - Infectious Disorders* **4**: 53-63.

Sen, S. & G. A. Churchill, (2001) A Statistical Framework for Quantitative Trait Mapping. *Genetics* **159**: 371-387.

Shapiro, T. A. & D. E. Goldberg, (2005) Chemotherapy of Protozoal Infections: Malaria. In: *Goodman & Gilman's The Pharmacological Basis of Therapeutics.* L. Brunton, J. Lazo & K. Parker (eds). McGraw-Hill, pp. 25.

Shortt, H. E., (1951) Life-cycle of the mammalian malaria parasite. *Br Med Bull* **8**: 7-9.

Sidhu, A. B., A. C. Uhlemann, S. G. Valderramos, J. C. Valderramos, S. Krishna & D. A. Fidock, (2006) Decreasing pfmdr1 copy number in plasmodium falciparum malaria heightens susceptibility to mefloquine, lumefantrine, halofantrine, quinine, and artemisinin. *J Infect Dis* **194**: 528-535.

Sidhu, A. B., S. G. Valderramos & D. A. Fidock, (2005) pfmdr1 mutations contribute to quinine resistance and enhance mefloquine and artemisinin sensitivity in Plasmodium falciparum. *Mol Microbiol* **57**: 913-926.

Sidhu, A. B., D. Verdier-Pinard & D. A. Fidock, (2002) Chloroquine resistance in Plasmodium falciparum malaria parasites conferred by pfcrt mutations. *Science* **298**: 210-213.

Su, X., M. T. Ferdig, Y. Huang, C. Q. Huynh, A. Liu, J. You, J. C. Wootton & T. E. Wellems, (1999) A genetic map and recombination parameters of the human malaria parasite Plasmodium falciparum. *Science* **286**: 1351-1353.

Su, X., L. A. Kirkman, H. Fujioka & T. E. Wellems, (1997) Complex polymorphisms in an approximately 330 kDa protein are linked to chloroquine-resistant P. falciparum in Southeast Asia and Africa. *Cell* **91**: 593-603.

Sun, A. Q., N. Balasubramaniyan, K. Xu, C. J. Liu, V. M. Ponamgi, H. Liu & F. J. Suchy, (2007) Protein-protein interactions and membrane localization of the human organic solute transporter. *Am J Physiol Gastrointest Liver Physiol* **292**: G1586-1593.

Teklehaimanot, A. & P. Mejia, (2008) Malaria and Poverty. *Annals of the New York Academy of Sciences* **1136**: 32-37.

Trager, W. & J. B. Jensen, (1976) Human malaria parasites in continuous culture. *Science* **193**: 673-675.

Tuteja, R., (2007) Malaria - an overview. *FEBS Journal* **274**: 4670-4679.

Uhlemann, A. C., T. Staalsoe, M. Q. Klinkerta & L. Hviid, (2000) Analysis of Plasmodium falciparum-infectedred blood cells. *MACS & More* **4**: 2.

Valderramos, S. G. & D. A. Fidock, (2006) Transporters involved in resistance to antimalarial drugs. *Trends Pharmacol Sci* **27**: 594-601.

van Vugt, M., A. Brockman, B. Gemperli, C. Luxemburger, I. Gathmann, C. Royce, T. Slight, S. Looareesuwan, N. J. White & F. Nosten, (1998) Randomized comparison of artemether-benflumetol and artesunate-mefloquine in treatment of multidrug-resistant falciparum malaria. *Antimicrob Agents Chemother* **42**: 135-139.

Vogt, A., (2008) Selection of trophozoites by using magnetic cell sorting (MACS). In: *Methods in Malaria Research.* K. Moll, I. Ljungström, H. Perlmann, A. Scherf & M. Wahlgren (eds). pp. 31-33.

Walker-Jonah, A., S. A. Dolan, R. W. Gwadz, L. J. Panton & T. E. Wellems, (1992) An RFLP map of the Plasmodium falciparum genome, recombination rates and favored linkage groups in a genetic cross. *Mol Biochem Parasitol* **51**: 313-320.

Wellems, T. E., L. J. Panton, I. Y. Gluzman, V. E. do Rosario, R. W. Gwadz, A. Walker-Jonah & D. J. Krogstad, (1990) Chloroquine resistance not linked to mdr-like genes in a Plasmodium falciparum cross. *Nature* **345**: 253-255.

Weniger, B. G., R. S. Blumberg, C. C. Campbell, T. C. Jones, D. L. Mount & S. M. Friedman, (1982) High-level chloroquine resistance of Plasmodium falciparum malaria acquired in Kenya. *N Engl J Med* **307**: 1560-1562.

White, N. Â J., (2008) Editorial Commentary: Plasmodium knowlesi: The Fifth Human Malaria Parasite. *Clinical Infectious Diseases* **46**: 172-173.

White, N. J., F. Nosten, S. Looareesuwan, W. M. Watkins, K. Marsh, R. W. Snow, G. Kokwaro, J. Ouma, T. T. Hien, M. E. Molyneux, T. E. Taylor, C. I. Newbold, T. K. Ruebush, 2nd, M. Danis, B. M. Greenwood, R. M. Anderson & P. Olliaro, (1999) Averting a malaria disaster. *Lancet* **353**: 1965-1967.

Wiesner, J., R. Ortmann, H. Jomaa & M. Schlitzer, (2003) Neue Antimalaria-Wirkstoffe. *Angewandte Chemie* **115**: 5432-5451.

Woodrow, C. J., R. K. Haynes & S. Krishna, (2005) Artemisinins. *Postgrad Med J* **81**: 71-78.

World Health Organisation, (2001) Roll Back Malaria Infosheet: Malaria in Pregnancy. http://www.rbm.who.int/cmc_upload/0/000/015/369/RBMInfosheet_4.htm Roll Back Malaria

World Health Organisation, (2003) Malaria during pregnancy. In: *Africa Malaria Report 2003.* pp. Chapter 4.

World Health Organisation, (2008) *World Malaria Report 2008*. World Health Organisation.

World Health Organisation, (2009) WHO Programs and Projects: Child and Adolescent Health and Development, Data Statistics, and Epidemiology. http://www.who.int/child_adolescent_health/data/child/en/index.html World Health Organisation

Wu, R., C.-X. Ma & G. Casella, (2007) *Statistical Genetics of Quantitive Traits*. Springer.

Yamauchi, L. M., A. Coppi, G. Snounou & P. Sinnis, (2007) Plasmodium sporozoites trickle out of the injection site. *Cell Microbiol* **9**: 1215-1222.

Yayon, A., Z. I. Cabantchik & H. Ginsburg, (1985) Susceptibility of human malaria parasites to chloroquine is pH dependent. *Proc Natl Acad Sci U S A* **82**: 2784-2788.

6. Appendices

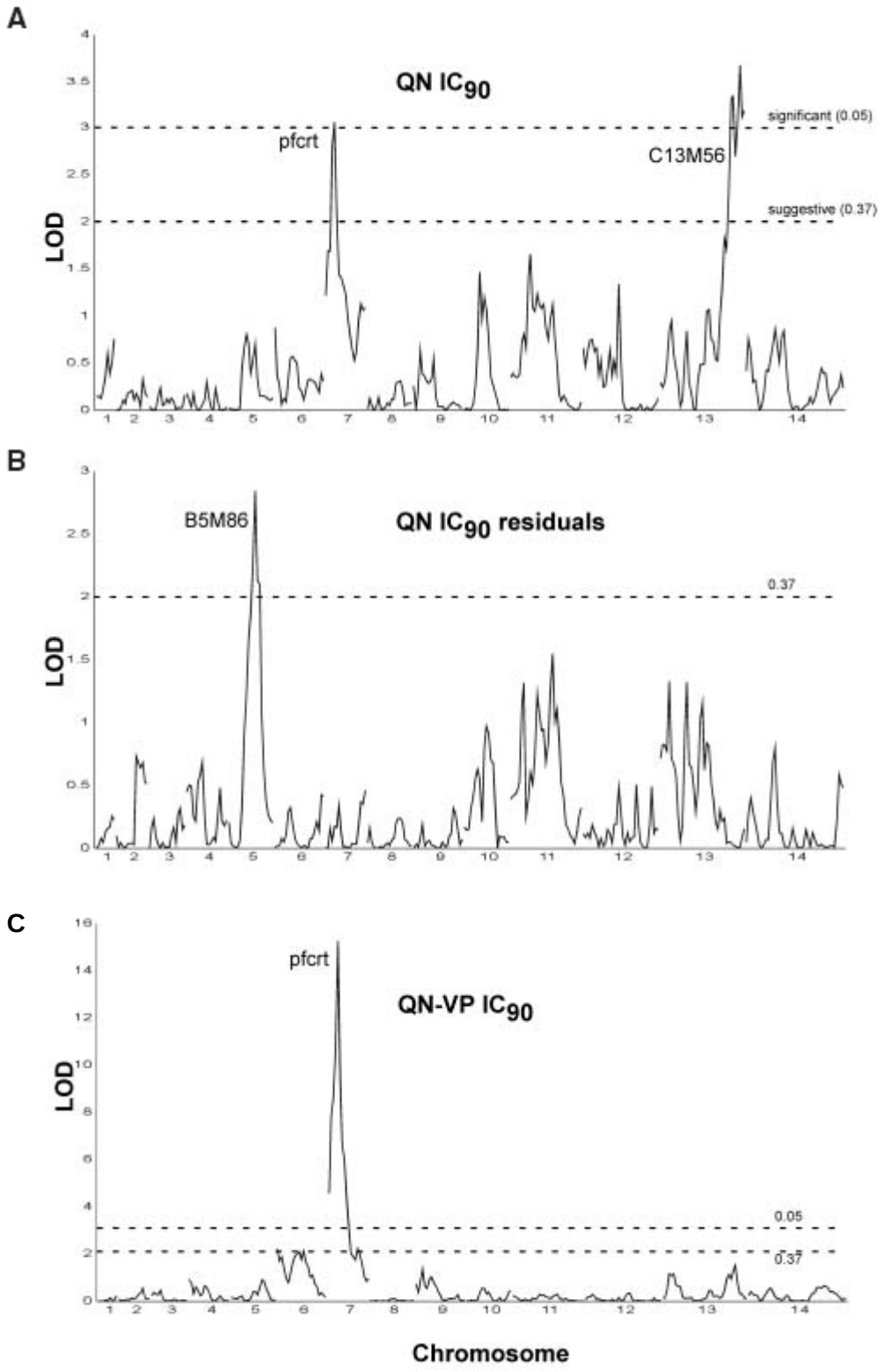

Appendix 1. Ferdig's QTL analysis of QN IC_{90} and QN-VP IC_{90} (Ferdig *et al.*, 2004)
(A) QN IC_{90} primary scan and **(B)** secondary scan, after removing the effect of *pfcrt* (C) QN-VP IC_{90} primary scan

B5M12 and *pfcrt* from HB3			B5M12 from Dd2 *pfcrt* from HB3			B5M12 from HB3 *pfcrt* from Dd2			B5M12 and *pfcrt* from Dd2		
Strains	**Accum.**	**IC_{90}**	**Strains**	**Accum.**	**IC_{90}**	**Strains**	**Accum.**	**IC_{90}**	**Strains**	**Accum.**	**IC_{90}**
HB3	168.49	382	C188	218.82	382	TC05	141.43	378	Dd2	115.89	925
B1SD	223.27	328	CH3-116	143.37	199	D43	186.41	452	3BA6	111.55	1038
QC13	213.88	539				7C111	172.44	540	1BB5	106.75	1044
QC01	168.68	456							3BD5	156.52	379
B4R3	203.91	202							SC01	144.57	736
SC05	202.56	428							QC34	110.25	673
TC08	184.35	262							QC23	119.92	528
GC03	169.16	351							GC06	115.97	755
CH3-61	159.39	322							C408	107.42	760
7C3	191.01	732							7C12	119.95	436
7C7	188.91	485							7C46	121.95	625
7C126	175.71	289							7C183	122.73	380
7C140	175.02	217							7C421	145.68	388
7C159	184.66	542							7C424	124.12	322
7C170	148.54	262									
7C16	185.50	287									
7C20	164.29	468									

Appendix 2. The QN accumulation and IC_{90} levels of strains grouped based on their inheritance of B5M12 and *pfcrt*.